ESSAYS ON THE EUROPEAN ELECTRICITY MARKETS

BY
HONG CAI

NHH

PhD THESIS

Department of Business and Management Science

ACKNOWLEDGMENTS

Thanks to Han, Xiaoluo (Erika), and Xiaoke (Leah), for always being there for me.

I want to first thank my advisor Endre Bjørndal. Thank you for bringing me in the PhD program and guiding me to the interesting research areas. Thank you for always encouraging me to explore interesting topics and giving me timely guidance and valuable suggestions. Thank you for always treating me equally in our discussions. Especially, thank you so much for your patience and consideration when I had to be away from work due to parental leave.

Thanks to my co-supervisor Mette Bjørndal. I have learnt so many things from you. You are so thoughtful and innovative in research. Without your guidance I can hardly imagine that I could finish the thesis with a publication in a quality journal.

But more importantly, I want to thank Mette for always being so considerate for the balance of my work and life. You always supported me when I was temporarily occupied by family-related issues (e.g., giving birth, moving to France, etc). Without that very precious support, many achievements in my life could have been impossible. Also, it is difficult to express how grateful I was when you generously helped me to find a visiting position in UC Berkeley in the third year of my PhD. The visiting year was extremely useful in broadening my horizons and was also a wonderful experience for my family.

Thanks to Pär Holmberg for being my dissertation committee member and providing very useful comments for the papers. Thank you for your extremely timely responses. I really appreciate.

Thanks to Norway and NHH. Studying for my Master and PhD in Norway changed my life and my life attitude. Without the Norwegian system, many wonderful things in my life would be impossible. Thanks to the Management Science Department, especially to Kurt

Jörnsten, Leif Sandal, Gunnar Eskeland, Stein Wallace, and Mario Guajardo, for your kindness and generous support.

Special thanks to Professor Ingolf Ståhl. It was so lucky that I took your course and got to know you during my master. I enjoy so much working with and learning from you. I remember that when I was in Norway, every year I was looking forward to your visit and talking to you. I really appreciate your kind support.

I want to thank Professor Shmuel Oren for coordinating my Berkeley visit and for your valuable comments on my work. I want to thank Professor Friedrich Kunz and Professor Anthony Papavasiliou, for your valuable comments and suggestions.

Thanks to my wonderful coauthor, friend, and "the Greek brother", Vangelis Panos. It was an extremely good experience working with you.

Thanks to my dear friends: Jenny and Stein, Xiaojia, Somayeh, Xinlu, Xiaoyu, Xiaomei, Guangzhi, Chunbo, Xunhua, Kiki and Trond, Kristina (Kiki), Yan, Chi, Meijuan, Jie, Xiaojing, Yushan, Zhongjia, Yizi, Weina and Xujun,

Special thanks to Professor Ole-Kristian Hope, the special one.

I dedicate this dissertation to my family, especially my uncle and aunt, my Grandma in-Law, and my Uncle and Aunt in-Law.

Chapter 1: Introduction

Over the last two decades Europe's energy policy has emphasized three main objectives. That is, energy in the European Union should be affordable and competitively priced, environmentally sustainable and secure for everybody. Under this circumstance, it is expected that a well-integrated internal energy market is a prerequisite to achieve these objectives in a cost-effective way. In 2011 the European Council set a clear deadline for the completion of an internal energy market by 2014, underlining that no EU Member State should remain isolated from the European gas and electricity networks after 2015.

Europe launched the Price Coupling of Regions (PCR) project, which aims at enhancing power exchange between different countries and creating a single European day-ahead market (EIRGRID, 2013). The project requires that fair and transparent determination of day-ahead electricity prices and trading volume of a bidding area across Europe could be given by using a single auction platform, called EUPHEMIA (acronym of Pan-European Hybrid Electricity Market Integration Algorithm). Now the project currently involves seven power exchanges (PXs), including EPEX SPOT, GME, Nord Pool, OMIE, OPCOM, OTE and TGE; PCR is used to couple the following countries: Austria, Belgium, Czech Republic, Denmark, Estonia, Finland, France, Germany, Hungary, Italy, Latvia, Lithuania, Luxembourg, the Netherlands, Norway, Poland, Portugal, Romania, Slovakia, Slovenia, Spain, Sweden and UK, i.e., about 75 % of European power consumption.

A larger connected area helps to secure the network reliability. In the European Union (28 countries), the share of energy from renewable sources in gross final consumption of energy steadily increased from 8.5 % in 2004 to 16.7 % in 2015. EU has set a target that 20% of the energy consumption is from renewable sources by 2020 and a more ambitious renewables target for 2030. The Commission has proposed to set such an EU-wide target of at least 27%. However, the variability and limited predictability of solar and wind power has challenged the current power systems. For instance, due to the effect of loop flow, countries that are close to wind farms might greatly suffer from unscheduled power exchange in the windy days. The Polish and Czech network operators claimed that unscheduled cross-border flows from wind generation in Germany overloaded their transmission networks more frequently, making their grids less stable and secure (Kunz, 2012).

The integration of the internal power market and the promotion of renewables in EU have greatly challenged the market design. One of the most important issues is how to price the electricity properly and handle cross-border power transfer. The four papers in this dissertation focus mainly on different congestion management methods applied in the European electricity day-ahead market and their economic consequences.

In "Nodal Pricing in a Coupled Electricity Market," [1]I investigate a market clearing model with a hybrid congestion management method, i.e. part of the system applies a nodal pricing scheme while the rest applies a zonal pricing scheme, and I test the model on a 13-node power system. Full nodal pricing is considered to better address network congestion than full zonal pricing. Within the area that is applying nodal pricing, prices and surpluses given by the hybrid pricing model match well with those given by the full nodal pricing model. However, due to the loop flow effect in the zonal pricing area, the prices given by the hybrid system may send wrong economic signals, which trigger unnecessary generation from existing capacities, exacerbate grid congestion, and induce higher re-dispatch costs.

In the European market, the promotion of wind power leads to more network congestion. Zonal pricing, which is the most commonly used method to relieve congestion in Europe, fails to provide adequate locational price signals regarding the energy resource scarcity and thus creates a large amount of unscheduled cross-border flows originating from wind-generated power, making the interconnected grid less secure. In "Hybrid

[1] The paper has been published at the *11th International Conference on the European Energy Market (EEM14)*, Krakow and was nominated for the best paper reward.

Pricing in a Coupled European Power Market with More Wind Power,”[2] I further investigate with more wind power, how nodal pricing works in a hybrid congestion management model, i.e. nodal pricing model for one country embedded in a zonal pricing system for the rest of the market, especially when we take the effects of re-dispatch into account. We find that, compared to full nodal pricing, hybrid pricing fails to fully utilize all the resources in the network and some wrong price signals might be given. However, hybrid pricing still performs better than zonal pricing. The results from the hybrid pricing model of Poland, Germany, Slovakia and the Czech Republic show that, within the area applying nodal pricing (Poland), better price signals are given; the need for re-dispatching reduces; more congestion rent is collected and the unit cost of power is reduced. The results also show that international power exchange increases between the nodal pricing area and the zonal pricing areas, especially on windy days. Moreover, the nodal pricing area has less unscheduled cross-border power flow from the zonal pricing area entering its network and collects more cross-border congestion rent.

In order to better monitor the power flow in an integrated European market, a so called “Flow-Based methodology” Market Coupling (FBMC) was developed by the European TSOs. In May 2015, the FBMC model replaced the zonal pricing model in Central Western Europe to determine the power transfer between countries (price areas). The FBMC model is expected to lead to increased social welfare in the day-ahead market and more frequent price convergence between different market zones. “Efficiency of the Flow-Based Market Coupling Model in the European Market” gives a discussion of the mathematical formulation of the FBMC model and the procedures of market clearing. I further examine the FBMC model in two test systems and show the difficulties in implementing the model in practice. I also find that a higher social surplus in the day-ahead market might come at the cost of more re-dispatching. We also find that the FBMC model might fail to relieve network congestion and to better utilize the

[2] The paper has been accepted by European Journal of Operational Research, Volume 264, Issue 3, 2018, Pages 919-931, ISSN 0377-2217, https://doi.org/10.1016/j.ejor.2017.06.048.

resources even when compared to the ATC model.

The FBMC model does not need to determine the maximum trading volume between two bidding zones before the marketing clearing. Compared to the zonal pricing model, it might be easier to change the bidding zone configuration in the FBMC model. “The Flow-Based Market Coupling Model and the Bidding Zone Configuration” runs a simulation in the IEEE RTS 24-bus test system and examines how the bidding zone configurations affect the performance of both the FBMC and ATC models. We show that by improving the zone configuration, the FBMC model outperform the ATC in terms of reducing the re-dispatch cost only when the systems operators have a higher level of cooperation in the real time market.

Reference

[1] EIRGRID. "Price Coupling of Regions (PCR) initiative and the North West Europe (NWE) project." *EIRGRID* (2013).

http://www.eirgrid.com/media/PCR_NWE_MO_TSO_Review.pdf

[2] Kunz, Friedrich. "Managing Congestion and Intermittent Renewable Generation in Liberalized Electricity Markets." *Dissertation* (2012).

Chapter 2: Nodal Pricing in a Coupled Electricity Market

Nodal Pricing in a Coupled Electricity Market

Endre Bjørndal, Mette Bjørndal, Hong Cai
Department of Business and Management Science
Norwegian School of Economics
Bergen, Norway
Endre.Bjorndal@nhh.no, Mette.Bjorndal@nhh.no, Hong.Cai@nhh.no

***Abstract*—This paper investigates a pricing model for an electricity market with a hybrid congestion management method, i.e. part of the system applies a nodal pricing scheme and the rest applies a zonal pricing scheme. The model clears the zonal and nodal pricing areas simultaneously. The nodal pricing area is affected by the changes in the zonal pricing area since it is directly connected to the zonal pricing area by commercial trading. The model is tested on a 13-node power system. Within the area that is applying nodal pricing, prices and surpluses given by the hybrid pricing model match well with those given by the full nodal pricing model. Part of the network is better utilized compared to the solutions given by the full zonal pricing model. However, the prices given by the hybrid system may send wrong economic signals which triggers unnecessary generation from existing capacities, exacerbates grid congestion, and induces higher re-dispatching costs.**

***Index Terms*—Congestion Management; Nodal Pricing; Zonal Pricing; Electricity Market.**

1. Nomenclature

Sets and Indices

N	Set of nodes
N^{Nodal}	Set of nodes in the nodal pricing area
L	Set of lines
L^{DC}	Set of DC lines
Z	Set of independent price areas
N^{Z}	Subset of nodes included in the price area z Î Z

Parameters Set and Indices

H_{ij}	Admittance of the line between the nodes i and j
CAP_{ij}	Thermal capacity limit of the line from i to j
CAP_{xz}	Upper limit on the flows from zone x to zone z
$p_i^s(q)$	Supply bid curve at node i
$p_i^d(q)$	Demand bid curve at node i

Variables

q_i^s	Generation quantity (MWh/h) at node i
q_i^d	Load quantity (MWh/h) at node i
f_{ij}	Load flow from node i to node j
q_i	Phase angle at node i

2. Introduction

In the European spot markets, zonal pricing is the most commonly used method to relieve grid congestion. Zonal pricing applies merit order to dispatch power from one location to another. It is a commercial pricing scheme which only to a limited extent takes physical laws and technical facts into account. A possible consequence of this is that there could be insufficient capacities in the network to transmit the contracted power, which requires the system operator to adjust the generation and consumption in order to change the physical flows in the network and to mitigate congestion [5]. Furthermore, zonal pricing gives a uniform price within each pricing area and thus does not provide sufficient price signals to market participants regarding scarce transmission capacity. In contrast, nodal pricing, which is first discussed by [7], gives the optimal value for each location and produces feasible flows within the network, and is considered to give clearer market signals [4].

Some European countries are considering adopting nodal pricing systems. For instance, Poland has prepared to implement nodal pricing since 2010 and the whole implementation is expected to be finished in 2015 [8]. However, as the Polish power grid is connected to other continental countries, it is inevitable to be affected by (and affect) flows from other areas. It is thus a research question whether nodal pricing in such a case can still work as efficiently as it is supposed to do.

In this paper, we first propose a hybrid pricing model, which could be applied to a joint power market, in which the market is divided into different sub-systems, where some apply nodal pricing and others apply zonal pricing. It is important to note that a nodal pricing sub-system is not isolated from the other parts of the system and still has commercial trading with the connected zonal pricing sub-systems. In such a case, generation or consumption changes in the zonal pricing areas could still have an effect on the nodal pricing area because of the impact of loop flows. A 13-node power system serves to illustrate the hybrid pricing model. We compare the hybrid pricing scheme to the zonal and nodal pricing schemes to investigate how much a single pricing area can gain by applying nodal pricing in the context where its neighborhood areas apply zonal pricing.

The congestion management methods discussed in this paper, i.e., nodal pricing, zonal pricing, and hybrid pricing, are based on centralized optimization subject to the power flow control method chosen by the system operator to relieve grid congestion. The description of the models is provided in Section II. Section III gives a numerical example and compares attained results for different pricing schemes. Some preliminary conclusions are given in Section IV.

3. Model

The power market consists of two types of pricing areas, i.e., the nodal pricing and zonal pricing areas. The objective of the system is to maximize the social welfare (1), considering different network constraints ((2)-(5)). Equation (1) is the objective function, expressing the difference between the customers' willingness to pay and the production cost. The difference is defined as social welfare.

$$\max_{q^d, q^s, f, \theta} \sum_{i \in N} \left[\int_0^{q_i^d} p_i^d(q)dq - \int_0^{q_i^s} p_i^s(q)dq \right] \quad (1)$$

$$q_i^s - q_i^d = \sum_{j:(i,j)\in L} f_{ij} - \sum_{j:(j,i)\in L} f_{ji}, \forall i \in N \quad (2)$$

$$f_{ij} = H_{ij}(\theta_i - \theta_j), (i,j) \in l \setminus L^{DC}, \forall i,j \in N^{Nodal} \quad (3)$$

$$-CAP_{ji} \le f_{ij} \le CAP_{ij}, \forall i,j \in N^{Nodal} \quad (4)$$

$$-CAP_{zx} \le \sum_{\substack{(i,j)\in L \\ i\in N^x \\ j \in N^z}} f_{ij} - \sum_{\substack{(i,j)\in L \\ j\in N^x \\ i \in N^z}} f_{ji} \le CAP_{xz} \quad (5)$$

In the nodal pricing area, the DC approximation [9] is used to approximate the power flow. The DC approximation gives much faster solution than the full alternating current (AC) solution, and the results given by the DC approximation match fairly well with the full AC solution [6]. The network flows in the nodal pricing areas are constrained by (2) to (4). Equation 2 is the energy balance equation, ensuring the difference of supply q_i^s and demand q_i^d at node *i* is equal to the difference of the power which is transported from (f_{ij}) and to (f_{ji}) node *i*. Equation (3) is the loop flow law, which determines the power flow f_{ij} on a transmission line by the admittances H_{ij} of the line and the difference of load angles (q_i - q_j) of its two connected points. Equation (3) also introduces a set for high voltage direct current (HVDC) transmission lines, L^{DC} . This set does not follow the loop flow law because flows on HVDC lines can be treated as controllable. Power flows on transmission lines are restricted by the thermal capacity limits CAP_{ij} (4). Flows within the nodal pricing area are physically feasible and thus are called physical flows. Physical flows could go from a high price node to a low price node, because of the loop flow constraints.

Within each zonal pricing area, there are no restrictions on the physical flows, i.e. loop rule and thermal capacity limits. Therefore, power will always go from a low price node to a high price node until prices for all nodes are the same, i.e., there are no opportunities to buy power from a lower price node. These flows are not necessarily feasible because they only take the economic but not physical restrictions into account. We refer to such flows as commercial flows. The networks in the zonal pricing areas are constrained by the energy balance equations (2) and aggregate capacity limits CAP_{xz} are used to restrict inter-zonal trading between two connected pricing areas x and z (5). This creates price differences among zones.

As the zonal pricing model does not include the loop flow law (3), the model does not give solutions for the phase angle variables q_i . Hence, flows on the lines connecting the zonal pricing areas and the nodal pricing areas cannot be modeled taking into account the physical law (3). That is, traded flows between the different pricing areas have to be treated as commercial flows. Therefore nodes in a nodal pricing area connected to a zonal pricing area are constrained by both the physical power exchange within the nodal pricing area and the commercial exchange within the zonal pricing area. Trading between the zonal and nodal pricing markets is also restricted by aggregate capacity limits (5), which is the same as in a full zonal pricing market (i.e., the whole network applies zonal pricing).

The dual variables of (2), which are the marginal costs/benefits of increasing injections in the nodes by one unit, are the nodal prices. Prices within each zonal pricing area are uniform as there are no restrictions on the intra-zonal trading. However, prices within the nodal pricing areas could be different, as the model takes both the physical laws and thermal capacity limits into account.

4. Numerical Example

A. Data

[3] uses a strongly simplified and rather aggregated model of the Nordic power market with different load scenarios to investigate the possibility of improving the capacity utilization of the transmission grid by varying the zone definitions. We choose this power system as an example for our analysis. Fig. 2-1 exhibits the topology and the zone definition of this power market.

There are in total 13 nodes in this system. Nodes 1 to 5 are within Norway (NO) and Nodes 6 to 10 are within Sweden (SE). Node 11 represents Finland (FI) and Node 12 and Node 13 represent Denmark (DK). This power market is decomposed into 4 zones according to their jurisdictions. There are in total 21 lines in the model and most of them are AC interconnections, except for Lines 1-13, 10-13, and 9-11, corresponding to HVDC cables. All the lines are assumed to have identical admittances.

This power system and its corresponding data are used as a starting point for examining the hybrid pricing method. We assume in the hybrid model that zone NO applies nodal pricing and that the rest use area prices.

B. Aggregate capacity limits

Aggregate capacity limits are used to restrict commercial trading

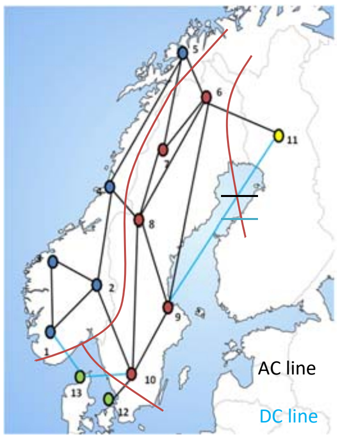

Fig. 2-1: Topology

between different pricing areas. In practice, setting adequate aggregate capacity limits is a challenging task because low limits would fail to fully use the network capacity while high ones could cause lots of congestion within a pricing area. In our analysis, we use the flows given by the full nodal pricing solution, i.e., where the whole network applies nodal pricing, as a basis to set the aggregate capacity limits. The limits are equal to the absolute value of accumulated flows between two pricing areas given by the nodal pricing solution.[1] The main reason for setting aggregate capacity limits in such a way is that the nodal pricing solution could be regarded as the optimal benchmark as it takes both the physical and economic constraints into account. These limits could be considered to optimize the utilization of the network given perfect information. Furthermore, this setting makes all the three pricing mechanisms (i.e., nodal pricing, zonal pricing, and hybrid pricing) comparable, because the traded volumes between two pricing areas are the same. When there is a price difference between two nodes connecting two different pricing areas, trading will continue until the price difference is eliminated or the aggregate capacity limit is reached. Note however that the actual flows resulting from the zonal and hybrid market clearings may still be infeasible.

We also assume that the aggregate capacity limits between two price areas are the same in both directions. For instance, the aggregate capacity limits from Norway to Sweden are equal to those from Sweden to Norway.

C. Some results from a high load scenario

Since congestion is likely to happen when demand is high, we choose a high demand hour for the following analyses. The total consumption volume given by the full nodal pricing solution is approximately 86% of the consumption prognosis at "10 years" winter temperature [1]. Data on the model and supply and demand information[2] are presented in the appendix.

Prices

Fig. 2-2 gives the prices at each node in different congestion management schemes. Prices within the zonal pricing market (Nodes 6 to 13) given by the hybrid pricing solution are identical to those given by the zonal pricing solution. This shows that if the aggregate capacity limits remain the same and the same proportion of the aggregate capacity limits is used, the prices within the zonal pricing market will not be affected by the congestion management scheme in the nodal pricing market.

The comparison between the prices in the nodal part of the hybrid system (i.e., Nodes 1 to 5) and the nodal prices for the whole system generates some interesting observations. In general, the two series of prices, presented in Fig. 2-2, match fairly well, with a notable exception for Node 5. At Node 5 the price given by the hybrid system is 132.5 NOK, while the full nodal price is only 91.6 NOK.

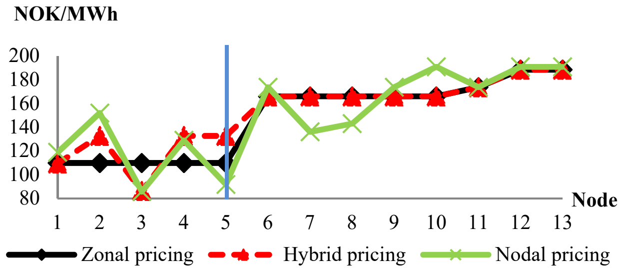

Fig. 2-2: Prices in different congestion management schemes

The reason for the high price at Node 5 in the hybrid system is that the three nodes that are directly connected with Sweden (i.e., Nodes 2, 4 and 5) face high demands from Sweden. In the hybrid system, the prices at these three points are set to be identical because flows going from these nodes to Sweden are modeled as direct flows without considering physical restrictions (i.e., the loop flow law).

As long as the thermal capacity of the lines connecting these three nodes to the zonal pricing area has not been fully used, i.e., there is no congestion in these lines, the prices at the three nodes should be equal. Otherwise, Sweden could always choose to buy power from the node with the lowest price, since the zonal pricing model does not take the laws of physics entirely into account. Therefore, Node 5 in the hybrid system gets a price as high as those at Nodes 2 and 4.

Fully loaded and overloaded lines

Physical flows[3] given by the zonal pricing scheme might not be feasible because it does not take scarce transmission capacity and the laws of physics into account. In the hybrid pricing model, the physical constraints are modeled for only parts of the system, so that there can still be infeasible flows in the zonal pricing area. Furthermore, areas applying nodal pricing are connected to other AC network areas applying zonal pricing, and could be affected by the loop flows in such areas. Investigating the capacity utilization of a transmission line, which is defined as the ratio of the physical flow to thermal capacity, helps to explain the reason why the price at Node 5 in the hybrid system is higher than the one in the nodal pricing system.

In the full nodal system, Nodes 2, 4 and 5 also face high demand from Sweden. Nodes 2 and 4 are indeed given high prices because of this. In comparison, the price at Node 5 is much lower, because Line 5-6 is fully-loaded. Fig. 2-3 displays

---

[1] For instance, the transfer capacity from Norway to Sweden is calculated as $CAP_{NO,SE} = \sum_{\substack{(i,j)\in L \\ i\in N^{NO} \\ j\in N^{SE}}} f_{ij}^* - \sum_{\substack{(i,j)\in L \\ j\in N^{NO} \\ i\in N^{SE}}} f_{ji}^*$, where f_{ij}^* and f_{ji}^* are solutions given by nodal pricing model.

[2] Formats of Supply and demand curves are displayed in Fig. A1. The corresponding data for parameters can be founded in Table AI and Table AII.

[3] To calculate the physical power flows of the zonal and hybrid pricing solution, we fix the values of nodal load q_i^d, generation q_i^s and flows over the DC lines f_{ij} $(\mathrm{where}(i,j) \in L^{DC})$ using the solutions given by the models. We use these values as inputs for a detailed network model to re-compute the final line flows. This network model takes loop flow into consideration ((2) to (3)), minimizes the losses caused by dispatching, but does not consider thermal capacity constraints (4). Thus we obtain the power flows that will result from injections and withdrawals in the nodes given by the zonal and hybrid pricing solutions.

the overloaded and fully loaded lines regarding these three different congestion management schemes. Congestion in Line 5-6 makes it impossible to transmit more power generated at this node to other areas, so the extra generation has significantly less value. In other words, low generation cost is not the only reason for the low price at Node 5. More importantly, the low price is due to the congestion which limits the power to be supplied to other areas. Without the congestion, production at Node 5 will be higher and at a higher marginal cost, implying a higher nodal price.

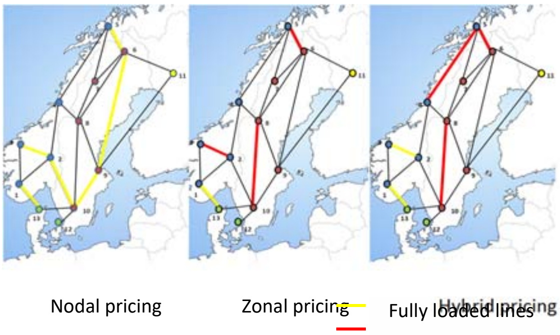

Consequently, the high price at Node 5 in the hybrid system gives wrong economic signals, which may cause short term and long term problems. First, more power will be generated by the existing generation capacity. This extra generation is unnecessary, because it cannot be transmitted to other areas due to the capacity constraint. Second, more generation will exacerbate congestion in those lines connecting Node 5 and other nodes. Note that Line 5-6 is fully loaded in the full nodal price solution. In the hybrid system, however, it becomes overloaded. Line 4-5 also becomes overloaded, despite it being within limits in the full nodal and zonal price solutions. Finally, the situation may worsen if the high price triggers more investments in generation capacity. Extra generation capacity in this area is unnecessary, and it will only intensify grid congestion. The extra congestion must be solved by re-dispatching, which leads to increased cost because the system uses more costly power in re-dispatching.

As discussed before, the nodal pricing area can be affected by the changes in the zonal pricing area. Therefore, there can also be infeasible flows in the nodal pricing area. As in Fig. 2-3, compared to the zonal pricing scheme, congestion in Line 2-3 is alleviated in the hybrid pricing scheme. However, congestion happens in Lines 5-6 and 4-5, even if the flow on Line 4-5 is feasible in the zonal pricing scheme. This can be explained by the previous discussion regarding the high generation at Node 5. Increased generation at Node 5 causes both Line 5-6 and Line 4-5 to be overloaded.

Table summarizes the traded volumes between different pricing areas for all three pricing schemes. Traded volumes between the nodal pricing area (Nodes 1-5) and other pricing areas are the same for all three mechanisms. However, the zonal pricing and hybrid pricing schemes fail to optimally utilize the existing network.

We notice that in the full nodal pricing model, the price at Node 7 in zone SE is relatively low, which creates counter flows going from Node 7 to Nodes 5 and 6. The counter flows alleviate the congestion in Line 5-6 and Line 4-5. However, the full zonal pricing or hybrid pricing models do not give clear price signals at Node 7 to reflect its cost competitiveness. Furthermore, prices in Norway are much lower than those in other pricing areas, so there will not be counter flows in the zonal and hybrid system to relieve congestion.

Table 2-1: Traded volumes between pricing areas (Unit: MWh)

		Zonal pricing	Nodal pricing	Hybrid pricing
1 to 5 (NO)[a]	6 to 10 (SE)	2804	2804	2804
1 to 5 (NO)	12 to 13(DK)	1000	1000	1000
6 to 10 (SE)	11 (FI)	219	219	219
12 to 13(DK)	6 to 10 (SE)		31[b]	

a. NO is the area applying nodal pricing while SE, DK, FI are the pricing areas applying zonal pricing.

b. Among Node 10, 12 and 13, Node 13 has the lowest price. However, this fact is not known in either the zonal or the hybrid pricing schemes. Therefore, there will not be flow going from DK to SE.

Nodal pricing in a hybrid pricing context could help to relieve grid congestion to a certain extent. However, we find that it could also intensify the grid congestion. For instance, in Lines 4-5, 5-6 and 8-10, the utilization rates all increase compared to those given by the zonal pricing scheme. This example also shows that congestion not only becomes worse in the area applying nodal pricing (Line 4-5, from 98% to 107%), and on the cross border links (Line 5-6, from 130% to 140%), but also in the area applying zonal pricing (Line 8-10, from 108% to 110%). Increased congestion in these lines could increase cost associated with re-dispatching.

Table 2-2: Utilization rate of overloaded lines for different pricing schemes

	Zonal pricing	Nodal pricing	Hybrid pricing
Line 2-4	114%	100%	100%
Line 4-5	98%	71%	107%
Line 5-6	130%	100%	140%
Line 8-10	108%	100%	110%

In conclusion, the wrong price signal given at Node 5 and the corresponding increased congestion is the result of two factors. First, the flows over the cross-border lines between the nodal pricing and zonal pricing areas cannot be modeled taking into account the full power flow laws. Second, one of the lines connecting Node 5 and the zonal pricing area (i.e., Line 5-6) is the bottleneck of the whole system. The two factors together lead to the wrong price signal at Node 5. These results highlight the importance of the interface between the nodal pricing and zonal pricing areas in the design of the hybrid pricing system.

Surplus

Table 2-3 summarizes the social surpluses and grid revenue in different pricing solutions. The total surpluses are not directly comparable because the flows in the zonal and hybrid solutions in general are infeasible and re-dispatching costs are not addressed. However, the different surpluses reflect that the zonal pricing area is affected by the pricing scheme in the nodal pricing area. Within the zonal part of the hybrid system, i.e., Nodes 6 to 13, the consumer and producer surpluses are identical to the zonal price solution, but the grid revenue decreases. As the zonal pricing area has the more expensive power sources in this case, it is always willing to import power from the nodal price area. Given the same traded volumes, the average price to import power from the nodal price area increases greatly from 109.7 in the zonal pricing scheme to 132.5 in the hybrid pricing scheme. This reduces the grid revenue obtained by the zonal pricing area from 120 to 88.

Table 2-3: Surpluses differences (Unit: 1000 NOK)

	Nodes 1 to 5 (Nodal pricing area, i.e., NO)			
	Producers	***Consumers***	***Grid***[a]	***Sum***
Zonal pricing	1501	19301	118	20920
Hybrid pricing	1588	19064	282	20934
Nodal pricing	1638	18931	393	20963
	Nodes 6 to 13 (Zonal pricing areas, i.e., SE,DK and FI)			
Zonal pricing	4237	38912	120	43268
Hybrid pricing	4237	38912	88	43236
Nodal pricing	4220	38708	257	43185

a. Also referred to merchandizing surplus (MS) (see [9]). The mathematical formulation for MS of an area is $MS = \sum_i p_i q_i = \sum_i \sum_j (p_j - p_i) f_{ij}$. Revenues from cross-border commercial trading are equally shared by the two system operators.

Meanwhile, the grid revenue for the nodal pricing area (i.e., Nodes 1 to 5) is greatly improved from 118 to 282. The total social welfare in the hybrid pricing scheme increases slightly by 14 compared to the zonal pricing scheme. The increase in grid revenue comes at the expense of a reduction in consumer surplus. The decrease in consumer surplus is associated with a decrease in consumption in Norway, as displayed in Table 2-4. This means that the nodal pricing part of the hybrid model reallocates the producer surpluses, consumer surpluses and grid revenue compared to the zonal pricing model. The surpluses of the hybrid solution are becoming closer to those given by the full nodal system.

Table 2-4: Production and consumption

	Zonal pricing		**Nodal pricing**		**Hybrid pricing**	
	Production	***Consumption***	***Production***	***Consumption***	***Production***	***Consumption***
NO	24225	20421	24026	20223	24098	20294
SE	21583	24168	21448	24064	21583	24168
FI	11958	12177	11958	12177	11958	12177
DK	5212	6212	5234	6203	5212	6212

5. Conclusion

This paper presents a model with hybrid congestion management methods for a hypothetical joint market and tests it in a 13-node power system. Results show that the hybrid pricing model works well in such a context, using the full nodal pricing solution as a benchmark. However, when cross-border lines happen to be the bottlenecks of the whole system, the hybrid pricing model may give wrong price signals for the nodes connecting such lines and trigger more congestion. The results highlight the importance of the interface between the nodal pricing and zonal pricing areas in the design of the hybrid pricing system.

Acknowledgment

The authors thank Stein. W. Wallace, Evangelos Panos for their comments and help on this paper.

References

[3] Bjørndal, Mette, and Kurt Jörnsten, "Benefits from coordinating congestion management — The Nordic power market." *Energy policy* 35, no. 3 (2007): 1978-1991.

[4] Hogan, William W. "Contract networks for electric power transmission." *Journal of Regulatory Economics* 4, no. 3 (1992): 211-242.

[5] Kunz, Friedrich. "Managing Congestion and Intermittent Renewable Generation in Liberalized Electricity Markets." Ph.D. dissertation, Technische Universität Dresden, 2012 .

[6] Overbye, Thomas J., Xu Cheng, and Yan Sun. "A comparison of the AC and DC power flow models for LMP calculations." In System Sciences, 2004. *Proceedings of the 37th Annual Hawaii International Conference* on, pp. 9-pp. IEEE, 2004.

[7] Schweppe, Fred C., Richard D. Tabors, M. C. Caraminis, and Roger E. Bohn. "Spot pricing of electricity." (1988).

[8] Sikorski, Tomasz. "Nodal pricing project in Poland." *34th IAEE International Conference*, Institutions. Efficiency and Evolving Energy Technologies. Stockholm. 21June. 2011.

[9] Wu, Felix, Pravin Varaiya, Pablo Spiller, and Shmuel Oren. "Folk theorems on transmission access: Proofs and counter examples." *Journal of Regulatory Economics* 10, no. 1 (1996): 5-23.

Appendix

Table AI: Line capacity

Line	Lower limit	Upper limit	Line	Lower limit	Upper limit
1-2	2000.0	2000.0	6-7	16500.0	16500.0
1-3	16500.0	16500.0	6-8	16500.0	16500.0
1-13	1000.0	1000.0	6-9	2000.0	2000.0
2-3	2800.0	2800.0	6-11	1500.0	900.0
2-4	800.0	800.0	7-8	16500.0	16500.0
2-10	2000.0	2000.0	8-9	2000.0	2000.0
4-5	400.0	400.0	8-10	2000.0	2000.0
4-8	600.0	600.0	9-10	2000.0	2000.0
5-6	400.0	400.0	9-11	550.0	550.0
5-7	400.0	400.0	10-12	1300.0	1700.0
			10-13	670.0	640.0

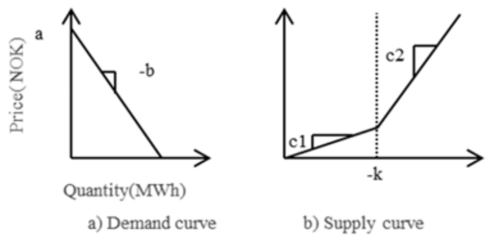

Fig. A1: Supply and demand Curves

Table AII: Parameters for bidding curves at nodes

Node	Demand		Supply		
	a	***b***	***c1***	***c2***	***K***
1	2000	0.88	0.025	0.15	3600
2	2000	0.2	0.016	0.09	5500
3	2000	0.5	0.011	0.1	9000
4	2000	0.5	0.023	0.25	4400
5	2000	1.5	0.05	0.25	2000
6	2000	1.7	0.04	0.2	2500
7	2000	1.7	0.04	0.2	2500
8	2000	0.5	0.02	0.1	5000
9	2000	0.2	0.018	0.2	5500
10	2000	0.2	0.025	0.15	3600
11	2000	0.15	0.011	0.035	10,000
12	2000	0.7	0.047	0.22	1910
13	2000	0.5	0.047	0.22	2545

Chapter 3: Hybrid Pricing in a Coupled European Power Market with More Wind Power

Hybrid Pricing in a Coupled European Power Market with More Wind Power

Endre Bjørndal[§], Mette Bjørndal[§], Hong Cai[§‡], Evangelos Panos[†]

Abstract: In the European electricity market, the promotion of wind power leads to more network congestion. Zonal pricing (market coupling), which does not take the physical characteristics of transmission into account, is the most commonly used method to relieve network congestion in Europe. However, zonal pricing fails to provide adequate locational price signals regarding scarcity of energy and thus creates a large amount of unscheduled cross-border flows originating from wind-generated power. In this paper, we investigate the effects of applying a hybrid congestion management model, i.e. a nodal pricing model for one country embedded in a zonal pricing system for the rest of the market. We find that, compared to full nodal pricing, hybrid pricing fails to fully utilize all the resources in the network and some wrong price signals might be given. However, hybrid pricing still outperforms zonal pricing. The results from the study cases show that, within the area applying nodal pricing, better price signals are given; the need for re-dispatching is reduced; more congestion rent is collected domestically and the unit cost of power is reduced.

Keywords: OR in energy, nodal pricing, zonal pricing, re-dispatching, renewable energy

1. Introduction

Power markets constitute an interesting and important application area where concepts from economic theory, like welfare optimization, is implemented by explicit optimization of market outcomes based on bids for generation and demand and a

---

We are grateful for help and comments from Xiaojia Guo, Friedrich Kunz, Shmuel S. Oren, Stein W. Wallace, seminar participants at UC Berkeley, and conference participants at INFORMS Annual Meeting 2014 in San Francisco.

[§]Norwegian School of Economics, Helleveien 30, 5045 Bergen, Norway

[‡] Corresponding author, Hong.Cai@nhh.no

[†] Energy Economics Group, PSI, 5232 Villigen PSI, Switzerland

representation of available network resources. Even if the general principles are similar across regions, different power markets have implemented different procedures and algorithms in order to take account of various technical and economic characteristics like hydro scheduling, thermal start-ups, renewable resources, ramping constraints and network flows, giving rise to different optimization problems to be solved in practice, including linear, quadratic, integer and stochastic programs. Even in Europe, under EU rules, there are differences between countries, although market integration, with a joint day-ahead market covering a large fraction of Europe, has progressed rapidly over the last 8-10 years.

One of the main differences between market clearing algorithms is the way they deal with network flows and network constraints. Most power systems are alternating current (AC) and the problem that we ideally would like to solve is an alternating current optimal power flow (ACOPF) problem. This is a difficult problem to solve, due to non-linearities and non-convexities. Thus, in practical applications a direct current (DC) approximation is used to solve DCOPFs, like in the nodal pricing systems in the US, or even simpler network flow approximations, without considering Kirchhoff's loop rules, like in the European zonal pricing models. Network constraints in the presence of new renewable capacity in European power markets is the main topic of this paper.

Efforts to meet the renewable energy target of the Renewable Energy Directive 2009/28/EC have led to a large number of wind capacity installations in EU countries. Promotion of renewable energy sources has challenged the current power system. As wind power requires high upfront capital investment and its operation costs are low, it is placed in the beginning of the merit order curve and has priority access under the current European power network which relies on zonal pricing to handle congestion. Due to the uncertainty of wind generation, excess wind power might lead to grid congestion. Furthermore, the installed wind power plants are usually located in places without sufficient consumption. Therefore, the utilization of wind energy often requires long distance transportation, which creates an extra burden for the network and may exacerbate congestion. The impact of wind energy on network congestion has been observed in the German electricity network, in which huge amounts of power are transported from the northern part, where the main installations of wind turbines are located, to the southern and mid-western parts where the demand is high (Deutscher Bundestag, 2010).

Power grids are connected between European countries, therefore, the effect of wind power is not limited by national borders. The use of zonal pricing (uniform pricing) for congestion management in most of the European countries has made this problem difficult to solve. Within the domestic market, zonal prices are calculated regardless of the constraints imposed by physical laws and the network capacity. International commercial power exchange between two countries is limited by a pre-planned Net Transfer Capacity (NTC) value. Therefore, the scheduled commercial power exchange is not necessarily equal to the real (physical) power exchange. In windy days, due to the effect of loop flow, countries that are close to wind farms might greatly suffer from unscheduled power exchange. For example, the Polish and Czech network operators claim that unscheduled cross-border flows from wind generation in Germany overload their transmission networks more frequently, making their grids less stable and secure (Kunz, 2012). Moreover, Aravena and Papavasiliou (2016) show that a zonal market clearing can undermine system performance by leading to suboptimal commitment of slow generators and creating significant unscheduled flows in day-ahead markets.

In practice, in order to limit the large amount of loop flow caused by wind/solar generation from Germany, Poland uses a very low Net Transfer Capacity (NTC) to reduce the power exchange with Germany. However, a low NTC can only restrict physical power exchange by restricting commercial trading between two connected countries. It cannot prevent the wind-generated power in northern Germany from entering the network because information about the location of power generation within Germany and the detailed network constraints is not used in the day-ahead market. Figure 3-1 shows the unplanned power flows, measured by the differences between the day-ahead scheduled commercial flows and the physical power flows between the

50Hertz area (Germany) and the PSE area (Poland) for the period between January and April 2014[1].

The values of the unplanned power flows mostly range between -300 MW and 1,600 MW, with a maximum of 3,286 MW (end of March) and a minimum of -484 MW (mid-April). In comparison, the two interconnectors between Germany and Poland consist of a northern line with capacity 914 MW and a southern line with capacity 2771 MW (Siewierski, 2011). Compared to the capacity of the interconnectors, the unplanned power flows are substantial, and may lead to serious overloads. The unplanned power flows are expected to increase when wind power capacity increases in northern Germany. This is because demand is located in the south of Germany and Germany is represented by a single price area in the day-ahead market clearing model. This means that there are no constraints on commercial flows within Germany in the day-ahead market. When power is transported from north to south in the real grid, however, due to loop flow, power will also be transmitted along parallel paths in neighboring countries, including Poland. This is part of the unplanned power flows, which may overload the interconnectors between Germany and Poland, but also overload internal transmission lines within Poland. The large magnitudes of unplanned flows shown in Figure 3-1 may indicate that a lower NTC did not help Poland to eliminate the loop flow caused by the wind-generated power from Germany during this period.

[1] With this measure, unplanned power flows may arise both due to the simplified network model in the day-ahead market and because uncertain wind generation and demand have changed from day ahead, causing re-dispatch in real time. Ideally, we would like to distinguish between the two effects, since in this paper, we are more interested in the first. A better measure of unplanned power flows due to the lack of congestion management could be to compare commercial flows including the effects from trades in the intraday markets. Intraday markets are open until close to real time, thus a considerable part of the uncertainty is revealed before they close, and typically intraday markets use the same network model as the day-ahead markets for cross-border and inter-area trades. Unfortunately, however, we have not been able to find data to make this comparison. Although intraday markets increase in importance, so far, volumes traded and the commercial use of interconnectors by intraday markets have been low compared to day-ahead markets (< 10 %), see for instance ACER/CEER (2016).

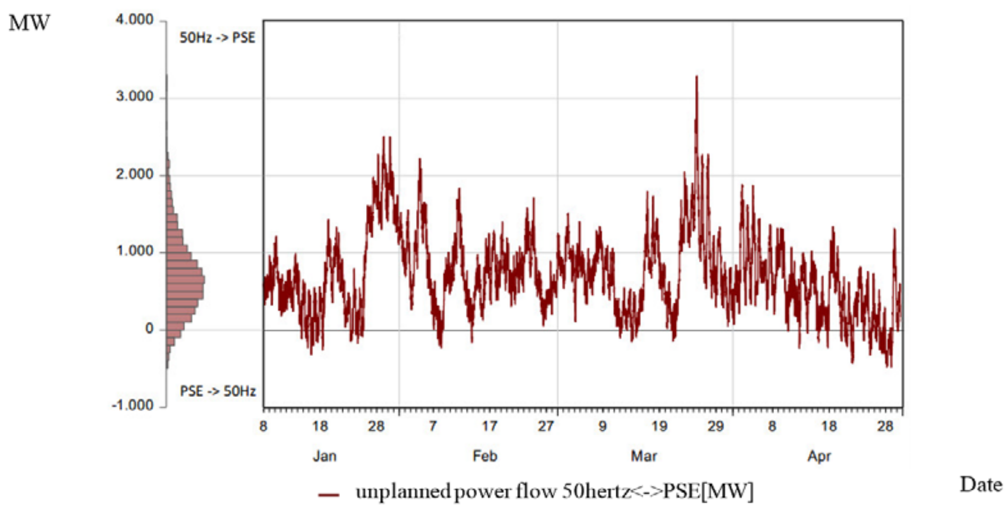

Source: 50Hertz (2014)

Figure 3-1: Unplanned power flows between the 50Hertz area (Germany) and the PSE area (Poland)

In contrast to zonal pricing, nodal pricing gives the value of power for each location by including all the physical and technical constraints (Schweppe et al., 1988). Nodal pricing limits the need for re-dispatching and reduces the corresponding cost. Furthermore, it gives the correct incentives for future investments by reflecting the value of scarce transmission capacity (Hogan, 1992).

Leuthold et al. (2008) have shown that the nodal pricing scheme is economically superior to the zonal pricing scheme for the integration of wind and solar power into the German grid. However, Leuthold et al. (2008) do not examine how intercountry power exchange affects the application of nodal pricing. This question is crucial because Europe has launched a Price Coupling of Regions (PCR) project in order to enhance power exchange among different countries and create a single European day-ahead market (EIRGRID, 2013). This project now involves power exchanges including APX/Belpex, EPEX SPOT, GME, Nord Pool Spot, OMIE, and OTE (NordPool, 2014), which account for more than 75% of European electricity demand. Therefore, applying nodal pricing in a single European country should not ignore the loop flow effect from the other countries.

Bjørndal et al. (2014) investigate a pricing model for an electricity market with a hybrid congestion management method, i.e. part of the system applies the nodal pricing scheme and the rest applies the zonal pricing scheme, and test the model in a 13-node power system. The model determines prices and net transfers for all the involved regions using a joint calculation. Their results indicate that part of the network is better utilized by applying nodal pricing in such a hybrid context. However, due to the influence of the zonal pricing areas, nodal pricing fails to function fully as it is supposed to. They find that wrong price signals are given at nodes (within the nodal pricing area) connected to the zonal pricing area, which might trigger more unplanned power flow.

Poland planned to implement nodal pricing within its domestic market in 2015 (Sikorski, 2011), but the project has been abandoned. For a long time, nodal pricing has been questioned within the European market. One of the main concerns is that nodal pricing might impede market harmonization as it imposes more restrictions (e.g., network capacity constraints) than zonal pricing, and thus could limit power exchange. However, applying zonal pricing might also reduce international power trades, and even to a larger extent, as in practice, NTC capacities are often reduced to very low levels compared to the thermal capacities of the power lines that they represent, see for instance Bjørndal et al. (2012a) and ACER/CEER (2016). Moreover, Sensfuss et al. (2008) argue that the merit-order effect would decrease the day-ahead market prices in Germany as more wind mills are installed, and thus, Germany would reduce its power import.

In our study, we apply the hybrid scheme proposed by Bjørndal et al. (2014) in a joint power market for Poland, Germany, the Czech Republic, and Slovakia. The four countries which are chosen for the study are included in the PCR project. We assume that Poland applies nodal pricing and that the rest of the countries apply zonal pricing. The Polish network is inter-connected with other continental countries, and even if Poland applies nodal pricing, it is still inevitable that the network will be affected by the flows from zonal pricing areas. In our study, we compare the hybrid pricing scheme to the full nodal pricing scheme (i.e., all the four countries apply nodal pricing) and the full zonal pricing scheme (i.e., all the four countries apply zonal pricing). We find that hybrid pricing helps to provide price signals by identifying the power resource scarcity within the Polish market, and that this results in increased international power exchange between Poland and the rest of the countries.

An interesting research question raised by our study is to test whether hybrid pricing can help Poland in integrating its neighboring wind-generated power into the grid when the Polish nodal-pricing market is surrounded by zonal-pricing countries. We investigate a Business-as-Usual (BAU) scenario and a High-Wind-Level (HIGH WIND) scenario for comparison. Specifically, we study the following questions: First, does hybrid pricing perform as well in the HIGH WIND scenario as it does in the BAU scenario in terms of giving correct pricing signals? Second, what is the impact of wind penetration on day-ahead market prices and cross-border power exchange when hybrid pricing is applied? Third, does hybrid pricing affect the physical power exchange?

2. MODEL

The target model for the European day-ahead power market is to simultaneously determine volumes and prices in all relevant zones based on the marginal pricing principle (ACER, 2013). In this paper, we apply the hybrid pricing model in a joint day-ahead market, in which there are two different pricing schemes, i.e., zonal pricing and nodal pricing. Different areas are not isolated from each other and commercial trading is considered regardless of the pricing schemes. This implies that both the day-ahead volumes and later re-dispatch in the zonal pricing areas will affect the nodal pricing areas.

Assumptions regarding the day-ahead market clearing and re-dispatching are briefly illustrated in Figure 3-2. We have a step-wise supply bidding curve which assumes that all the generators bid at their marginal cost. Wind/solar-generated power is placed at the beginning of the supply curve, with very low marginal cost. The system is to maximize social welfare and the day-ahead market clearing price (P*) and quantity (Q*) are determined by the intersection of supply and demand bidding curves. Due to the network constraints, which are not taken into account in the day-ahead market, some of the contracted power cannot be dispatched, and therefore re-dispatching is needed. In the re-dispatching model, we assume that power plants that are re-dispatched downwards would pay their saved marginal cost to the market and power plants that increase their generation in order to satisfy the demand would be compensated by their short-run marginal cost of production. I.e., no economic profit is accruing from the re-dispatching procedure, neither for generation nor load. Increased generation, which replaces the downward dispatched supply, is more expensive and leads to an extra cost, which is shown as the yellow area in Figure 3-2. The model is kept close to the European market design, assuming an energy only market without central coordination of unit commitment. If unit commitment decisions were included in the market clearing, there is a risk of starting the wrong units in the day-ahead market (see the discussion in Aravena and Papavasiliou, 2016) and the re-dispatch cost would be higher. With higher re-dispatch cost, the benefits of nodal pricing should be higher.

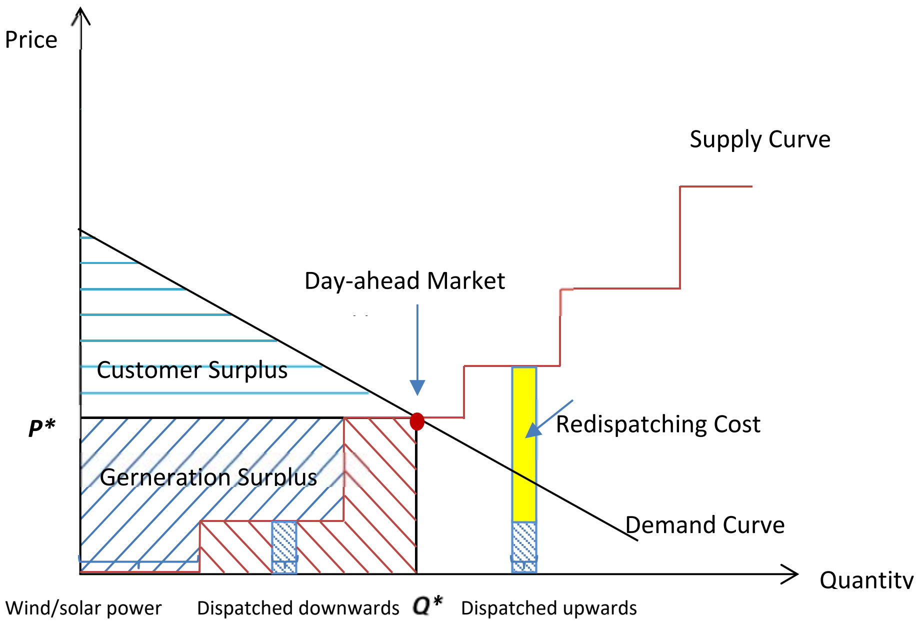

Figure 3-2: Market clearing procedure and re-dispatching (without load/supply shedding)

The complete mathematical formulations of the models used are given below:

Sets

$c \in C$ Set of conventional power plants

C_n	Set of conventional power plants located in node n
C_z	Set of conventional power plants located in zone z
$n, nn \in N$	Set of all nodes
$NODAL$	Set of nodes in the nodal pricing area
$ZONAL$	Set of nodes in the zonal pricing area
$HYBRID$	Set of nodes that are in the nodal pricing area and connected to the zonal pricing area
$l \in L$	Set of all transmission lines
$l \in L\_NODAL$	Set of transmission lines within the nodal pricing area
$z, zz \in Z$	Set of all zones

Parameters

a_n	Intercept of the demand function at node n
$bvector_{n,nn}$	Series susceptance of line n, nn [1/Ω]
$ccur$	Curtailment cost [EUR/MWh]
cg_c	The electricity generation cost for power plant c [EUR/MWh][2]
gda_c	Contracted generation of plant c in the day-ahead market [MW]
$gmax_c$	Maximum generation of plant c [MW]
$gsolar_n$	Solar generation at node n [MW]
$gwind_n$	Wind generation at node n [MW]
m_n	Slope of the demand function at node n
$ntc_{z,zz}$	Net transfer capacity between zone z and zz [MW]
$pmax_{n,nn}$	Thermal transmission limit of transmission line l [MW]
qda_n	Contracted demand at node n in the day-ahead market [MW]

Variables

Δ_n	Voltage angle at node n [rad]
$G_{c,n}$	Generation of plant c located at node n [MW]
GDN_c	Decreased generation of plant c [MW]
GUP_c	Increased generation of plant c [MW]
$LF_{n,nn}$	Power flow between nodes n and nn [MW]

2 The electricity generation cost is composed of two parts (i.e., fuel cost and carbon cost).

$LOADSHED_n$	Load curtailment at node n [MW]
NI_n	Net input at node n [MW]
p_n	Price at node n
Q_n	Demand at node n [MW]
$SOLSHED_n$	Solar power curtailment at node n [MW]
$TF_{n,nn}$	Commercial trade between nodes n and nn [MW]
$WINDSHED_n$	Wind power curtailment at node n [MW]

Details of the nodal pricing and zonal pricing schemes are based on the ELMOD framework described in Leuthold et al. (2012). The full explanation of the model is given below.

2.1. Day-ahead market model[3]

$$\max_{Q,G} \sum_n (a_n * Q_n + 0.5 * m_n * Q_n^2) - \sum_c cg_c * G_c \tag{6}$$

Subject to:

$$NI_n = \sum_{c \in C_n} G_{c,} + gwind_n + gsolar_n - Q_n, \forall n \in NODAL \tag{2.a}$$

$$\sum_{nn} \left(TF_{n,nn} - TF_{nn,n}\right) = \sum_{c \in C_n} G_c + gwind_n + gsolar_n - Q_n, \forall n \in ZONAL \tag{2.b}$$

$$NI_n + \sum_{nn} \left(TF_{n,nn} - TF_{nn,n}\right) = \sum_{c \in C_n} G_c + gwind_n + gsolar_n - Q_n \text{ }, \forall n \in HYBRID \tag{2.c}$$

$$G_c \leq gmax_c, \forall c \in C \tag{3}$$

$$LF_{n,nn} = bvector_{n,nn} \left(\Delta_n - \Delta_{nn}\right), \forall (n, nn) \in L\_NODAL, \forall\, n, nn \in NODAL \tag{4}$$

$$NI_n = \sum_{nn:(n,nn) \in L\_NODAL} LF_{n,nn} - \sum_{nn:(nn,n) \in L_{NODAL}} LF_{nn,n} \text{ }, \forall n \in NODAL \tag{5}$$

---

[3] The model assumes a linear inverse electricity demand function of the form: $p_n(Q_n) = a_n + m_n \cdot Q_n$ at each node n of the network. In the appendix, it is shown how to determine the intercept a_n and slope m_n by using a reference price and demand together with a given demand elasticity. The model maximizes the total social welfare, which is defined as $\sum_n \int_0^{Q_n} p_n(Q_n) d\, Q_n - \sum_c \int_0^{G_c} cg_c(G_c) d\, G_c$. Inserting the linear inverse demand function into the social welfare function, the expression becomes $\sum_n \left[\int_0^{Q_n} (a_n + m_n \cdot Q_n) d\, Q_n\right] - \sum_c \int_0^{G_c} cg_c(G_c) d\, G_c = \sum_n (a_n Q_n + \frac{m_n}{2} Q_n^2) - \sum_c cg_c(G_c)$..

$$-pmax_{n,nn} \leq LF_{n,nn} \leq pmax_{n,nn}, \forall (n, nn) \in L\_NODAL, \forall\ n, nn \in NODAL \qquad (6)$$

$$\Delta_{n'} = 0, n' = slackbus\ in\ the\ nodal\ pricing\ area \qquad (7)$$

$$\sum_{n \in z} \sum_{nn \in zz} TF_{n,nn} \leq ntc_{z,zz}, \forall z, zz \in Z,\ z \neq zz \qquad (8.a)$$

$$\sum_{nn \in z} TF_{n,nn} \leq ntc_{n,z}, \forall n \in HYBRID, z \in Z \qquad (8.b)$$

$$\sum_{nn \in z} TF_{nn,n} \leq ntc_{z,n}, \forall n \in HYBRID, z \in Z \qquad (8.c)$$

$$G_c \geq 0, Q_n \geq 0, TF_{n,nn} \geq 0 \qquad (9)$$

The objective of the day-ahead market model is to maximize social welfare Eq. (1), considering the network constraints. The model distinguishes between nodal pricing and zonal pricing areas.

2.1.1. Nodal pricing area

The areas applying nodal pricing are constrained by energy balance (Eq. (2.a)), maximum generation capacity of thermal power plants (Eq. (3)), and restrictions on power transmission (Eq. (4)-(6)). Energy balance (Eq. (2.a)) ensures that at node n, net input or withdrawal NI_n is equal to the difference between power generation (including all the conventional power generation G_c at node n, wind generation $gwind_n$, and solar generation $gsolar_n$) and nodal demand Q_n . Conventional power generation is restricted by the maximum generation requirement $gmax_c$ (Eq. (3)). The Direct Current approximation (DC) approach (see Chao et al. (2000) and Sauma and Oren (2006)) is used to determine the load flows $LF_{n,nn}$ (Eq. (4)) in each line and the resulting injection or withdrawal NI_n (Eq. (5)) at each node in the nodal pricing area. Eq. (6) limits the absolute physical exchange between system nodes and Eq. (7) is to specify the slack bus.

2.1.2. Zonal pricing areas

In the areas applying zonal pricing, we assume free trading within the domestic market regardless of constraints imposed by physical laws and network capacity. Therefore, trading within a zonal pricing area is only constrained by the energy balance (Eq. (2.b)) and capacity restrictions of power plants (Eq. (3)). The commercial flows between two nodes $TF_{n,nn}$ introduced in Eq. (2.b) will never be directed from a higher price area to a lower price area[4].

2.1.3. Interfaces5

The nodes that are within a nodal pricing area but connected to a zonal pricing area(s) are constrained by both types of pricing schemes (Eq. (2.c)). We assume that the power exchange between such nodes and the zonal pricing area is commercial trading. That is, the flow between a nodal pricing area and a zonal pricing area is not modeled by taking physical laws into account. How to model the interface between the nodal and zonal pricing areas is discussed in Cai (2013).

Commercial transfers between connected pricing areas are limited by NTC-values, which are set by the Transmission System Operator (TSO) before the clearing of the day-ahead market (Eq. (8.a-c))[6]. We assume that commercial trading is limited not only between two connected zonal pricing areas (Eq. (8.a)) but also between a nodal pricing area and its connected zonal pricing areas (Eq. (8.b-c)). NTC values have two directions, i.e., one for importing and another for exporting power from/to other areas. In the full zonal pricing scheme, between two countries, only one direction of NTC values will be used, and power exchange happens only from a lower price area to a higher price area. However, in the hybrid pricing scheme, power exchange could happen in both

---

4 The variable $LF_{n,nn}$ denotes a flow within the nodal pricing area, that is subjected to loop flow constraints. It is positive if the power flow goes from the defined starting point of line l, i.e. from n to nn, and negative otherwise. The variable $TF_{n,nn}$ on the other hand, is required to be non-negative and will not take on positive values in direction from high price to low price, that is $TF_{n,nn} = 0 \; if \; p_n > p_{n,nn}$. The flow $LF_{n,nn}$ however, could go from high price to a low price due to the effect of loop flow in the nodal pricing model.

5 The mathematical formulation allows more than one isolated nodal pricing area.

6 At least two different approaches could be used to formulate the NTC constraints in the full zonal pricing scheme, i.e., the gross approach which sets the gross commercial flows in each direction to be no larger than the pre-defined NTC value (e.g., CASC.EU (2014), Kunz (2012)) and the net approach which sets the net commercial flows in each direction to be no larger than the NTC value (e.g., Bjørndal et al. (2014)). When formulating the NTC constraints between a nodal pricing area and a zonal pricing area, these two approaches might give different results. The gross approach is stricter than the net approach since both directions of the NTC constraints can be binding at the same time. Our formulation corresponds to the gross approach.

directions between a nodal pricing area and a zonal pricing area since the prices in the nodal pricing area are not uniform.

2.2. Re-dispatching model

Because the zonal pricing areas consider only restrictions on inter-zonal transfers, a separate re-dispatching model has to be specified to manage physical congestion within the zones. However, a nodal pricing area is inevitably affected by the zonal pricing areas due to the impact of loop flows. Thus, re-dispatching could be needed in nodal pricing areas as well. The uncertainties regarding supply (wind and solar) and demand are not modeled in this paper, and re-dispatching occurs only due to the physical network constraints that are not taken into account in the day-ahead market.

We assume that the re-dispatch model takes a pay-as-bid approach. Power plants increasing their generation are compensated by their short-run marginal cost of production; power plants decreasing their generation pay their saved marginal costs. In practice, the TSOs may not always find the cheapest available power for the re-dispatch, and thus an even higher re-dispatching cost could occur. We further assume that the TSOs can only access the re-dispatching resources within their own area[7].

Below the formulation of the re-dispatch model is given:

$$min[\sum_c (cg_c * GUP_c - cg_c * GDN_c) + \sum_n ccur * (WINDSHED_n + SOLSHED_n + LOADSHED_n)] \quad (10)$$

Subject to:

$$NI_n = \sum_{c \in C_n} (gda_c + GUP_c - GDN_c) + (gwind_n - WINDSHED_n) + (gsolar_n - SOLSHED_n) - (qda_n - LOADSHED_n), \forall n \in N \quad (11)$$

$$0 \leq gda_c + GUP_c - GDN_c \leq gmax_c, \forall c \in C \quad (12)$$

$$LF_{n,nn} = B_{n,nn} (\Delta_n - \Delta_{nn}), (n, nn) \in l, \forall n, nn \in N \quad (13)$$

[7] See Oggioni and Smeers (2013), Aravena and Papavasiloiu (2016), and Kunz and Zerrahn (2016), which discuss different degrees of coordination among the TSOs in the re-dispatching models.

$$NI_n = \sum_{nn:(n,nn)\in L} LF_{n,nn} - \sum_{nn:(nn,n)\in L} LF_{nn,n}, \forall n \in N \quad (14)$$

$$-pmax_{n,nn} \leq LF_{n,nn} \leq pmax_{n,nn}, \forall (n,nn) \in L, \forall n, nn \in N \quad (15)$$

$$\Delta_{n'} = 0, n' = slackbus \quad (16)$$

$$\sum_{c\in C_z}(GUP_c - GDN_c) = 0, \forall z \in Z \quad (17)$$

$$GUP_c \geq 0, GDN_c \geq 0 \quad (18)$$

The objective is to minimize total re-dispatch costs (Eq. (10)). The generation from the hybrid model can be increased by GUP_c or decreased by GDN_c. To ensure feasibility of the re-dispatch, the model allows for curtailment of load ($LOADSHED_n$) and reduction in renewable generation; solar ($SOLSHED_n$) and wind ($WINDSHED_n$). However, the marginal costs for these alternatives are assumed to be significantly higher ($ccur \gg 0$) than any other marginal generation cost[8].

The dispatch from the day-ahead model is treated as input in the re-dispatch model, which implies that both demand $\mathrm{Q_n}$ and generation $\mathrm{G_c}$ are now given and represented in the re-dispatch model by the parameters $\mathrm{qda_n}$ and $\mathrm{gda_c}$, respectively. The energy balance constraints (Eq. (11)) and the generation capacity constraints (Eq. (12)) have to be respected. Again, the DC approximation approach is used to reflect the physical flow in the network (Eq. (13) – (16)). We assume that the system operators are fully aware of operations by other system operators in the re-dispatch model. However, re-dispatching is restricted to the same pricing area. That is, the system operators can only increase or decrease generation within their own jurisdiction, and total reduction in generation must be equal to total increase in generation within the same pricing area (Eq. (17)).

[8] We have used a high penalty for curtailment of load or reduction in renewable generation in the re-dispatch model. In the given formulation, the penalties for load shedding and renewable downregulation are the same, however, they could also differ. A measure of value of lost load (VOLL) is frequently used to penalize loadshedding. A justification for using a penalty on the reduction in renewable generation is that it has priority access to the grid in real time, consistent with the Renewable Energy directive (2009/28/EC), or that it is subsidized by feed in tariffs or premiums, although in this case, the curtailment compensation is not necessarily very high (see WindEurope, 2016).

The day-ahead market model is a quadratic problem and the re-dispatch model is linear. Models are coded in GAMS. The time frame is 1 hour. To simplify, unit commitment decisions and block bids are not taken into account.

3. Power System and Data

3.1 Network

We apply the models in the previous section to a hypothetical joint market for Germany, Poland, Slovakia, and the Czech Republic. The network topology and the AC lines' physical properties are derived from Kunz (2012)[9], by choosing the nodes and lines relevant to the countries under consideration (i.e., Germany, Poland, Slovakia and the Czech Republic). Interconnections of these countries with the rest of the European countries are not taken into account. In total, 529 buses, 835 lines, and 411 power plants are used for this analysis. The transmission network for these countries is displayed in Figure 3-3. The capacity of transmission lines is de-rated to 80 % of their nominal capacity to approximate N-1 security constraints in the network[10].

[9] The original dataset is based on 2008 market data and has been updated to 2011 market data.

[10] An alternative would be to include contingency constraints, like the ones that the Norwegian TSO is using for the Norwegian power market (see for instance Bjørndal et al. (2014) for a description). However, we do not have access to similar cut-constraints/security-constraints for the German and Eastern European power markets. Consequently, in this paper, we have chosen to follow Neuhoff et al. (2013) and Leuthold et al. (2012), who are using the 80 % approach for the German and European power markets. For a comparison of the two methods, and the effect on nodal prices, see Bjørndal et al. (2012b).

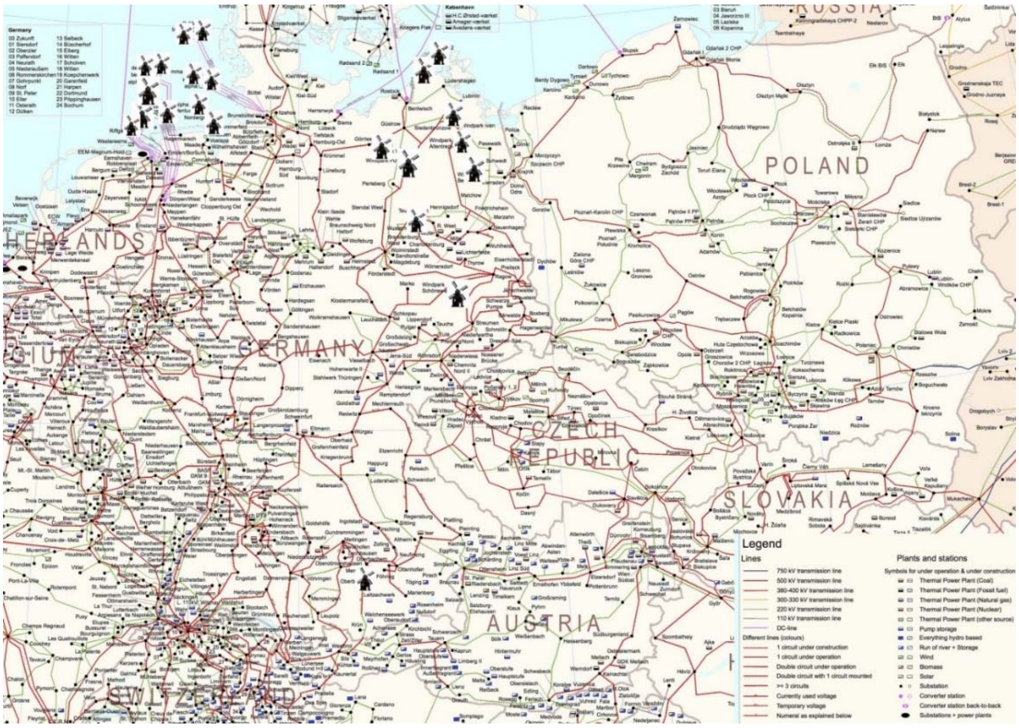

Source: ENTSO-E

Figure 3-3: Map of Grid and the German Wind Power Plants Distribution

3.2. Market data

In order to get more realistic results, we have collected data on load, prices and NTCs from the involved day-ahead markets. As congestion most likely happens in the hours with high demand, we define a high load hour (i.e., 1.2 times the average hourly load in 2012) for the analysis. Therefore, we arbitrarily choose a specific hourly load (i.e., 9 am on 2012-03-01) which is approximately equal to 1.2 times the average hourly load in 2012, and use the corresponding day-ahead market prices as reference.

Net Transfer Capacities (NTCs)[11], which limit the commercial trades between the countries, are given in Table 3-1. The Polish TSO defines a separate NTC for Slovakia and the Czech Republic, as well as a joint NTC (1700 MW for export and 200 MW for import) for all Polish cross-border exchanges, including the borders with Germany (DE), the Czech Republic (CZ) and Slovakia (SK). The official documents do not explicitly state how the Polish TSO allocates transmission capacity to each of its

[11]Data regarding NTCs are obtained from the ENTSO-E portal.

interconnections in the day-ahead market clearing procedure. In our model we implement the joint NTC by adding an extra constraint to the day-ahead market model, in which the three interconnections of Poland (i.e., with Germany, the Czech Republic and Slovakia) are considered as a whole, and the sum of the trades is limited by the joint NTC[12].

From	TO	EXPORT NTC	IMPORT NTC
DE	CZ	1400	1800
PL	CZ-DE-SK	1700	200
PL	SK	600	500
SK	CZ	1200	1800
CZ	PL	600	400
			Sources: ENTSO-E

Table 3-1: NTC values (in MW)

As described in the introduction, NTCs are sometimes also used in attempts to limit physical power exchanges between areas. When wind generation is particularly high in northern Germany, the Polish TSO may publish very low NTCs towards Germany in order to avoid power going from north to south in Germany to transit through Poland. However, in a zonal pricing system, where it is implicitly assumed that the internal transmission capacity within Germany is unlimited, even an NTC of zero on the German-Polish border may not be enough, and transiting power may still enter the Polish power system as unplanned flows and exacerbate internal Polish capacity limits, making the system less secure and increasing the need for re-dispatch in the Polish area.

[12] The joint NTC constraint is similar to the cut constraints that have been used in Nord Pool Spot, for instance to limit total exchange into and out of Sweden and Western Denmark. A reason for the cut constraints in the Nordic power market was that the internal network capacity in Sweden and Western Denmark was limited, but instead of reducing all the individual NTCs to and from these areas proportionally, a joint constraint was given to the market clearing algorithm, so that the most beneficial power exchange across all the borders could be chosen by the operation of the day-ahead market. So for instance for Western Denmark, where total import was limited to 1000 MW, due to an internal constraint in Jutland, while the NTC from Norway was 1000 MW and the NTC from Sweden was 500 MW, the joint constraint of 1000 MW could imply that all trade into Western Denmark came from Norway, if this was most beneficial. The alternative was to reduce the individual NTCs to 667 MW (from Norway) and 333 MW (from Sweden).

3.3. Definition of scenarios

The wind and solar installations (Table 3-2) are assumed to be at 2011 levels (Source: EWEA 2013, EPIA 2013). Germany accounts for more than 90% of the wind and solar installations in the four countries. Wind power locations are concentrated to a few specific areas and cause large amounts of loop flow in our case study. We specifically estimate how the power system would be affected by increased wind power by defining two different scenarios, the Business-as-Usual (BAU) scenario and the High-Wind-Level (HIGH WIND) scenario. We assume that the availability of wind power is 21% of the total installed capacity in the BAU scenario[13] and higher, i.e. 50% of installed capacity, in the HIGH WIND scenario[14].We keep the availability of solar power to be 9% of total installed capacity in both scenarios.

Country	Wind	Solar
CZ	217	1959
DE	29071	24807
SK	3	508
PL	1616	3

Table 3-2: Wind and Solar installations (in MW)

4. RESULTS

In this part, we first clarify some concepts in order to conduct further analysis.

1. p_n

   Market price (p_n): The dual variable of Eq. (2), i.e., the marginal cost/benefit of increasing one unit of power at node n, defines the price at node n. Price within each zonal pricing area is uniform as there are no restrictions on intra-zonal trading. Prices within the nodal pricing area can be different as the model takes both the physical laws and thermal capacity limits into account.

2. $DC = \sum_n p_n Q_n$ (19)

[13] The mean capacity factor for wind power (the ratio of average delivered power to theoretical maximum power) during the period 2003-2008 for Europe is close to 21% (Boccard 2009).

[14] The HIGH WIND scenario shows the impact of adding more wind generation into the grid. We assume a higher wind availability in our analyses, however, an alternative interpretation is that existing wind capacity is expanded.

Demand cost (DC): Defined as the sum of the products of nodal demand Q_n and nodal or zonal day-ahead price.

3. $GI = \sum_n \left[p_n \sum_{c \in C_n} gda_c\right] + \sum_c [cg_c GUP_c] - \sum_c [cg_c GDN_c]$ (20)

Generation incomes (GI): Defined as income earned in the day-ahead market plus income from re-dispatching if up-regulation is required minus costs caused by re-dispatching if down-regulation is required.

4. $GC = \sum_c [cg_c (gda_c + GUP_c - GDN_c)]$ (21)

Generation cost (GC): Refers to the cost of the final generation dispatch, given the re-dispatching results.

5. $GS = GI - GC$ (22)

Generation surplus (GS): Defined as generation income (GI) minus generation cost (GC)[15].

6. $RC = \sum_c [cg_c GUP_c] - \sum_c [cg_c GDN_c]$ (23)

Re-dispatching cost (RC) is the cost caused by re-dispatching.

7. $CR = \sum_n p_n Q_n - \sum_n p_n \sum_{c \in C_n} gda_c = \frac{1}{2} \sum_n \sum_{nn} (p_{nn} - p_n) \times$ $TF_{n,nn} + \sum_n \sum_{nn} (p_{nn} - p_n) \times LF_{n,nn})$ (24)

Congestion rent (CR) collected from the day-ahead market can generally be described as the difference between day-ahead market payment received from consumers and day-ahead market payment to generators[16].

In a full zonal pricing regime, congestion rents for the transmission system operators only result from allocation of international net transfer capacity (i.e., $TF_{n,nn}$) during the day-ahead market clearing. That is, because the day-ahead prices are uniform within areas, no congestion rents will be collected within the areas (countries) that apply zonal pricing. In contrast, within

[15] For simplicity, we have assumed that the re-dispatch model takes a pay-as-bid approach. Power plants that increase their generation are compensated by their short-run marginal cost of production; power plants that decrease their generation pay their saved marginal costs. As displayed in Figure 3-2, the total generation surplus does not increase (or decrease) after re-dispatch.

[16] Also referred to as merchandizing surplus (MS) (Wu et. al 1996).

countries applying nodal pricing, congestion rent results not only from international trades but also from the differences in locational marginal prices. We assume that the rent from cross-border commercial trading is equally shared by the two system operators.

4.1. Day-ahead market prices

Table 3-3 presents the day-ahead market prices (without re-dispatching cost) for the four countries in the two scenarios and under different pricing schemes. Prices are volume weighted by consumption. In the BAU scenario, the full zonal solution shows that Poland has the lowest price among the four countries, mainly due to the low marginal generation cost of its coal and gas-fired generation. Therefore, Poland does not import power from the other three countries. In the hybrid pricing model, the average price within Poland increases after taking into consideration the physical constraints. Therefore, power from the other three countries becomes comparatively cheaper (without considering re-dispatching cost), and in this case Poland imports power from the other countries.

In the HIGH WIND scenario, market prices given by all the three pricing schemes generally decrease given the input of low-cost wind power. The full zonal pricing scheme gives similar prices for all the four countries (and identical prices for the Czech Republic, Germany and Slovakia). Poland has the highest price mainly because it restricts power exchange with other countries by setting a low NTC value. In the hybrid pricing scheme, Poland again has the highest price, mainly due to the consideration of network constraints. The prices for the other three countries are lower without counting the re-dispatch cost. Moreover, the uniform prices in the zonal-pricing areas makes it difficult for Poland to identify low-cost power opportunities. For instance, power in North Germany should have been cheaper on a windy day, and Poland could have imported this power, however, it does not happen due to the uniform price in Germany.

Pricing Scheme	BAU			HIGH WIND		
	Zonal	Hybrid	Nodal	Zonal	Hybrid	Nodal
Czech Republic	50.89	50.30	48.13	48.25	48.08	49.34
Germany	50.89	51.03	52.67	48.25	48.08	49.15
Poland	49.76	52.49	52.11	48.88	50.45	49.95
Slovakia	50.89	50.30	48.51	48.25	48.08	48.43

*** Nodal prices are weighted by consumption volumes where applicable**

Table 3-3: Day-ahead prices (in € per MWh)

Compared to zonal pricing, hybrid pricing helps Poland to reduce its cost for re-dispatching and to collect a great amount of congestion rent. This is further discussed in Section 4.3 and 4.4. Table 3-4 gives the unit prices for both the zonal and hybrid pricing schemes after taking into consideration the re-dispatching cost and congestion rent (i.e., the prices include re-dispatching cost but deduct congestion rent). In both the BAU and HIGH WIND scenarios, the hybrid pricing solution reduces the unit prices for Poland. As consumers in many countries bear the largest part of grid costs and the system operation costs of the TSOs, consumers in Poland can potentially benefit from this reduction in unit price.

Pricing Scheme	BAU		HIGH WIND	
	Zonal	Hybrid	Zonal	Hybrid
Czech Republic	51.01	50.25	48.29	48.09
Germany	51.54	51.71	48.60	48.43
Poland	50.98	49.72	49.66	48.79
Slovakia	50.81	50.24	48.24	48.08

Table 3-4: Unit prices with re-dispatching cost and congestion rent (in € per MWh)

In the following, we further assess whether the hybrid pricing model in Poland can truly reflect network congestion. We compare the prices in Poland given by the hybrid pricing scheme to those given by the full nodal pricing scheme in Figure 3-4. Moreover, we use t-tests to identify statistical differences between the hybrid prices and the full nodal prices, for both scenarios.

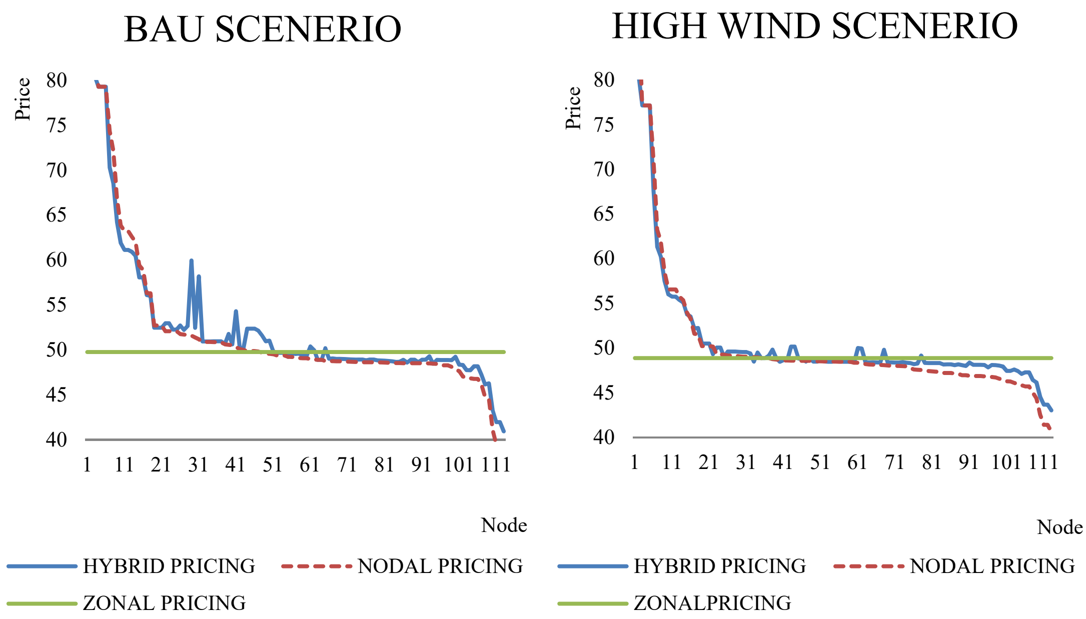

Figure 3-4: Day-ahead Price comparison in Poland

In both the BAU and HIGH WIND scenarios, the hybrid prices fluctuate, but generally match rather well with the full nodal prices, indicating that hybrid prices in such a context are able to capture the congestion signals within the network. However, in both scenarios, the average hybrid prices are higher than the average nodal prices[17]. The differences between the prices are statistically significant at a five-percent level in a t-test. This indicates that hybrid pricing cannot fully utilize all the available resources in the network. The major reason is that the lack of price signals in the zonal pricing areas (i.e., uniform prices within Germany, the Czech Republic, and Slovakia) prevents Poland from trading optimally. For example, in the full nodal pricing solution of the BAU scenario, prices in the southern part of Poland are lower than those in the northern part. This induces Polish export to the Czech Republic, which is further exported to serve the great demand for power in southern Germany. In contrast, in the hybrid system, uniform prices are given for the interconnected countries (i.e., Germany, the Czech Republic, and Slovakia) and thus no price signals are received by Poland. As a result, compared to full nodal pricing, Poland exports more power to Germany and Slovakia but less power to the Czech Republic (as shown by the flows in Figure 3-5).

[17] The actual average hybrid prices should be even higher if re-dispatch cost is considered.

This increases the prices at nodes within Poland that are connected to Germany and Slovakia. Because no price signals are revealed within the Czech market, Poland does not export its power from the best interconnected nodes indicated by the full nodal price solution. Therefore, some interconnected nodes experience higher prices (i.e., exporting more power) while others have lower prices (i.e., exporting less power) compared to the full nodal price solution.

Furthermore, the trading cap (i.e., NTC value) in the hybrid pricing scheme further restricts some optimal trades suggested by the full nodal pricing scheme. This is especially important in the HIGH WIND scenario, in which the input of wind power reduces the prices in the full nodal price solution. The low NTC value restricts Poland from importing cheap power from Germany, leading to an even higher price difference compared to nodal pricing.

Hybrid prices are more variant in the BAU scenario than in the HIGH-WIND scenario. This is shown by the higher standard deviation of the price differences in Table 3-5, which means that the difference between hybrid prices and nodal prices vary more in the BAU scenario than in the HIGH-WIND scenario. In the BAU scenario, Poland has more commercial trading with other countries and therefore is more likely to be affected by the zonal pricing area. In the HIGH-WIND scenario, Poland greatly limits its import from other countries and becomes a relatively more independent system, thus getting less affected by the zonal pricing areas. This indicates that more frequent interactions with other zonal pricing areas will enlarge the variation of the price differences between hybrid prices and nodal prices.

	BAU SCENERIO	HIGH WIND SCENERIO
Mean (Price differences)	0.36 €	0.47 €
Observed Number (Nodes)	113	113
Standard Deviation (Variation of price differences)	1.98	1.09
T-statistic	1.94	4.58

Table 3-5: Price matches for nodal pricing and hybrid pricing in Poland

4.2. Power exchange

Figure 3-5 shows the commercial cross-border trading volumes in both the BAU and HIGH WIND scenarios for different pricing schemes [18,19]. We find that international exchange would be reduced in the HIGH WIND scenario; however, the hybrid pricing scheme has more international exchange than full zonal pricing. International power exchange is reduced in the HIGH WIND scenario because Germany, as the main importing country in the BAU scenario, produces wind power that satisfies its own load. Another reason leading to the low international power exchange is that Germany's uniform pricing system does not allow other countries to take advantage of the cheap wind power. Therefore, countries, such as Poland, are not able to import as much power as indicated by the solution of the full nodal pricing scheme. For example, in the full nodal pricing scheme, Germany exports 623 MW to Poland. In comparison, Germany exports only 100 MW to Poland in the full zonal pricing scheme, and 200 MW in the hybrid pricing scheme. The zonal-pricing areas (e.g., Germany) therefore can hold their cheap energy within their own countries before they have transactions with the interconnected countries, leading to a reduction in international power exchange. Besides, this indicates that Germany is using the Polish network to transport its power without paying corresponding congestion rent. This is further discussed in section 4.3.

Further, we find that the power exchange for Poland under hybrid pricing is affected by the zonal pricing areas. In the BAU scenario under the hybrid pricing scheme, Poland exports most of its available commercial trading amount and also imports 200 MW from Germany to help relieve its grid congestion[20]. This is because price signals indicate more congestion in the northern part of Poland and it would cost less for Poland to import than to produce the power. However, in the full nodal pricing, Poland does not import power from other countries in the day-ahead market.

---

[18] Commercial flows given by the full nodal pricing solution are the same as the physical flows.

[19] Commercial trades between areas with identical prices may not be unique. Congestion rent between such areas is always 0.

[20] Poland has several nodes connecting with other countries. As the prices vary within the Polish network, Poland could import power at some of the connected nodes while export power at other nodes.

Under the HIGH WIND scenario, large amounts of wind generated power bring down the price in Germany, greatly reduce its power imports, and create an uncongested power market for Germany, the Czech Republic, and Slovakia (i.e., identical market price for these three countries) in the hybrid pricing scheme. The market prices for these three countries do not provide transparent signals for Poland. As a result, the interface node (nodes) in Poland with the least cost (i.e., lowest market price) trades with the zonal-pricing areas. In the hybrid pricing case then, power is traded from Poland to Germany although, the physical power exchange given by the full nodal pricing solution indicates that no power flows should go directly from Poland to Germany. Flows should first go to the Czech Republic and then enter the German jurisdiction.

4.3. Re-dispatching and unplanned physical flows

We assume that the actual physical power flows between the nodes can be calculated by the DC approximation of the alternating current (AC) power flows[21]. Since we assume that there is no uncertainty with regards to generation or demand, power flows are feasible and re-dispatch is not needed in the full nodal pricing model. However, day-ahead markets that apply zonal pricing or hybrid pricing produce commercial power flows, which are not necessarily equal to actual physical power flows and might need re-dispatching in order to relieve grid congestion. Table 3-6 and Table 3-7 show the commercial and physical power flows for the two scenarios. Physical power flows before re-dispatching are calculated based on the day-ahead market solution[22]. Physical

[21] Thus, real power flows will differ from the flows predicted by the DC approximation. For the Polish system, the results from a DC market clearing model could be tested against AC power flow models, models that the TSOs often apply for other purposes (like assessing power losses). Presently, as far as we know, market clearing algorithms that take into account power flows, use DCOPF. The experiences from power markets in the US (like PJM) suggest that the accuracy of commercial flows improve significantly when moving from transportation type models (with "contract" paths) to DCOPF and nodal pricing. AC power flow models impose challenges like non-linearities and non-convexities, and there is considerable research into improving optimal power flow models to take into account AC characteristics, i.e. ACOPF, see for instance Castillo et al. (2016).

[22] In order to calculate the physical power flows of the zonal and hybrid price solutions, we fix the values of nodal load and generation, consistent with the corresponding market clearing solutions. We then use these values as inputs in a detailed network model to re-compute the line flows based on the DC approximation. Thus, when computing the power flows resulting from the zonal and hybrid market

power flows might not be feasible, and in order to ensure feasible power flows, re-dispatching is needed.

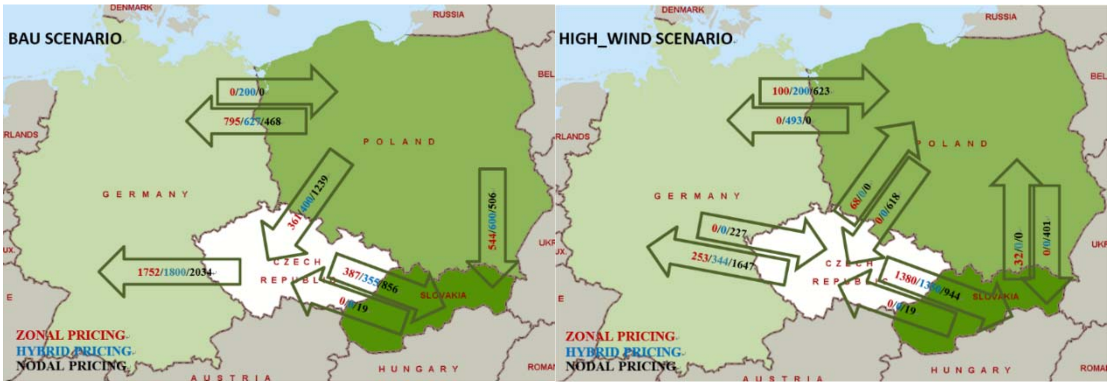

Figure 3-5: Cross-border commercial trades (in MW)

In the BAU scenario, Poland, as the main exporting country, is only to a limited extent influenced by flows from other countries. Under both full zonal and hybrid pricing, the net physical power exchange between Poland and its neighboring countries is close to the net commercial power exchange: power flow is rearranged on the border.

Commercial Exchange (Day-ahead market)						Physical Power Exchange (without re-dispatching)						Physical Power Exchange (with re-dispatching)					
Zonal pricing						Zonal pricing						Zonal pricing					
To From	CZ	DE	PL	SK	SUM	To From	CZ	DE	PL	SK	SUM	To From	CZ	DE	PL	SK	SUM
CZ	-	1752	0	387	2139	CZ	-	2271	0	639	2910	CZ	-	2269	0	592	2861
DE	0	-	0	0	0	DE	0	-	0	0	0	DE	0	-	0	0	0
PL	361	795	-	544	1700	PL	1022	275	-	403	1700	PL	966	278	-	456	1700
SK	0	0	0	-	0	SK	110			-	110	SK	117	0	0	0	117
SUM	361	2547	0	931	3839	SUM	1132	2547	0	1041	4720	SUM	1083	2547	0	1048	4678
Hybrid Pricing						Hybrid Pricing						Hybrid Pricing					
To From	CZ	DE	PL	SK	SUM	To From	CZ	DE	PL	SK	SUM	To From	CZ	DE	PL	SK	SUM
CZ	-	1800	0	355	2155	CZ	-	2026	0	595	2621	CZ	-	2147	0	603	2750
DE	0	-	200	0	200	DE	0	-	0	0	0	DE	0	-	50	0	50
PL	400	627	-	600	1627	PL	784	201	-	442	1427	PL	895	131	-	451	1478
SK	0	0	0	-	0	SK	81	0	0	-	81	SK	100	0	0	-	100
SUM	400	2427	200	955	3983	SUM	865	2227	0	1036	4129	SUM	995	2278	50	1055	4378

solutions, we take into consideration the loop flow characteristics of power network, but the computed power flows may violate thermal and other network constraints. When nodal generation and demands are fixed, the DC power flows are also fixed (see also a similar discussion in Bjørndal et al., 2012).

Table 3-6: Cross-border Power flows in the BAU scenario (in MW)

In the HIGH WIND scenario, Poland imports in total 200 MW from other countries in the day-ahead market, given the full zonal pricing solution. However, the physical power flows entering the Polish network given by the day-ahead market and re-dispatching models are 1122 MW (i.e. 922 MW of unplanned power flows) and 1342 MW (1142 MW of unplanned power flows), respectively. Thus, a low NTC in the zonal pricing solution does not prevent power flows from entering the Polish network. This large amount of unplanned power flows indicates that other countries have utilized the Polish network to transport power, which might threaten the Polish network security. By applying the hybrid pricing model, Poland still imports in total 200 MW in the day-ahead market. However, Poland is able to export power and thus reduces the unplanned import power flows. Specifically, instead of importing from all the other three countries under full zonal pricing, hybrid pricing suggests that Poland should only import power from Germany (to relieve its grid congestion in the northern part) and export power in its southern part. Ideally, Poland should have exported power to the Czech Republic and Slovakia as the nodal pricing model indicates. Although Poland exports power to Germany instead, this could still to a large degree prevent the Polish network from being occupied by the German wind power. As a result, the physical power flows entering the Polish network given by the day-ahead market and re-dispatching models are reduced to 730 MW (530 MW unplanned power flow) and 863 MW (663 MW unplanned power flow). That is, applying hybrid pricing could help Poland to reduce unplanned power flow from entering its network by around 35%.

Cross-border Exchange (Day-ahead market)						Physical Power Exchange (without re-dispatching)						Physical Power Exchange (with re-dispatching)					
Zonal pricing						Zonal pricing						Zonal pricing					
To / From	CZ	DE	PL	SK	SUM	To / From	CZ	DE	PL	SK	SUM	To / From	CZ	DE	PL	SK	SUM
CZ	-	253	68	1380	1700	**CZ**	-	1586	19	1189	2795	**CZ**	-	1837	0	894	2730
DE	0	-	100	0	100	**DE**	331	-	1103	0	1434	**DE**	342	-	1342	0	1684
PL	0	0	-	0	0	**PL**	763	0	-	158	922	**PL**	688	0	-	454	1142
SK	0	0	32	-	32	**SK**	0	0	0	-	0	**SK**	0	0	0	-	0
SUM	0	253	200	1380	1832	**SUM**	1094	1586	1122	1348	5150	**SUM**	1030	1837	1342	1348	5557

Hybrid Pricing						Hybrid Pricing						Hybrid Pricing					
To From	CZ	DE	PL	SK	SUM	To From	CZ	DE	PL	SK	SUM	To From	CZ	DE	PL	SK	SUM
CZ	-	344	0	1350	1694	**CZ**	-	1680	20	905	2605	**CZ**	-	1848	0	885	2733
DE	0	-	200	0	200	**DE**	333	-	710	0	1043	**DE**	348	-	863	0	1211
PL	0	493	-	0	493	**PL**	578	0	-	446	1023	**PL**	690	0	-	466	1156
SK	0	0	0	-	0	**SK**	0	0	0	-	0	**SK**	0	0	0	-	0
SUM	0	837	200	1350	2388	**SUM**	911	1680	730	1350	4671	**SUM**	1039	1848	863	1350	5100

Table 3-7: Cross-border Power flows in the HIGH WIND scenario (in MW)

Table 3-8 summarizes the re-dispatching cost given by the full zonal pricing and hybrid pricing schemes. As expected, Poland could greatly reduce its re-dispatching cost in the hybrid pricing model. Compared to the full zonal pricing scheme, re-dispatch costs for Poland have been reduced by 93% in the BAU scenario and 88% in the HIGH WIND scenario, even when only Poland uses nodal pricing.

	BAU		HIGH WIND	
	ZONAL PRICING	HYBRID PRICING	ZONAL PRICING	HYBRID PRICING
CZ	1220	646	448	374
DE	43481	46609	24209	23537
PL	24346	1624	15061	1732
SK	0	0	0	0
SUM	69047	48879	39718	25642

Table 3-8: Re-dispatching Cost

4.4. Congestion rent

Changes in cross-border trades lead to the reassignment of congestion rent. In the full zonal pricing scheme, prices are uniform within each zone and therefore congestion rent is only collected for cross-border trades. In the hybrid pricing scheme, Poland could also collect congestion rent within its domestic market. Table 3-9 summarizes congestion rent for cross-border trades. We assume that the congestion rent resulting from cross-border commercial trading is equally shared by the two system operators. Table 3-10 gives the congestion rent collected by each country for their inter-zonal and intra-zonal trade.

BAU					HIGH WIND				
Zonal pricing					**Zonal pricing**				
To / From	**CZ**	**DE**	**PL**	**SK**	**To / From**	**CZ**	**DE**	**PL**	**SK**
CZ	-	0	0	0	**CZ**	-	0	43	0
DE	0	-	0	0	**DE**	0	-	64	0
PL	411	905	-	620	**PL**	0	0	-	0
SK	0	0	0	-	**SK**	0	0	20	-
Hybrid Pricing					**Hybrid Pricing**				
To / From	**CZ**	**DE**	**PL**	**SK**	**To / From**	**CZ**	**DE**	**PL**	**SK**
CZ	-	1314	0	0	**CZ**	-	0	0	0
DE	0	-	284	0	**DE**	0	-	346	0
PL	737	0	-	430	**PL**	0	0	-	0
SK	0	0	0	-	**SK**	0	0	0	-

Table 3-9: Cross-border congestion rent (in €)

BAU					HIGH WIND				
	ZONAL PRICING		**HYBRID PRICING**			**ZONAL PRICING**		**HYBRID PRICING**	
	Inter-zonal	**Intra-zonal**	**Inter-zonal**	**Intra-zonal**		**Inter-zonal**	**Intra-zonal**	**Inter-zonal**	**Intra-zonal**
CZ	205	×	1025	×	CZ	22	×	0	×
DE	452	×	799	×	DE	32	×	173	×
PL	968	×	725	53062	PL	64	×	173	33123
SK	310	×	215	×	SK	10	×	0	×

Note: Revenues from cross-border commercial trading are equally shared by the two system operators

Table 3-10: Congestion rent collected by each country (in €)

In the full zonal pricing solution under the BAU scenario, price differences only exist between Poland and the other countries. Therefore, congestion rent is collected only on the Polish border. In the hybrid pricing solution, more congestion rent could be collected as more power has been transferred among the countries. In the hybrid pricing model, Poland exports less power to Germany, which increases the price in Germany and creates price differences between Germany and other countries. Because of this, Poland collects less cross-border congestion rent while the other countries collect more.

However, Poland would collect a great amount of congestion rent within the domestic market if applying nodal pricing.

In the HIGH WIND scenario, because more power is traded in the hybrid pricing scheme, more congestion rent is collected than in the full zonal pricing solution. However, the total international congestion rent is greatly reduced compared to the BAU scenarios. Less international power exchange is the main contributor of the reduction in congestion rent. Prices outside the Polish network are the same in both the zonal pricing and hybrid pricing solutions. Therefore, congestion rent could only be collected on the Polish border.

4.5. Supply and demand adjustment

The re-dispatch model allows the option to curtail nodal load, solar and/or wind generation in order to ensure a feasible solution[23]. There is no need for curtailment of solar and wind generation for any of the cases studied (refer Table 3-11)[24]. Load curtailment happens in all the studied cases, however, only for very few (1-4) nodes. Hybrid pricing yields a lower load curtailment than zonal pricing. In the full zonal pricing scheme, Germany and Poland are the only two countries (i.e., Table 3-12) that face load shedding. Poland does not need to curtail its load in the hybrid pricing scheme.

	BAU		**HIGH WIND**	
	ZONAL PRICING	HYBRID PRICING	ZONAL PRICING	HYBRID PRICING
Load Shedding	107.92	28.71	82.62	14.75
Solar Curtailment	×	×	×	×
Wind Curtailment	×	×	×	×

Table 3-11: Curtailment for different pricing schemes (in MW)

[23]Following Kunz (2013), we assume that the load, wind and solar shedding costs are 500 €/MWh (higher than any marginal cost of electricity production).

[24] For must-take renewables the anticipated wind and solar electricity generation is exogenously given in the day-ahead market and is typically fully accepted due to low marginal cost. The TSOs have the option to curtail wind/solar electricity during re-dispatch, however at a high cost of 500 €/MWh, which can be considered a must-take penalty. Thus, the shedding cost for wind/solar electricity will only affect the results of the re-dispatching model. Since demand is assumed to be high in the cases studied in this paper, the results reported are not sensitive to the size of the assumed penalty.

	BAU		HIGH WIND	
	ZONAL PRICING	HYBRID PRICING	ZONAL PRICING	HYBRID PRICING
CZ	×	×	×	×
DE	YES	YES	YES	YES
PL	YES	×	YES	×
SK	×	×	×	×

Table 3-12: Load shedding countries

5. CONCLUSION

This paper attempts to investigate how efficiently the hybrid pricing scheme works in a coupled European power market as more wind-generated power enters the grid. The paper applies a pricing model with two types of congestion management methods (Bjørndal et al. 2014). Four countries, i.e., the Czech Republic, Germany, Poland, and Slovakia are involved in the research, of which Poland applies nodal pricing. We construct two different wind levels (i.e., BAU and HIGH WIND) to test how nodal pricing performs in different perspectives.

We find that countries that are greatly affected by neighboring wind-generated power, such as Poland, would benefit from applying nodal pricing to address their network congestion. In the HIGH WIND scenario, international power exchange has been greatly reduced in the full zonal pricing as wind-generated power satisfies a significant portion of the demand within the German market. However, the real (physical) power exchange does not accordingly reduce due to the physical characteristics of power transmission. Therefore, a large amount of unscheduled power flow enters the Polish power grid. Though transparent price signals are missing in Polish neighbor countries, nodal pricing helps Poland to identify resource scarcity within its domestic market. Poland has more demand in its northern part while cheaper resources in its southern part. Therefore, Poland could import power in its northern part but export power in its southern part in the nodal pricing scheme. This helps Poland to reduce the unplanned power flows from Germany.

We also find that if using nodal pricing, Poland would reduce its need for re-dispatching and collect a great amount of congestion rent domestically. The Polish consumers might benefit from applying the nodal pricing scheme. Taking the re-dispatching cost and congestion rent into account, the average unit price given by the hybrid pricing solution decreases compared to the zonal price solution. We also find that nodal pricing would reduce the need for load curtailment.

Another interesting result is that countries with a great amount of wind-generated power, such as Germany, will benefit from keeping zonal pricing. In such a way, Germany would be able to keep the low-cost energy within the country. Furthermore, they could transmit the power using their neighboring grid and without paying the corresponding congestion rent.

References

[10] 50Hertz. "Report on vPST pilot phase experience." *50Hertz* (2014).

http://www.50hertz.com/Portals/3/Content/Dokumente/AnschlussZugang/Engpassmanagement/vPST-pilot-phase-report-2014.pdf

[11] ACER. "Coordination Group for Electricity Regional Initiatives, ERI Quarterly Report #6 April 2013 – June 2013, Ref: A13-ERI-02." *Agency for cooperation of Energy Regulators* (2013).

http://www.acer.europa.eu/Official_documents/Acts_of_the_Agency/Publication/6th ERI Quarterly Report - Q2 2013.pdf.

[12] ACER/CEER. "Annual Report on the Results of Monitoring the Internal Electricity Markets in 2015." *Agency for cooperation of Energy Regulators/Council of European Energy Regulators* (2016).

[13] Aravena, Ignacio, and Anthony Papavasiliou. "Renewable energy integration in zonal markets." *IEEE Transactions on Power Systems* (2016).

[14] Bjørndal, E., Bjørndal M. and Hong Cai. " Nodal pricing in a coupled electricity market." In *11th International Conference on the European Energy Market (EEM14)*, pp. 1-6. IEEE (2014).

[15] Bjørndal, E., Bjørndal M. and Gribkovskaia, V. "Congestion Management in the Nordic Power Market – Nodal Pricing versus Zonal Pricing." (SNF report 15/12). " *SNF* (2012).

[16] Bjørndal, E., Bjørndal M. and Gribkovskaia, V. " Simulation of congestion management and security constraints in the Nordic electricity market." In *9th International Conference on the European Energy Market (EEM12),* IEEE (2012).

[17] Bjørndal, E., M. Bjørndal, and V. Gribkovskaia (2014). "A Nodal Pricing Model for the Nordic Electricity Market". *Discussion Paper 43/2014*, Department of Business and Management Science, NHH.

[18] Boccard, Nicolas. "Capacity factor of wind power realized values vs. estimates." *Energy Policy* 37.7 (2009): 2679-2688.

[19] Cai,Hong. "Hybrid congestion management in Nordpool", NFB conference (2013).

[20] CASC.EU "Documentation of the CWE FB MC solution as basis for the formal approval-request." *CASC.EU* (2014).

[21] Castillo, Anya, Paula Lipka, Jean-Paul Watson, Shmuel Oren, Richard P. O'Neill, "A Current-Voltage Successive Linear Programming Approach to Solving the ACOPF." *IEEE Transactions on Power Systems*, 13(4), July 2016, pp. 2752-2763.

[22] Chao, H. P., Peck, S., Oren, S., & Wilson, R. (2000). "Flow-based transmission rights and congestion management." *The Electricity Journal*,*13*(8), 38-58.

[23] Bundestag, Deutscher. "Rahmenbedingungen für den Aufbau eines Overlay-Stromnetzes." *Drucksache* 17 (2010): 4336.

[24] EPIA. "Global Market Oulook for Photovoltaics 2013-2017. Market Outlook." *European Photovoltaic Industry Association* (2013).

[25] EIRGRID. "Price Coupling of Regions (PCR) initiative and the North West Europe (NWE) project." *EIRGRID* (2013).

http://www.eirgrid.com/media/PCR_NWE_MO_TSO_Review.pdf

[26] EWEA. "Pure Power Wind energy targets for 2020 and 2030." *European Wind Energy Association* (2011).

http://www.ewea.org/fileadmin/ewea_documents/documents/publications/reports/Pure_Power_III.pdf

[27] EWEA. "Wind in power: 2012 European statistics 2013." *European Wind Energy Association* (2013).

http://www.ewea.org/fileadmin/files/library/publications/statistics/Wind_in_power_annual_statistics_2012.pdf

[28] Hogan, William W. "Contract networks for electric power transmission." *Journal of Regulatory Economics* 4, no. 3 (1992): 211-242.

[29] Kunz, Friedrich. "Managing Congestion and Intermittent Renewable Generation in Liberalized Electricity Markets." *Dissertation* (2012).

[30] Kunz, Friedrich and Alexander Zerrahn, "Coordinating Cross-Country Congestion Management: Evidence from Central Europe." *Energy Journal* 37 (2016).

[31] Leuthold Florian U. "Economic engineering modeling of liberalized electricity markets: approaches, algorithms, and applications in a European context." *Dresden, Techn. Univ., Diss., 2010* (2010).

[32] Leuthold, Florian U., Hannes Weigt, and Christian von Hirschhausen. "Efficient pricing for European electricity networks–The theory of nodal pricing applied to feeding-in wind in Germany." *Utilities Policy*, (2008): 16(4), 284-291.

[33] Leuthold, Florian U., Hannes Weigt, and Christian von Hirschhausen. "A large-scale spatial optimization model of the European electricity market." *Networks and spatial economics* 12, no. 1 (2012): 75-107.

[34] Neuhoff, Karsten, et al. "Renewable electric energy integration: Quantifying the value of design of markets for international transmission capacity." *Energy Economics* 40 (2013): 760-772.

[35] Nordpool."4M Market Coupling launches successfully by using PCR solution." *Nordpool* (2014).

http://www.nordpoolspot.com/globalassets/download-center/pcr/pcr-pr_4m-mc-launch.pdf

[36] Oggioni, Giorgia, and Yves Smeers. "Market failures of Market Coupling and counter-trading in Europe: An illustrative model based discussion." *Energy Economics* 35 (2013): 74-87.

[37] Papaemmanouil, Antonios. "Coordinated transmission expansion planning of future interconnected power systems." *PhD diss., University of Patras* (2011).

[38] Parkinson, Giles, "Poland builds electronic wall to keep out German renewables." (2013).

http://reneweconomy.com.au/2013/poland-builds-electronic-wall-to-keep-out-german-renewables-72084.

[39] Schweppe, Fred C., Michael C. Caramanis, Richard D. Tabors, and Roger E. Bohn. "Spot pricing of electricity." (1988).

[40] Sensfuss, Frank, Mario Ragwitz, and Massimo Genoese. "The merit-order effect: A detailed analysis of the price effect of renewable electricity generation on spot market prices in Germany." *Energy Policy* 36.8 (2008): 3086-3094.

[41] Sikorski, Tomasz. "Nodal pricing project in Poland*." In 4th IAEE International Conference: Institutions. Efficiency and Evolving Energy Technologies. Stockholm* (2011).

[42] Siewierski, Tomasz. "Transmission Networks Developments and the Role of Interconnections with Neighbouring Countries" *CGEMP Conference, Paris 9-10 June 2011* (2011).

[43] Siewierski, Tomasz. "Empirics of Intraday and Real-time Markets in Europe: POLAND. " (2015).

[44] Wu, Felix, Pravin Varaiya, Pablo Spiller, and Shmuel Oren. "Folk theorems on transmission access: Proofs and counter examples." *Journal of Regulatory Economics* 10, no. 1 (1996): 5-23.

[45] Sauma, E. E., & Oren, S. S. (2006). "Proactive planning and valuation of transmission investments in restructured electricity markets." *Journal of Regulatory Economics*, 30(3), 261-290.

[46] WindEurope. "WindEurope views on curtailment of wind power and its links to priority dispatch." *WindEurope* (2016).

Appendix

I. Determination of a_n and m_n in the inverse electricity demand function using a reference price and demand[25]

The model assumes a linear inverse electricity demand function of the form:

$$p_n(Q_n) = a_n + m_n * Q_n$$

Demand function: $Q_n(p_n) = -\frac{a_n}{m_n} + \frac{1}{m_n} * p_n$

Definition of elasticity: $= \frac{\partial Q_n}{\partial p_n} * \frac{p_n}{Q_n}$. The elasticity is assumed to be -0.25.

$$\varepsilon = \frac{1}{m_n} * \frac{p_n}{Q_n}$$

$$m_n = \frac{p^{ref}}{d^{ref}} * \frac{1}{\varepsilon}, a_n = p^{ref} - m_n * Q_n{}^{ref}$$

II. Tables

	load (MW)	Ref. Price (Euro)
CZ	8636	57.01
DE	64421	62.01
PL	19499	48.68
SK	3692	57.01

Table AI :Electricity load and reference prices for the four countries on 2012-03-01[26]

[25] The ELMOD pre-defines a fixed demand share for each node within a country (i.e., the sum of demand share for the whole country is 100%). The reference demand for each node is thus calculated as the fixed demand share multiplied by the reference demand load for the whole country. Then the demand function for each node could be defined, as shown in appendix I.

[26] Hourly day-ahead prices for Germany are available from the European Power Exchange Spot. Electricity trading in Poland is conducted both in the bilateral contract market (i.e., Auction 1) and at the Polish Power Exchange Towarowa Giełda Energi (i.e., Auction 2) (Siewierski, 2015). The day-ahead price for Poland is calculated as the quantity-weighted mean value of three auction prices (transactions concluded in Auction 1 and 2 and continuous trading during the transaction period) provided by the Polish Power Exchange.

Chapter 4: Efficiency of the Flow-Based Market Coupling Model in the European Market

Efficiency of the Flow-Based Market Coupling Model in the European Market

Endre Bjørndal[§], Mette Bjørndal[§], Hong Cai[§‡]

Abstract: In May 2015, the Flow-Based Market Coupling (FBMC) model replaced the Available Transfer Capacity (ATC) model in Central Western Europe to determine the power transfer among countries (price areas). The FBMC model aims to enhance market integration and to better monitor the physical power flow. The FBMC model is expected to lead to increased social welfare in the day-ahead market and more frequent price convergence between different market zones. This paper gives a discussion of the mathematical formulation of the FBMC model and the procedures of market clearing, and we discuss the relationships between the nodal pricing, ATC, and FBMC models. In addition to an illustrative 3-node example, we examine the FBMC model in two test systems and show the difficulties in implementing the model in practice. We find that a higher social surplus can come at the cost of more re-dispatching. We also find that the FBMC model might fail to relieve network congestion and better utilize the power resources even when compared to the ATC model.

1. Introduction

Europe has launched the Price Coupling of Regions (PCR) project, which aims at enhancing power exchange among different countries and creating a single European day-ahead market (EIRGRID, 2013). The project has involved a number of power exchanges (PXs), including APX/Belpex, EPEX SPOT, GME, Nord Pool Spot, OMIE, and OTE (NordPool, 2014), accounting for more than 75% of Europe's electricity demand. Currently, most of the European countries rely on the ATC (Available Transfer Capacity) model to process power exchange with other countries. In this model, it is assumed that power can be directly transferred between any two adjacent areas. Only a pre-defined ATC value is used to limit the maximum commercial trading volume between two areas (mostly countries) in the day-ahead market. However, as a matter of fact, the AC power flow between any two nodes follows the paths designed

§ Norwegian School of Economics, Helleveien 30, 5045 Bergen, Norway

‡ Corresponding author, Hong.Cai@nhh.no

by Kirchhoff's laws and is also restricted by the thermal limit of the transmission lines. Therefore, the commercial power transfer is not necessarily equal to the real physical power exchange. Solutions given by the ATC model do not guarantee a congestion-free network. Hence, re-dispatching would be needed and it incurs extra costs.

In contrast to the ATC model, nodal pricing (Schweppe et al., 1988), reduces the needs for re-dispatching by including all the physical and technical constraints in the market-clearing process. The nodal pricing model has been successfully implemented in many regions and countries, such as Pennsylvania – New Jersey – Maryland (PJM), California, and New Zealand. Within Europe, Poland planned to implement nodal pricing in its domestic market in 2015 and estimated that it would reduce generation cost (Sikorski, 2011). However, the project has now been abandoned. In the European context nodal pricing has not been accepted as the standard tool for integrating the European electricity market. One of the main concerns is that nodal pricing might impede market harmonization as it imposes more restrictions (e.g., network capacity constraints) than the ATC model, and thus could limit power exchange between countries.

In recent years, more and more renewable energy has been connected to the power system. This requires more accurate monitoring of power flows, the reason being that installed renewable energy power plants (like wind turbines) are usually located in places without sufficient consumption. Therefore, the utilization of such energy resources often requires long distance transportation, which creates an extra burden for the network and may exacerbate congestion. For example, due to the large wind capacity installation, Germany and its neighboring countries found that their transmission networks had been overloaded more frequently, making their grids less stable and secure (Kunz, 2012). Furthermore, the ATC model may constitute a crude approximation of real power flows, since the locations of generation plants within a price area do not affect the model solutions and it is assumed that the cheaper power within an area can always be dispatched first. In real-time dispatch, however, physical power follows the laws of physics and it is not necessarily equal to the commercial flow defined by the ATC model. Moreover, Bjørndal et al. (2018) found that when the penetration level of renewable energy is high, applying a low ATC value (i.e., to restrict the commercial power exchange in the day-ahead market) was not sufficient to limit physical power exchange between two connected countries.

In order to better monitor the power flow in an integrated European market, a so called "Flow-Based methodology" Market Coupling (FBMC) was developed by the European TSOs (Schavemaker et al., 2008). Van den Bergh et al. (2016) give a description of the FBMC model. The FBMC model is developed from the nodal pricing model, i.e. the nodal pricing model where we use the power transfer distribution factors (PTDF) to calculate flows. The FBMC model imposes an aggregate (or zonal) PTDF matrix on certain areas/lines in order to limit the power exchange between price areas. Therefore, the solutions given by the FBMC model may still be infeasible in some parts of the network and re-dispatching may be needed. The FBMC model tries to reduce the explicit limitations to cross-border trades, which is an indirect way of dealing with individual line constraints, and instead focuses on selected critical branches (CBs) that are the ones most likely to be influenced by cross-border trading.

In May 2015, Central Western Europe (CWE), a region consisting of the Netherlands, Belgium, France, Luxembourg, and Germany, started to implement the FBMC model. The CWE TSOs have been working on the FBMC calculation method since 2007 and this methodology has been tested with 2-year off-line parallel runs. The Parallel Run performance report (CASC, 2015) claims that the FBMC model performs better than the ATC model as it significantly increases the social welfare in the day-ahead market and leads to more frequent price convergence between different market zones based on the parallel runs results.

Nevertheless, to fully evaluate how the FBMC model works in the European power markets, two crucial questions deserve careful examination. First, because the non-CBs are not properly monitored, flows on the non-CBs could affect the accuracy of the FBMC model due to Kirchhoff's loop flow effect. It is necessary to test to what extent the FBMC model helps to relieve the congestion on the CBs. Second, a higher social welfare generally implies that more power is sold/exchanged in the market. However, it is possible that some contracted power in the day-ahead market could not be dispatched in real time due to network limitations. The following re-dispatch may lead to extra cost for the end consumers. Therefore, it is critical to examine whether the increased social welfare comes at the cost of more re-dispatching.

The rest of the paper is organized as follows. In section 2, we provide the mathematical formulations of different day-ahead market clearing models (nodal pricing, FBMC, and ATC) as well as the real-time re-dispatch. In section 3, we discuss some formal relationships between the day-ahead market clearing models, illustrated by a 3-node example. Section 4 shows different model results in two numerical examples, a 6-bus test system and the IEEE 24-bus test system. Some conclusions are given in section 5.

2. Market procedures and models

2.1 Notation

Sets and Indices

$i, j \in N$	Set of nodes
$l \in \mathrm{L}$	Set of directed lines
N_z	set of nodes belonging to zone z
CB	Set of critical branches
$z, zz \in Z$	Set of price areas

Parameters

$atc_{z,zz}$	Upper limit on the flows from zone z zone zz
cap_l	Thermal capacity limit of the line l
$gsk_{i,z}$	Generation shift keys
$nptdf_{l,i}$	Node to line PTDF matrix
$zptdf_{l,z}$	Zone to line PTDF matrix

Variables

$BEX_{z,zz}$	The exchange from z to zz
${FL_l}^N$	Load flow on line l in the nodal pricing model
${FL_l}^{FBMC}$	Flows on line l in the FBMC model
NEX_z	The net position of a zone z
NI_i	Net injection at node i
Q_i^s	Generation quantity (MWh/h) at node i
Q_i^d	Load quantity (MWh/h) at node i
P_i^s	Supply curve at node i
P_i^d	Demand curve at node i
GUP_i	Increased generation at node i
GDN_i	Decreased generation at node i
$LOADSHED_i$	Load curtailments at node i

In this section, we discuss the sequential structure and necessary procedures of day-ahead and real time re-dispatch markets. We also state the mathematical models used in this paper. Generally, three distinct phases can be identified in the operational procedure of FBMC, i.e. pre-market coupling, market coupling and post-market coupling.

2.2 Pre-market coupling

Pre-market coupling is the preparation phase where the TSOs prepare the input for the day-ahead market models. The pre-market coupling starts on the evening of Day -2 and lasts until 10:00 on Day -1. For the FBMC model, to prepare the input data, the TSOs first create a “base case” which contains the load and generation information for each bidding zone and the expected state of the detailed grid topology. Given the “base case,” the TSOs then will derive the Generation Shift Keys (GSKs), zonal PTDF matrices, Critical Branches (CBs), and other factors. These data are sent to the power exchanges and used as input for the day-ahead market. For the ATC model, the TSOs will assign the maximum trading volume between two connected price areas.

We notice that there might be substantial forecast errors for these input data as they are collected/generated one or two days before market clearing. The inaccuracy might affect the performance of the day-ahead models in practice. However, in this paper, we do not measure the uncertainty regarding the load, generation, or network topology. We assume that these data are kept unchanged for all the three phases involved.

We further assume that the results given by the nodal pricing model (i.e., the optimal solution and nodal prices) serve as the “base case.” The nodal pricing model is considered to be able to utilize all the available recourses within the network. Because the FBMC model originates from the nodal pricing model, results given by the nodal pricing model could be considered as the best possible estimation for the input data. As the input data in this paper are based on better predictions than what we can expect in practice, the results from the FBMC model should be on the optimistic side.

Nodal pricing model

$$\max \sum_i \left[\int_0^{Q_i^d} P_i^d(Q)dQ - \int_0^{Q_i^s} P_i^s(Q)dQ \right] \quad (1)$$

Subject to:

$$NI_i = Q_i^s - Q_i^d, \forall i \in N \quad (2)$$

$$\sum_i NI_i = 0 \quad (3)$$

$$FL_l{}^N = \sum_i nptdf_{l,i} \times NI_i, \forall l \in L \quad (4)$$

$$\left|FL_l{}^N\right| \le cap_l, \forall l \in L \tag{5}$$

The objective of the nodal pricing model is to maximize the social welfare, i.e., Eq. (1)). Net injection, NI_i, to each node i is equal to the difference between generation, Q_i^s, and demand, Q_i^d, i.e., Eq.(2)). Total generation should be equal to demand (Eq. (3)), i.e. we are not considering losses. The nodal power transfer distribution factor, $nptdf_{l,i}$, which is derived from the lossless DC power flow approximation (Christie et al., 2000), illustrates the linearized impact on line l by injecting 1 MW power at node i and subtracting it from the reference node. The total power flow on line l is given in Eq. (4), and it is restricted by the line thermal capacity limit in Eq. (5).

A generation shift key (GSK) is a factor describing the most probable change in net injection at a node, relative to a change in the net position of the zone that it belongs to (Epexspot, 2011). The set of GSKs is crucial in the FBMC model (De Maere d'Aertrycke and Smeers, 2013). Although the GSKs should be defined before market clearing, in reality they cannot be known until the FBMC calculation is completed. The TSOs calculate the GSKs using a "base case" by predicting the anticipated grid topology, net positions, and corresponding power flows for each hour of the day of delivery. In practice, a precise procedure to define the GSKs is missing.

In this paper, we define GSKs as the nodal weight of the net position within each zone:[1]

$$gsk_{i,z} = \frac{Q_i^s - Q_i^d}{\sum_{i \in N_z}(Q_i^s - Q_i^d)}, \forall z \in Z, i \in N_z \tag{6}$$

Q_i^s and Q_i^d are unknown before the market clearing, however, we use the solution given by the nodal pricing model (i.e., Q_i^{s*} and Q_i^{d*}) to calculate the GSKs because the nodal pricing model is considered to best utilize the network resources.

[1] The GSKs cannot be defined in a balanced price area (i.e., $\sum_{i \in Z}(Q_i^{s*} - Q_i^{d*}) = 0$).

Next, TSOs use both GSKs and nodal PTDF matrices to calculate the zonal PTDF matrices, $zptdf_{l,z}$. The zonal PTDF matrices are used to estimate the influence of the net position of any zone on the lines in the FBMC model.

$$zptdf_{l,z} = \sum_{i \in N_z} nptdf_{l,i} \times gsk_{i,z}, \forall l \in L, z \in Z \tag{7}$$

$$zptdf_l^{z,zz} = zptdf_{l,z} - zptdf_{l,zz}, \forall l \in L, z \in Z, zz \in Z \tag{8}$$

In the FBMC model, the physical restrictions are only imposed on the selected CBs. The CBs are defined as the transmissions lines that are significantly impacted by cross-border trading (JAO.EU, 2014). A CB is considered to be significantly impacted by CWE cross-border trades if its maximum CWE zone-to-zone PTDF $zptdf_l^{z,zz}$ (Eq. (8)) is larger than a fixed threshold value (JAO.EU, 2014). The TSOs publish the CBs and their corresponding Remaining Available Margin (RAM) before market clearing. The RAM is the line capacity that can be used by the day-ahead market. The RAM is calculated as:

$$ram_l = cap_l - F_l{}' \tag{9}$$

where cap_l is the thermal capacity limit and $F_l{}'$ includes three components: (1) flows caused by transactions outside the day-ahead market (e.g., re-dispatching, bilateral trades, forward market), (2) an adjustment value based on TSO knowledge, and (3) a safety margin that is needed to compensate for the approximations and simplifications made by the FBMC model. In this paper, we simply assume that $ram_l = cap_l$, however it is clear that this way of deciding the RAM leaves a lot of discretion in the hands of the TSOs.

2.3 Market coupling[2]

2.2.1 FBMC model

$$\max \sum_i \left[\int_0^{Q_i^d} P_i^d(Q)dQ - \int_0^{Q_i^s} P_i^s(Q)dQ \right] \tag{10}$$

Subject to:

$$NI_i = Q_i^s - Q_i^d, \forall i \in N \tag{11}$$

$$\sum_i NI_i = 0 \tag{12}$$

$$NEX_z = \sum_{i \in N_z} (Q_i^s - Q_i^d), \forall z \in Z \tag{13}$$

$$FL_l^{FBMC} = \sum_z zptdf_{l,z} \times NEX_z, \forall l \in CB \tag{14}$$

$$\left| FL_l^{FBMC} \right| \leq cap_l, \forall l \in CB \tag{15}$$

The objective of the FBMC model is to maximize the social welfare (Eq. (10)). The Net Exchange Position of zone z, NEX_z, is equal to the difference between the total generation and demand within zone z (Eq. (13)). A positive sign of NEX_z indicates that zone z is a net export area and a negative sign indicates a net import area. The zonal PTDF matrix is applied only to calculate flows on the CBs (Eq. (14)), and these flows are restricted to be less than the thermal capacities (Eq. (15)).

2.2.2 ATC model

$$\max \sum_i \left[\int_0^{Q_i^d} P_i^d(Q)dQ - \int_0^{Q_i^s} P_i^s(Q)dQ \right] \tag{16}$$

Subject to:

$$NI_i = Q_i^s - Q_i^d, \forall i \in N \tag{17}$$

$$\sum_i NI_i = 0 \tag{18}$$

[2] The models in this part are not exactly how they would be formulated in practice. In order to compare the different day-ahead models, including the need for re-dispatch, the detailed information about supply, demand and the grid are given.

$$NEX_z = \sum_{i \in N_z} Q_i^s - Q_i^d, \forall z \in Z \tag{19}$$

$$\mathrm{NEX}_z = \sum_{zz} (BEX_{z,zz} - BEX_{zz,z}), \forall z \in Z \tag{20}$$

$$0 \leq BEX_{z,zz} \leq atc_{z,zz}, \forall z, zz \in Z \tag{21}$$

Compared to the FBMC model, the ATC model[3] does not have specific limitations on any selected lines. However, it restricts the total transfer between two price areas to a pre-defined cap $atc_{z,zz}$, as in Eq. (21). The net position of a zone NEX_z is equal to the difference of its total export and import (Eq. (20)).

2.4 Post-market coupling (re-dispatch model)

Though the FBMC model tries to take the real physical characteristics of the power system into account, it introduces more approximations and simplifications than the nodal pricing model. The zonal PTDF matrices do not accurately represent the characteristics of the power system. The GSKs are based on the prediction of the market-clearing results, which implies that GSKs are subject to forecast errors. It also assumes that any change in the zonal net injection is distributed on the nodes of the zone corresponding to the GSKs. Therefore, the power transfer given by the FBMC model is not equal to the real physical power flow[4], and re-dispatch may be needed in order to obtain a feasible flow in the real network.

[3] In this paper, we do not consider gaming opportunities. However, in reality, it might happen that the producers in a zonal market could bid at a lower price (than the marginal cost) in the day-ahead market to guarantee that their bids are accepted. Then, due to export constraints in the real time, the contracted power in the day-ahead market cannot be dispatched, and the producer will buy back power at a lower price (than the day-ahead price) in the re-dispatch market. This is referred to as the increase-decrease (inc-dec) game, and the producers can profit from this action. It is important to note that the inc-dec game could happen in reality and thus increase the re-dispatching cost (Holmberg and Lazarczyk (2015)).

[4] Although the "base case" in this paper is the solution of the nodal pricing model, the FBMC model is not necessarily converging to the nodal pricing model.

We would like to test whether the FBMC model could truly help to relieve the congestion on the CBs. If so, the need for re-dispatching should be reduced. We introduce the re-dispatching model to examine whether the re-dispatching cost will be reduced after applying the FBMC model.

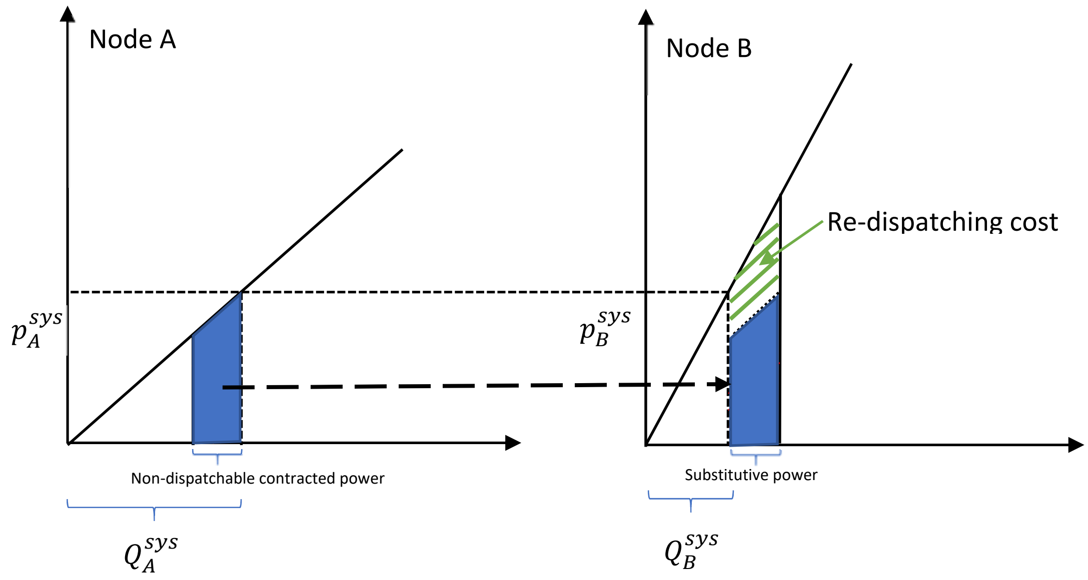

Figure 4-1: Example of re-dispatching

Figure 4-1 further illustrates the mechanism of the re-dispatching model, using a two-node example where we assume that the prices are equal after the day-ahead market clearing. The day-ahead market determines the clearing price and quantity based on the supply and demand information. The supply curve at node A is less steep than that at node B, which implies that the next unit power at node A is cheaper. However, we assume that due to network constraints, some of the contracted power at node A cannot be dispatched. Therefore, in order to satisfy the demand, generation at node B has to be increased. We assume that the generators bid at their marginal cost and that there is perfect price discrimination. Generators that fail to dispatch the contracted power would pay their saved marginal cost to the market and generators that increase their generation in order to satisfy the demand would be compensated by their short-run marginal cost of production (i.e., no economic profit is generated from the re-dispatching procedure, neither for generation nor for load). The increased generation that replaces the non-dispatchable contracted power is more expensive and leads to an extra cost, which is shown as the area filled with green slashed lines. In our study, we assume that the re-dispatch market is regulated in this way, i.e. there are no bids, the system operator simply observes the marginal cost curve of each producer, and compensates them for the costs that they have in the re-dispatch stage. These assumptions are conservative, and may give a much lower re-dispatching cost than what can be expected in practice. In real life, the re-dispatching cost will increase because the generators might bid at a higher price (i.e., marginal price plus the opportunity cost) and because other cost (e.g., start-up cost) would be taken into account.

$$\min \sum_i \int_{Q_i^{s'}}^{Q_i^{s'}+GUP_i+GDN_i} P_i^s(Q)dQ + \sum_i voll \times LOADSHED_i \tag{22}$$

Subject to:

$$NI_i = \left(Q_i^{s'} + GUP_i - GDN_i\right) - (Q_i^{d'} - LOADSHED_i), \forall i \in N \tag{23}$$

$$\sum_i NI_i = 0 \tag{24}$$

$$FL_l{}^N = \sum_i nptdf_{l,i} \times NI_i, \forall l \in L \tag{25}$$

$$\left|FL_l{}^N\right| \le cap_l, \forall l \in L \tag{26}$$

$$GUP_i, GDN_i, LOADSHED_i \ge 0, \forall i \in N \tag{27}$$

The objective of the re-dispatch model is to minimize total re-dispatch costs (Eq. (22)), including load-shedding, if necessary. The generation $Q_i^{s'}$ and the demand $Q_i^{d'}$ from the day-ahead model are used as input. Generation can be increased by GUP_i or decreased by GDN_i. The option to curtail consumer's load ($LOADSHED_n$) is possible only when the feasibility of the re-dispatch model cannot be guaranteed. We assume that the marginal cost of such an option is significantly higher ($voll \gg 0$) than any other marginal generation cost. The re-dispatch model guarantees that the solution gives feasible flows by applying the nodal PTDF matrix and thermal capacity limits (Eq.(25) and (26)).

3. Day-ahead model relationships

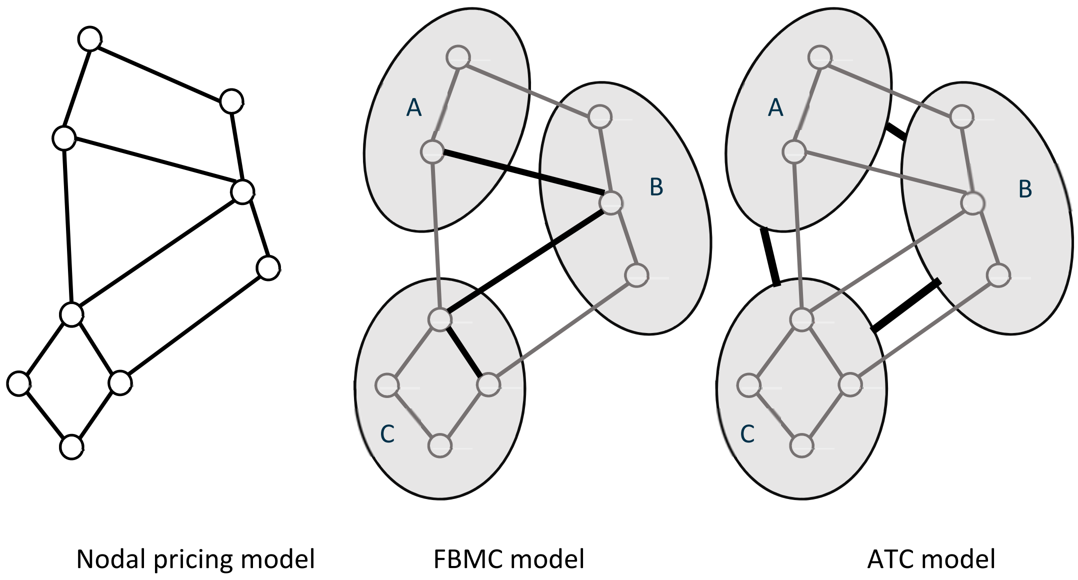

Figure 4-2: Day ahead market models

Figure 4-2 gives a brief illustration of different market clearing models. Among the three models, the nodal pricing model needs most detailed information regarding the grid topology. All the elements (i.e., nodes and lines) are taken into account in the model. The laws of physics are applied to the whole network, and line flows are restricted by the thermal capacities. The topology information is only partially used in both the FBMC model and the ATC model. In the FBMC model, the nodes in the grid are divided into several price areas (zones). The laws of physics are only applied to certain individual lines (i.e., CBs); the other lines (i.e., non-CBs) have no physical restrictions. The CBs could be lines connecting two price areas (i.e., interties) or lines within a price area. In the ATC model, the network is also divided into several price areas. However, instead of using the capacity of individual lines, the ATC model limits power transfer between two price areas to be less than an aggregate capacity (i.e., ATC value). No physical restrictions are applied to lines within a price area. Therefore, within the same area power can be freely traded.

In the following, we further discuss the relationship between these three models in terms of their mathematical formulations. Note from the previous section that the objective functions are the same in all three models.

3.1 The nodal pricing model and the FBMC model

Proposition 1:

a) If the GSKs are derived from a feasible solution to the nodal pricing model, then this solution is also feasible in the FBMC model.
b) If the GSKs are derived from an optimal solution to the nodal pricing model, then this optimal solution is feasible also in the FBMC model, and the optimal social surplus of the FBMC model is greater than or equal to the optimal social surplus of the nodal pricing model.
c) If only a subset of lines is selected as CBs, and if $CB_2 \subseteq CB_1 \subseteq L$, then the optimal solution values, v, are such that $v_{CB_2}^{fbmc} \geq v_{CB_1}^{fbmc} \geq v_L^{fbmc} \geq v^{nodal}$.

Proof:

a) We first assume that the GSKs are derived from a feasible solution to the nodal pricing model (i.e., satisfying Eq. (2)-(5) in Section 2). Let $NI_i{}' = Q_i^{s'} - Q_i^{d'}$ be the net nodal injection at node i for the feasible solution to the nodal pricing model, and let $NEX_z' = \sum_{i \in N_z} NI_i'$ for any zone z, where N_z is the set of nodes belonging to zone z. A feasible solution to the nodal pricing model must satisfy the capacity constraints, i.e.

$$\left| \sum_i nptdf_{l,i} \cdot NI_i{}' \right| \leq cap_l, \forall l \in L \tag{28}$$

Using Eq. (6) and (7), the zonal PTDFs can be expressed as

$$zptdf_{l,z} = \sum_{i \in N_z} nptdf_{l,i} \cdot \frac{Q_i^{s'} - Q_i^{d'}}{\sum_{i \in N_z}\left(Q_i^{s'} - Q_i^{d'}\right)} = \frac{\sum_{i \in N_z} nptdf_{l,i} \cdot NI_i'}{NEX_z'} \tag{29}$$

If we assume that all lines are CBs in the FBMC model, from (14) and (15) we have that

$$\left|\sum_{z} zptdf_{l,z} \cdot NEX_z\right| \leq cap_l \; \forall l \in L \tag{30}$$

Inserting (29) into (30), we get

$$\left|\sum_{z} \frac{\sum_{i \in N_z} nptdf_{l,i} \cdot NI_i'}{NEX_z'} \cdot NEX_z\right| \leq cap_l \; \forall l \in L \tag{31}$$

If $NEX_z = NEX_z'$ for all z, then Eq. (31) simplifies to

$$\left|\sum_{i \in \mathrm{N}} nptdf_{l,i} * NI_i'\right| \leq cap_l \; \forall l \in L \tag{32}$$

which is satisfied for a feasible solution to the nodal pricing model.

b) It follows from a) that if we use an optimal solution to the nodal pricing model to derive the GSKs, then this optimal solution will be feasible in the resulting FBMC model. Since the objective functions of the two models are the same, the optimal solution of the FBMC model must be at least as good as the optimal solution of the nodal pricing model.

c) The last inequality follows from b). Since the feasible area of the FBMC model is convex, the optimal solution values cannot decrease if we remove constraints from the model formulation.

3.2 The nodal pricing model and the ATC model

Proposition 2:

a) If the ATC-capacities, $atc_{z,zz}$, are greater than or equal to the sum of the thermal capacities of the individual lines across the interface, then the ATC model is a relaxation of the nodal pricing model.
b) If the ATC-capacities, $atc_{z,zz}$, are greater than or equal to the sum of the power flow going from zone z to zone zz in the optimal solution to the nodal pricing model, then the optimal social surplus of the ATC model is greater than or equal to the optimal social surplus of the nodal pricing model.

Proof:

a) The thermal constraints (i.e., Eq. (5)) imply that the sum of power going from zone z to zone zz is less than or equal to the sum of thermal capacities in any feasible solution to the nodal pricing model. Therefore, if the value of the $atc_{z,zz}$ is set to be greater than or equal to the sum of thermal capacities, any solution that is feasible in the nodal pricing model will also be feasible in the ATC model.

b) If we assume that the value of the $atc_{z,zz}$ is greater than or equal to the sum of power going from zone z to zone zz in the optimal solution to the nodal pricing model, then this solution to the nodal pricing model will always be feasible in the ATC model (Eq. (16) to (21)). In this case, the ATC model will have an optimal social surplus, which is greater than or equal to the optimal social surplus of the nodal pricing model.

3.3 Example with 3 nodes

We illustrate the relationships between the different congestion management methods for the day-ahead market by using a 3-node example as displayed in Figure 4-3. The nodes are connected by 3 identical lines (i.e., with the same thermal capacity and admittance). The network is divided into two zones, zone z1 with node 1 and zone z2 with nodes 2 and 3. We let Q_i denote net injection into node i, $Q_i > 0$ representing net generation and $Q_i < 0$ representing net withdrawal (demand).

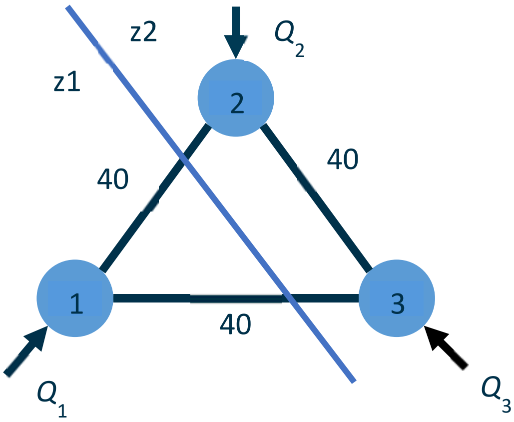

Figure 4-3: 3 node example

a) Nodal pricing model constraints

We assume node 1 to be the reference node and the corresponding nodal PTDFs are given in Table 4-1.

LINE	$nptdf_{l,1}$	$nptdf_{l,2}$	$nptdf_{l,3}$
21	0	$\frac{2}{3}$	$\frac{1}{3}$
31	0	$\frac{1}{3}$	$\frac{2}{3}$
23	0	$\frac{1}{3}$	$-\frac{1}{3}$

Table 4-1: nodal PTDF for the 3 node example

The nodal pricing constraints for the three lines are

$$-40 \leq \frac{2}{3}Q_2 + \frac{1}{3}Q_3 \leq 40 \qquad (33)$$

$$-40 \leq \frac{1}{3}Q_2 + \frac{2}{3}Q_3 \leq 40 \qquad (34)$$

$$-40 \leq \frac{1}{3}Q_2 - \frac{1}{3}Q_3 \leq 40 \qquad (35)$$

b) ATC model constraints

In the ATC model, only the transfer over the interface between the two zones is constrained

$$-ATC \leq Q_2 + Q_3 \leq ATC \tag{36}$$

In practice, setting the ATC transfer capacities between the areas is a challenging task. On the one hand, setting a too high capacity will typically result in infeasible flows, while setting it too low may constrain the system unnecessarily. In the example, we discuss two possibilities: The first is to sum the individual capacities for all the connecting lines (i.e., 80 in our example), and the second is to use a more restrictive value, taking into account the possibility of a "worst case" distribution of supply and demand within the zones (i.e., 60 in our example)[5]. In the example, it seems reasonable to use an ATC value between 60 and 80, however in practice, the ATC transfer limit may be even lower than 60, for instance in order to relieve intra-zonal constraints.

$$\text{Maximum capacity:} \quad -80 \leq Q_2 + Q_3 \leq 80 \tag{37}$$

$$\text{"Worst case" capacity:} \quad -60 \leq Q_2 + Q_3 \leq 60 \tag{38}$$

c) FBMC model constraints

We follow the procedure described, and start by defining the GSKs. For node 1, the GSK is equal to 1, and the PTDFs for zone 1 are zero for all lines. For nodes 2 and 3, the GSKs can be defined as

$$\text{Node 2: } \frac{Q_2'}{Q_2'+Q_3'} = \alpha \tag{39}$$

$$\text{Node 3: } \frac{Q_3'}{Q_2'+Q_3'} = 1 - \alpha \tag{40}$$

[5] Since in a zonal pricing context we do not know exactly where supply and demand bids are located, the "worst case" refers to a situation where generation and load is located in the most unfavorable way. In the example, if zone 2 is the exporting zone, the worst possible case is if all net generation was located in one of the nodes 2 or 3. If so, the maximum net generation that is feasible in the nodal model, would be 60 units (⅔ · 60 = 40). Setting the ATC transfer capacity at 60, would then secure that the net transfer is feasible in the nodal model, no matter how generation is distributed over the nodes in zone 2.

The PTDFs for zone 2 are then calculated by using the GSKs and the nodal PTDFs

$$zptdf_{21}^{z2} = \frac{1}{3} \cdot \alpha + \frac{1}{3} \tag{41}$$

$$zptdf_{31}^{z2} = -\frac{1}{3} \cdot \alpha + \frac{2}{3} \tag{42}$$

$$zptdf_{23}^{z2} = \frac{2}{3} \cdot \alpha - \frac{1}{3} \tag{43}$$

Assuming all three lines are critical, the FBMC model constraints are the following

$$-RAM_{21} \leq (\frac{1}{3}\alpha + \frac{1}{3}) \cdot (Q_2 + Q_3) \leq RAM_{21} \tag{44}$$

$$-RAM_{31} \leq (-\frac{1}{3}\alpha + \frac{2}{3}) \cdot (Q_2 + Q_3) \leq RAM_{31} \tag{45}$$

$$-RAM_{23} \leq (\frac{2}{3}\alpha - \frac{1}{3}) \cdot (Q_2 + Q_3) \leq RAM_{23} \tag{46}$$

The exact constraints depend on the value of α (the GSKs). However, we also notice that the FBMC model limits the sum of Q_2 and Q_3, and thus, like the ATC model, is not able to distinguish between the effects of net injections in node 2 versus node 3.

If $\alpha = \frac{1}{2}$ and $RAM_l = cap_l$, then the constraints for the three critical branches are

$$-40 \leq \frac{1}{2} \cdot Q_2 + \frac{1}{2} \cdot Q_3 \leq 40 \tag{47}$$

$$-40 \leq \frac{1}{2} \cdot Q_2 + \frac{1}{2} \cdot Q_3 \leq 40 \tag{48}$$

$$-40 \leq 0 \cdot (Q_2 + Q_3) \leq 40 \tag{49}$$

The two first constraints (for lines 21 and 31) are identical and equal to the ATC constraint, with ATC value of 80. The last equation (for line 23) is always satisfied, and not constraining in this case.

If we assume inelastic demand equal to 70 located in node/zone 1, and that the marginal cost for generation is low in node 2 and high in node 3, we obtain the following optimal solutions from the three models:

Nodal pricing:	$(Q_1^*, Q_2^*, Q_3^*) = (-70, 50, 20)$
ATC, capacity 80:	$(Q_1^*, Q_2^*, Q_3^*) = (-70, 70, 0)$
ATC, capacity 60:	No solution
FBMC:	$(Q_1^*, Q_2^*, Q_3^*) = (-70, 70, 0)$

In Figure 4-4 we show the feasible areas for the different congestion management models, varying the "base case" used to calculate the GSKs and the ATC transfer capacities. Since the energy balance implies that $Q_1 = -(Q_2 + Q_3)$, we only need to consider the Q_2 and Q_3 variables.

In Figure 4-4-a, we use $(Q_1{}', Q_2{}', Q_3{}') = (-70,70,0)$ as the "base case", and the ATC transfer capacity is set to 80. We notice that the feasible area of the ATC model covers the feasible points of the nodal pricing model, consistent with the ATC model being a relaxation of the nodal pricing model. The FBMC model on the other hand, includes points that are both feasible and infeasible in the nodal pricing model. Moreover, not all feasible solutions to the nodal pricing model are feasible in the FBMC model. Even if the "base case" is not feasible in neither the nodal pricing model nor the FBMC model, it still generates feasible points in the FBMC model.

In Figure 4-4-b, the ATC transfer capacity is reduced to 40, and the ATC model is no longer a relaxation of the nodal pricing model.

In Figure 4-4-c, we change the "base case" to $(Q_1{}', Q_2{}', Q_3{}') = (-5,70,-65)$. The ATC transfer capacity is 80. We find that the feasible area of the FBMC model is very restricted compared to the previous "base case". However, the new "base case" is now included in the feasible area of the FBMC model, showing that nodal feasibility is not a necessary condition for the "base case" to be feasible in the FBMC model.

In Figure 4-4-d, we use the optimal solution to the nodal pricing model in the example above, i.e. $(Q_1{}', Q_2{}', Q_3{}') = (-70,50,20)$, as the "base case". The "base case" is now included in the feasible areas of both the nodal pricing and the FBMC models, consistent with Proposition 1. The figure also illustrates that the FBMC model does not cover the feasible area of the nodal pricing model, showing that the FBMC model is not a relaxation of the nodal pricing model, even if a feasible solution to the nodal pricing model is used as the “base case”.

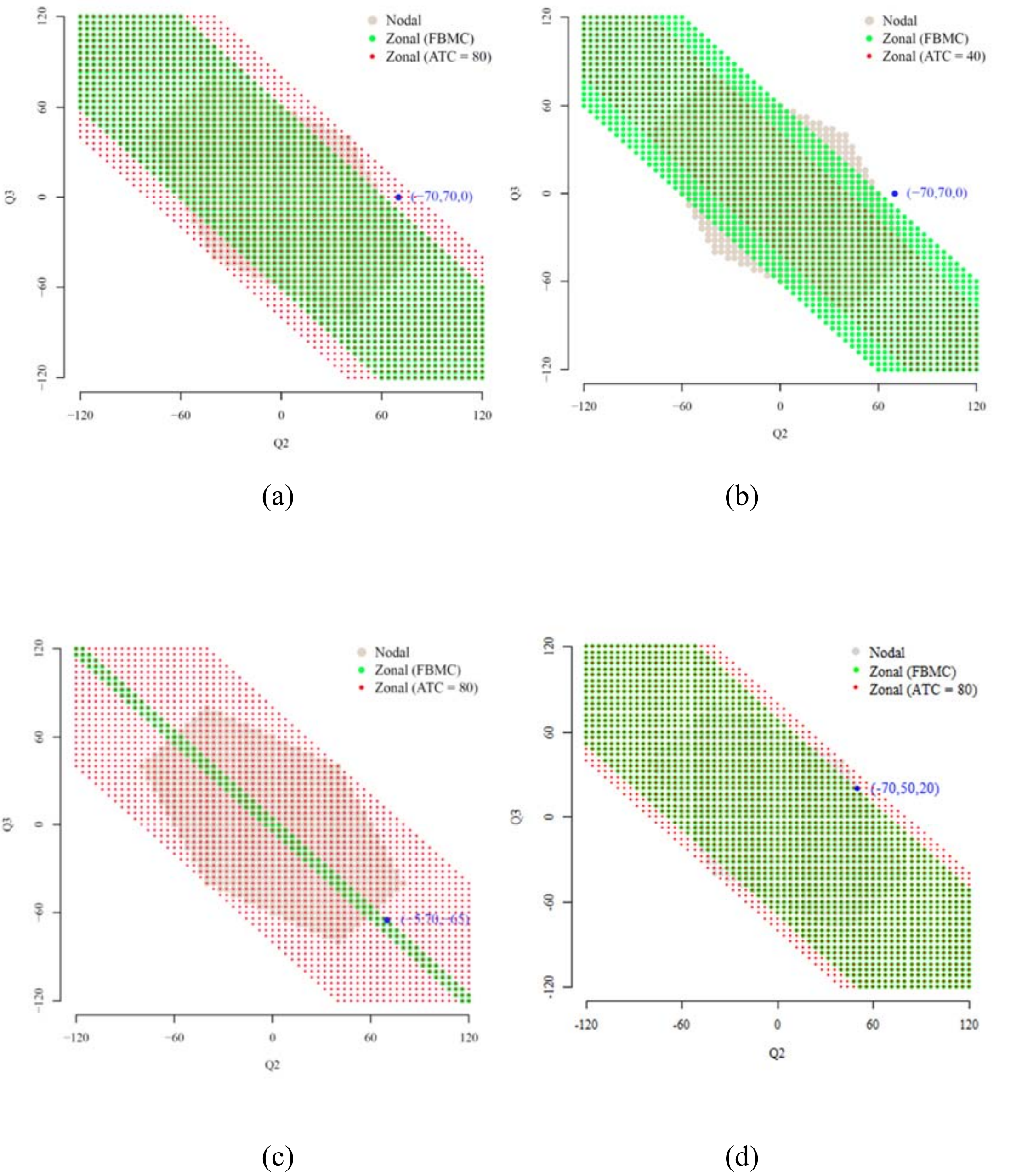

Figure 4-4: Feasible areas of the different dispatch models

The discussion above regarding the feasible areas of the FBMC model shows the importance of the choice of GSKs.

4. Numerical Examples

In this section, we follow the market procedures as discussed in Section 2 and use a 6-bus test system and the IEEE 24-bus test system (Subcommittee, 1979) to illustrate the impact of the implementation of the FMBC model.

4.1 A 6-bus test system

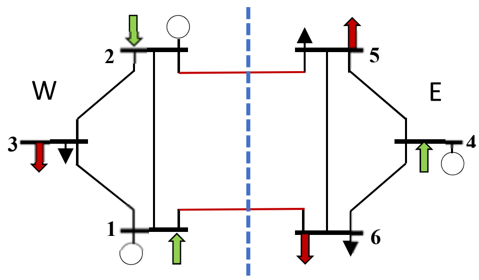

Figure 4-5: A 6-bus test system

We first consider a 6-bus network example as shown in Figure 4-5. This example is used in Chao and Peck (1998) and De Maere d'Aertrycke and Smeers (2013). Generation is located at buses 1, 2 and 4, while load is located at buses 3, 5 and 6. The supply and demand bids are assumed to be linear in quantity q, and they are given in Table 4-2. The parameters regarding the topology are shown in Table 4-3. The network is divided in a western (W) and eastern (E) zone, as shown in Figure 4-5.

Bus-ID	*Supply Bids*	*Bus-ID*	*Demand Bids*
1	10+0.05q	3	37.5-0.05q
2	15+0.05q	5	75−0.1q
4	42.5+0.025q	6	80−0.1q

Table 4-2: Bid functions for generation and load for the 6-bus system

	From Bus-ID	To Bus-ID	Area	Impedance	Capacity	Power flow (nodal pricing solution)
Line1	1	2	W	1	125	0
Line2	1	3	W	1	125	100
Line3	1	6	Intertie	2	200	200
Line4	2	3	W	1	125	100
Line5	2	5	Intertie	2	250	200
Line6	4	5	E	1	125	100
Line7	4	6	E	1	250	100
Line8	5	6	E	1	125	0

Table 4-3: Line parameters

Bus 1 is selected to be the reference node and the node-to-branch PTDF matrix is shown in Table 4-4. We solve the nodal pricing model and get the net input for each bus. We derive the GSKs as in Eq. (6) to determine the weight for each bus as shown in Table 4-5.

	Bus 1	Bus 2	Bus 3	Bus 4	Bus 5	Bus 6
Line1	0	-0.583	-0.292	-0.292	-0.333	-0.250
Line2	0	-0.292	-0.646	-0.146	-0.167	-0.125
Line3	0	-0.125	-0.063	-0.563	-0.500	-0.625
Line4	0	0.292	-0.354	0.146	0.167	0.125
Line5	0	0.125	0.063	-0.438	-0.500	-0.375
Line6	0	-0.042	-0.021	0.479	-0.167	0.125
Line7	0	0.042	0.021	0.521	0.167	-0.125
Line8	0	0.083	0.042	0.042	0.333	-0.250

Table 4-4: Node-to-branch PTDF matrix (Bus 1 is set to be the reference node)

Bus-ID		*Net Input (nodal pricing)*	*Price (nodal pricing)*	*GSKs*	
1	W	300	25	$gsk_{1,N}$	0.75
2		300	30	$gsk_{2,N}$	0.75
3		-200	27.5	$gsk_{3,N}$	-0.5
4	E	200	47.5	$gsk_{4,S}$	-0.5
5		-300	45	$gsk_{5,S}$	0.75
6		-300	50	$gsk_{6,S}$	0.75

Table 4-5: Generation shift keys

Using the GSKs and the node-to-branch PTDF matrix we calculate the zone-to-branch PTDF matrix (Eq. (7)).The zone-to-branch PTDF matrix is given in Table 4-6. Based on the PTDF matrix, the TSOs then decide the CBs. We notice that the zone-to-branch PTDF matrix changes as the reference node changes. However, the zone-to-zone PTDF matrix $zptdf_l^{z,zz}$ (Eq. (8)) remains the same even when the reference node changes[6]. The zone-to-zone PTDFs, $zptdf_l^{z,zz}$, could be interpreted as the influence on line l when transferring one unit of power from zone z to zone zz. This also indicates that in practice, the TSOs need to predict on which borders the international transfers happen in order to identify the CBs. This increases the difficulties in implementing the FBMC model.

	W	*E*	*W→E*	*Area*	*CB*
Line1	-0.292	-0.292	0	*W*	
Line2	0.104	-0.146	0.25	*W*	
Line3	-0.063	-0.563	0.5	*Intertie*	***
Line4	0.396	0.146	0.25	*W*	
Line5	0.063	-0.438	0.5	*Intertie*	***
Line6	-0.021	-0.271	0.25	*E*	
Line7	0.021	-0.229	0.25	*E*	
Line8	0.042	0.042	0	*E*	

Table 4-6: Zone-to-branch PTDF

CBs are those transmissions lines which are significantly impacted by cross-border trades. We select the lines with the highest values of zone-to-zone PTDFs as the CBs. In this example, lines 3 and 5 are chosen as the CB candidates. Both lines have the same highest zone-to-zone PTDF value among all the lines. We test whether these two lines are equally important in the FBMC model. We simulate three cases separately: either of the two CB candidates is chosen as the CB, and both candidates are chosen. The results are given in Table 4-7. We find that when line 3 is selected as the CB, the solutions are the same regardless of whether line 5 has been chosen or not. The reason

[6] This can be proved based on the fact that the sum of GSKs for a zone is constant and equal to 1, and the difference between two nodal PTDFs is the same regardless of the choice of reference node.

is that line 3 is the bottleneck of the system. Power exchange between areas W and E is mainly limited due to the lack of thermal capacity on line 3. Only 400 MW power can be traded between these two areas.

	CB=3	*CB=5*	*CB=3,5*	*Nodal pricing*
Price (W)	27.5	29.17	27.5	27.5*
Price (E)	47.5	45.83	47.5	47.5*
Social Surplus①	23187.50	25020.83	23187.50	23000
Re-dispatching cost②	250.95	2176.87	250.95	0
① -②	22936.55	22843.96	22936.55	23000
W→E(power exchange)	400	500	400	400
Total generation	800	800	800	800

*Supply volume weighted average price

Table 4-7: Results for 6-bus system

In the case when only line 5 is selected as the CB, power exchange increases to 500MW. This reduces the price difference and increases the social surplus given in the FBMC model. However, when we take the post-market coupling into account, re-dispatching cost increases significantly. We re-calculate the social surplus by subtracting the re-dispatching cost. We find that this case has the lowest social surplus when taking into account the re-dispatch cost.

This example shows the importance of choosing the “right” CBs before market clearing in the FBMC model. Based on the zone-to-zone PTDF matrices, both lines 3 and 5 show equal importance in terms of inter-zonal trading. However, the results reveal that line 3 is actually more important. If only line 5 is selected, a higher re-dispatch cost occurs, which leads to lower social surplus. In such a case, the end-consumers might have to bear the cost.

We further compare the FBMC model to the ATC model. We set the ATC value to 400 MW in the ATC model. That is to limit the maximum trading volume between W and E to 400 MW (the total capacity for the interties is 450 MW). We find that the solutions are exactly the same for both the ATC and FBMC models. This indicates that the FBMC model does not necessarily outperform the ATC model in terms of relieving the congestion on the CBs in this example.

Both the ATC model[7] and the FBMC model give a higher objective function value than the nodal pricing model (see Proposition 1 and 2). However, after taking the re-dispatch cost into account, the nodal pricing model gives the highest social surplus.

4.2 The IEEE 24-bus test system

We next apply the FBMC model to the IEEE 24-bus test system with topology shown in Figure 4-6. The supply and demand bid functions are derived from Deng et al. (2010) and shown in Table 4-8. Generators are located at buses 1, 4, 7, 11, 13, 15, 17, 21, 22 and 23. Loads are at the rest of the buses.

Bus-ID	*Supply Bids*	*Bus-ID*	*Demand Bids*
1	15.483+0.0150q	2	65.000−0.0820q
4	20.000+0.0161q	3	75.517−0.1129q
7	12.555+0.0352q	5	63.000−0.0925q
11	29.000+0.0362q	6	42.289−0.0847q
13	39.859+0.1012q	8	62.517−0.1016q
15	29.678+0.0220q	9	50.517−0.0876q
17	23.180+0.0295q	10	59.517−0.0502q
21	30.031+0.0270q	13	45.289−0.0733q
22	20.966+0.0268q	14	64.517−0.0851q
23	35.330+0.0552q	16	58.289−0.1146q
		18	76.547−0.0792q
		19	72.517−0.0682q
		20	63.289−0.1033q
		24	72.289−0.0733q

Table 4-8: Bid functions of generation and load for IEEE24 system

Previous research shows that in order to properly implement the ATC model, a zone should be aggregated in such a way that congestion seldom happens within the zone.

[7] The total volume of power transfer between the two price areas is the same in both the ATC and the nodal pricing models.

This might also be a critical issue in the FBMC model. However, in the European power market, most of the price areas are currently defined according to the national boundaries. Therefore, we do not study how to partition the nodes in this IEEE 24-bus system. We arbitrarily divide the system into two areas S and N. The S area contains buses 1 to 10 and the N area contains buses 11 to 24. We follow the same procedure as we demonstrated in the 6-bus system to find the CBs. We choose 6 lines (the red lines in Figure 4-6) which are considered to be most affected by cross-border trades indicated by the zone-to-zone PTDF matrix.

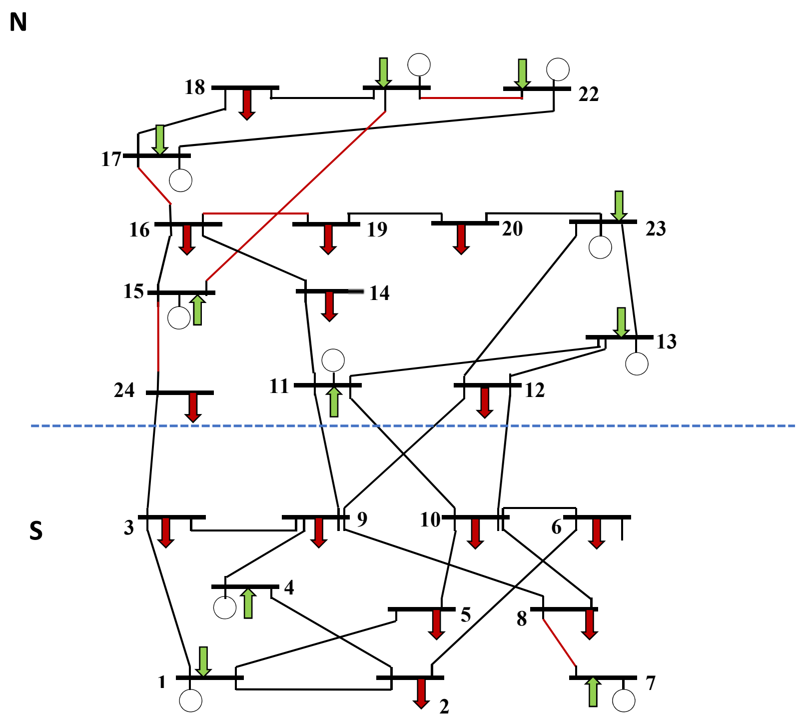

Figure 4-6: IEEE 24 network

As shown in Table 4-9, compared to the nodal pricing model, the FBMC model has a higher social surplus (i.e., objective value) as indicated by Proposition 1. However, the cost per unit of electricity that a customer pays could be much higher if the re-dispatch cost is taken into account. The power in the N area is generally cheaper than that in the S area. Due to the effect of Kirchhoff's law however, the power flow goes from the S area (high-price area) to the N area (low-price area) in the nodal pricing model.

However, this is not the case in neither the FBMC model nor the ATC model. Power flow goes from the N area (low-price area) to the S area (high-price area) regardless of Kirchhoff's laws. Therefore, the FBMC model is not working as well as the nodal pricing model in terms of following the physical constraints. This example also shows that proper partitioning of zones is an important issue to study even when implementing the FBMC model.

	ATC	*FBMC*	*Nodal pricing*
Price (N)	34.205	33.994	24.313*
Price (S)	37.314	37.444	38.941*
Social Surplus($)	104165	104044	90273
Re-dispatching cost($) (Gernetation part)	14353	14099	0
Load shedding(MW)	202	207	0
N→S(power exchange)(MW)	380	343	-343
Unit cost	32.229	32.232	28.464

**Supply volume weighted average price*

Table 4-9: Results for IEEE24 system

We then compare the FBMC results to the ATC model in which the ATC value is set to 380 MW. We find that the net inter-zonal power exchange is 343 MW in the FBMC model compared to 380 MW in the ATC model. Moreover, the average cost for each unit power is slightly higher in the FBMC model. We further check the physical power flow given by solutions to the day-ahead markets. We use Eq.(4) to calculate the physical power flow by fixing the value of nodal load and generation given by the day-ahead market models (i.e., ATC and FBMC models). From the results in Table 4-10, we notice that 3 out of 6 selected CBs are congested in both the ATC and FBMC models. In this example, applying the FBMC model does not help these lines to become congestion-free. We even find that two of these three lines become more congested in the FBMC model than in the ATC model.

	From	*To*	*Line Capacity*	*Actual Flow (ATC)*	*Actual Flow (FBMC)*
CB 1	7	8	350	615	609
CB 2	15	21	1000	-353	-360
CB 3	15	24	500	392	400
CB 4	16	17	500	-510	-519
CB 5	16	19	500	537	543
CB 6	21	22	500	-366	-369

Table 4-10: Actual flow for CBs

5. Conclusions

In this paper we discuss the FBMC model, which has recently been implemented in parts of the European electricity market. We illustrate the relationships between the various congestion management models in a 3-node example, and further test the FBMC model in a 6-bus system, as well as the IEEE 24-bus test system. In the paper we simplify the model to a great extent by neglecting the uncertainties regarding the load, generation, and network topology. However, we still find results showing that it is difficult to implement the FBMC model appropriately. Therefore, it might be a great challenge to apply the FBMC model in the current European power system.

We find it difficult to identify the CBs simply based on the zonal PTDF matrix. It requires that the TSOs forecast directions of the cross-border power exchange. Moreover, the TSOs might choose the wrong CBs based on the information given by the zonal PTDF matrix. In our example, a higher social surplus in the day-ahead market could occur if CBs are not correctly defined. However, this selection leads to a high re-dispatch cost in the post market coupling. This could do harm to the end-consumers as they might have to bear the high re-dispatch cost. We also find that the FBMC model does not necessarily outperform the ATC model in terms of helping to relieve the congestion and to better utilize the resources within the network.

We find that price areas are currently defined according to the national boundaries in the European power market, and that this might lead to power being exchanged in the wrong direction. This happens not only in the ATC model, but also in the FBMC model. This is an important issue to study when implementing the FBMC model.

Reference

[1] Aguado M, Bourgeois R, Bourmaud J, et al. Flow-based market coupling in the central western european region-on the eve of implementation[J]. CIGRE, C5-204, 2012.

[2] Endre Bjørndal, Mette Bjørndal, Hong Cai, Evangelos Panos, Hybrid pricing in a coupled European power market with more wind power, In European Journal of Operational Research, Volume 264, Issue 3, 2018, Pages 919-931, ISSN 0377-2217

[3] CASC 2015 CWE Flow Based Market- coupling project: Parallel Run performance report
http://www.casc.eu/media/Parallel%20Run%20performance%20report%2026-05-2015.pdf

[4] Chao, Hung-po, and Stephen C. Peck. "Reliability management in competitive electricity markets." Journal of Regulatory Economics 14.2 (1998): 189-200.

[5] Christie, Richard D., Bruce F. Wollenberg, and Ivar Wangensteen. "Transmission management in the deregulated environment." Proceedings of the IEEE 88.2 (2000): 170-195.

[6] de Maere d'Aertrycke G., Smeers Y. (2013) Transmission Rights in the European Market Coupling System: An Analysis of Current Proposals. In: Rosellón J., Kristiansen T. (eds) Financial Transmission Rights. Lecture Notes in Energy, vol 7. Springer, London

[7] EIRGRID (2013). "Price Coupling of Regions (PCR) initiative and the North West Europe (NWE) project." EirGrid, 2013.
http://www.eirgrid.com/media/PCR_NWE_MO_TSO_Review.pdf

[8] Epexspot (2011), "CWE_Flow_Based_Questions_and_Answers" https://www.epexspot.com/document/14065/CWE_Flow_Based_Questions_and_Answers.pdf

[9] Holmberg, Pär, and Ewa Lazarczyk. "Comparison of congestion management techniques: Nodal, zonal and discriminatory pricing." Energy Journal 36, no. 2 (2015): 145-166.

[10] JAO.EU (2014) "Documentation of the CWE FB MC solution As basis for the formal approval-request." JAO.EU, 2014

[11] Kunz, Friedrich. "Managing Congestion and Intermittent Renewable Generation in Liberalized Electricity Markets." Dissertation 2012.

[12] Nordpool (2014), "4M Market Coupling launches successfully by using PCR solution." http://www.nordpoolspot.com/globalassets/download-center/pcr/pcr-pr_4m-mc-launch.pdf

[13] Van den Bergh, Kenneth, Jonas Boury and Erik Delarue, The Flow-Based Market Coupling in Central Western Europe: Concepts and definitions, In The Electricity Journal, Volume 29, Issue 1, 2016, Pages 24-29, ISSN 1040-6190

[14] Schavemaker, P.H., et al., "Flow-based allocation in the Central Western European region", paper C5-307, CIGRE, 2008.

http://citeseerx.ist.psu.edu/viewdoc/download?doi=10.1.1.459.7550&rep=rep1&type=pdf

[15] Schweppe F C, Tabors R D, Caraminis M C, et al. "Spot pricing of electricity." 1988.

[16] Sikorski, Tomasz. "Nodal pricing project in Poland." 4th IAEE International Conference: Institutions. Efficiency and Evolving Energy Technologies. Stockholm, 2011.

[17] Subcommittee, P. M. "IEEE reliability test system." IEEE Transactions on Power Apparatus and Systems (1979): 2047-2054.

Chapter 5: The Flow-Based Market Coupling Model and the Bidding Zone Configuration

The Flow-Based Market Coupling Model and the Bidding Zone Configuration

Endre Bjørndal[§], Mette Bjørndal[§], Hong Cai[§‡]

Abstract: In May 2015, the Flow-Based Market Coupling (FBMC) model replaced the Available Transfer Capacity (ATC) model in Central Western Europe to determine the power transfer among bidding zones in the day-ahead market. It might be easier to change the bidding zone configuration in the FBMC model than in the ATC model as the FBMC model does not need to determine the maximum trading volume between two bidding zones. In our study, we run a simulation in the IEEE RTS 24-bus test system and examine how the bidding zone configurations affect the performance of both the FBMC and ATC models. We show that by improving the zone configuration, the FBMC model outperform the ATC in terms of reducing the re-dispatching cost only when the systems operators have a higher level of cooperation in the real-time market. Our results also indicate that better cooperation among the system operators would help to reduce the need for load shedding.

1. Introduction

A large amount of renewable energy has been installed in the EU countries in order to meet the renewable energy target of the Renewable Energy Directive 2009/28/EC. However, promotion of renewable energy sources has greatly challenged the current power systems. As the operation cost of renewable energy is usually much lower than conventional energy, it is placed in the beginning of the merit order curve in the day-ahead market and therefore, has priority access to the power network. However, the forecast errors of renewable energy have led to more network congestion and a higher requirement of back-up capacity in real time. Furthermore, the installed renewable power plants are usually located in places without sufficient consumption (e.g., off-shore wind turbines), and the utilization of such energy often requires long distance transportation. This creates an extra burden for the network and may exacerbate congestion. For instance, the impact of wind energy on network congestion has been

§ Norwegian School of Economics, Helleveien 30, 5045 Bergen, Norway

‡ Corresponding author, Hong.Cai@nhh.no

observed in the German electricity network, in which huge amount of power is transported from the northern part where the main installations of wind turbines are located, to the southern and mid-western parts where the demand is high (Deutscher Bundestag, 2010).

Since February 2014, the EU has launched its most ambitious market coupling project to date by using a single price coupling algorithm, which is called EUPHEMIA (acronym of Pan-European Hybrid Electricity Market Integration Algorithm) (EPEX SPOT et al. 2013). This project now involves power exchanges including APX/Belpex, EPEX SPOT, GME, Nord Pool Spot, OMIE, and OTE (NordPool 2014), which accounts for more than 75% of European electricity demand. One advantage of an integrated European power market is that it could help to better handle the renewable energy in the power system by matching supply and demand across a much wider market.

One crucial question in order to integrate the European power markets is to find a solution to manage the cross-border network congestion efficiently. Currently, most of the European countries rely on the ATC (Available Transfer Capacity) model to process power exchange with the other countries, and this model assumes that power can be directly transferred between any two locations within a bidding zone. Only a pre-defined ATC value is used to limit the maximum commercial trading volume between two bidding zones in the day-ahead market.

The ATC model has been criticized for a long time due to some of its features. Firstly, the ATC model does not take the physical characteristics of electricity into account. In contrast, in the real-time dispatch, power flows between any two locations have to follow the paths resulting from Kirchhoff's laws and are also restricted by the thermal limit of the transmission lines. The ATC model in the day-ahead market thus is not able to give correct information regarding the physical power flows in the system. Secondly, it is rather challenging to decide a proper ATC value between bidding zones. Generally, a high ATC value might promote the commercial transaction opportunities but could induce more network congestion, while a low value will unnecessarily limit the commercial transfer and reduce power network utilization. Furthermore, Bjørndal et al. 2017 find that in the cases where the penetration level of renewable energy is high, even a very low ATC value might not truly help to restrict physical power exchange. Thirdly, previous research shows that in order to properly implement the ATC model, a zone should be aggregated in a way such that congestion seldom happens within the zone. Bjørndal and Jörnsten (2001) show that the results of the ATC model could be greatly affected by the zonal configuration. However, currently most of the bidding zones are aggregated according to the national boundaries and stay unchanged during the market clearing procedures, and bottlenecks may occur frequently within a bidding zone.

In recent years, as more and more renewable energy has been connected to the power system, it is required that the power flows should be more accurately monitored. Leuthold et al. (2008) have shown that the ATC model is not the best option in terms of integrating the wind and solar power into the grid. In May 2015, a so called "Flow-Based methodology" Market Coupling (FBMC), which was developed by the European TSOs (Schavemaker et al. 2008), was implemented to replace the ATC model in Central Western Europe (CWE), a region consisting of the Netherlands, Belgium, France, Luxembourg, and Germany. Van den Bergh et al. (2016) give a description of the FBMC model. The FBMC model applies the physical limitations (e.g., the Kirchhoff's law and the thermal limit) to certain transmission lines (i.e., the critical branches). The system operators aim to have better control over the power flow given the fact that the physical constraints are imposed on the important transmission lines during the day-ahead market clearing.

Compared to the ATC model, in the FBMC model, the system operators do not need to limit the maximum power exchange volume between bidding zones in the day-ahead market. In the perspective of mathematical formulations, the FBMC model only directly imposes limitations on selected transmission lines, which are called critical branches (CBs) that are most likely to be the bottlenecks in the system. Therefore, it might be easier for the TSOs to change the configuration of bidding zones using the FBMC model and achieve a better market outcome. This raises the research question for this paper. We would like to test whether the FBMC model will outperform the ATC model by testing different zonal configuration. Currently, the bidding zones are defined mostly according to the national boundaries. The way to define the bidding zones might be a crucial point to implement the FBMC model successfully. In this paper, we test whether higher efficiency could be achieved for the FBMC model by improving the zonal configuration.

The rest of the paper is organized as follows. In section 2 we provide the mathematical formulations of different day-ahead market clearing models (nodal pricing, FBMC, and ATC) as well as real-time redispatch. In section 3 and 4 we describe the data and show different model results in the numerical examples. Some conclusions are given in section 5.

2. Markets, Assumptions and Models

Generally, three distinct phases can be identified in the operational procedure of the markets. That is the preparation phase, the day-ahead market coupling phase and the real-time re-dispatching phase. The preparation phase is where the TSOs prepare the input for the market coupling models (e.g., the ATC and FBMC models in the European markets). In the day-ahead market coupling phase, the market coupling models will produce output, such as prices and contracted power. However, due to the supply and load uncertainties and the incompleteness of the market coupling models (e.g., physical characteristics of the power system are not fully taken into account), re-dispatching is needed in order to guarantee a congestion free network in the real time. The contracted power in the day-ahead market might be adjusted. This would induce an extra cost. The cost of re-dispatching is an important index to evaluate the performance of the market coupling models.

Sets and Indices

$i, j \in N$	Set of nodes
$l \in \mathrm{L}$	Set of lines
N_z	set of nodes belonging to zone z
CB	Set of critical branches
$z, zz \in Z$	Set of independent price zones

Parameters

$atc_{z,zz}$	Upper limit on the flows from zone z zone zz
cap_l	Thermal capacity limit of the line l
$lscost$	The cost of loadshedding
$nptdf_{l,i}$	Node to line PTDF matrix
$qwind_i$	Expected wind generation at node i (bidding volume) in the day-ahead market
$rqwind_i$	Wind generation at node i in real time
$zptdf_{l,z}$	Zone to line PTDF matrix

Variables

$BEX_{z,zz}$	The Exchange from bidding zone z to zz
${FL_l}^N$	Load flow on line l in the nodal pricing model
${FL_l}^{FBMC}$	Flows on line l in the FBMC model
GUP_i	Increased generation at node i
GDN_i	Decreased generation at node i
$LOADSHED_i$	Load curtailments at node i
$WINDSHED_i$	Wind curtailments at node i
NI_i	Net injection at node i
Q_i^s	Conventional Generation quantity (MWh/h) at node i
Q_i^d	Load quantity (MWh/h) at node i
P_i^s	Supply bid curve at node i
P_i^d	Demand bid curve at node i

2.1 The ATC model[1]

$$\max \sum_i (\int_0^{Q_i^d} P_i^d(Q)dQ - \int_0^{Q_i^s} P_i^s(Q)dQ) \quad (1)$$

Subject to:

$$NI_i = Q_i^s + qwind_i - Q_i^d, \forall i \in N \quad (2)$$

$$NEX_z = \sum_{i \in N_z} NI_i, \forall z \in Z \quad (3)$$

$$\sum_{z \in Z} NEX_z = 0 \quad (4)$$

$$\mathrm{NEX}_z = \sum_{zz} (BEX_{z,zz} - BEX_{zz,z}), \forall z \in Z \quad (5)$$

$$0 \leq BEX_{z,zz} \leq atc_{z,zz}, \forall z, zz \in Z \quad (6)$$

The objective of the ATC model is to maximize the social welfare (Eq.(1)). The Net Exchange Position of zone z NEX_z is equal to the difference between the total generation (i.e., the conventional generation Q_i^s and wind generation, $qwind_i$) and demand within zone z (Eq.(2) and (3)). The volume of wind generation is the expected value of the real time wind power and is given exogenously.[2] The whole system has to be balanced (Eq. (4)). A positive sign of NEX_z indicates that zone z is a net export zone and a negative sign indicates a net import zone. The net position of a zone NEX_z is equal to the difference of its total export and import (Eq. (5)). The total transfer between two bidding zones is limited to a pre-defined cap $atc_{z,zz}$, as in Eq. (6).

2.2 The FBMC model

The FBMC model is a simplification of the nodal pricing model using PTDFs or power transfer distribution factors. Although the nodal pricing model has been successfully implemented in many regions and countries, such as Pennsylvania – New Jersey-

---

[1] In practice, the model will not be solved like this, since the location on nodes is not known, only the zonal location of a bid is given.

[2] Using the expected wind power may not be the optimal bidding strategy for the wind generators or the system as a whole. However, in this paper, we do not investigate the bidding strategy for the wind generators in the day ahead market. See Bjørndal et al. (2016)

Maryland (PJM), California, and New Zealand, it has not been implemented in any of the European countries. It is considered as an effective method of handling network congestion. The nodal pricing model takes the physical and technical constraints in the whole network into account, which would help to limit the needs for re-dispatching and reduce the corresponding cost. Furthermore, it gives the correct incentives for future investments by reflecting the value of scarce transmission capacity (Hogan 1992). In its simplified version (i.e., the FBMC model), the physical limitations are only applied to part of the network. We display the connections and differences between these models below.

2.2.1 Nodal pricing model

$$\max \sum_i \left(\int_0^{Q_i^d} P_i^d(Q)dQ - \int_0^{Q_i^s} P_i^s(Q)dQ \right) \tag{7}$$

Subject to:

$$NI_i = Q_i^s + qwind_i - Q_i^d, \forall i \in N \tag{8}$$

$$\sum_i NI_i = 0 \tag{9}$$

$$FL_l{}^N = \sum_i nptdf_{l,i} * NI_i, \forall l \in L \tag{10}$$

$$\left|FL_l{}^N\right| \le cap_l, \forall l \in L \tag{11}$$

The objective of the nodal pricing model is again to maximize the social welfare (i.e., Eq. (7)). The net injection NI_i at each node is equal to the difference between its generation $Q_i^s + qwind_i$ and demand Q_i^d (i.e., Eq. (8)). The total generation should be equal to the demand (i.e., Eq. (9)). The nodal power transfer distribution factor $nptdf_{l,i}$, which is derived from the lossless DC power flow approximation (Christie et al. 2000), illustrates the linearized impact on line l by injecting 1 MW power at node i and subtracting it from the reference node. The power flow on line l is given in Eq. (10) and is restricted by the line thermal capacity limit Eq. (11).

2.2.2 FBMC model

$$\max \sum_i \left(\int_0^{Q_i^d} P_i^d(Q)dQ - \int_0^{Q_i^s} P_i^s(Q)dQ \right) \tag{12}$$

Subject to:

$$NI_i = Q_i^s + qwind_i - Q_i^d, \forall i \in N \tag{13}$$

$$NEX_z = \sum_{i \in N_z} NI_i \,, \forall z \in Z \tag{14}$$

$$\sum_{z \in Z} NEX_z = 0 \tag{15}$$

$$FL_l^{FBMC} = \sum_z zptdf_{l,z} * NEX_z, \forall l \in CB \tag{16}$$

$$\left| FL_l^{FBMC} \right| \leq cap_l, \forall l \in CB \tag{17}$$

In the FBMC model, the physical limitations are only applied to the critical branches (CBs) (Eq.(16) and (17)). The zonal PTDF matrices $zptdf_{l,z}$ are used to estimate the influence of the net position of any zone on the CBs. The zonal PTDF matrices are derived from both the Generation Shift Keys (GSKs) and the nodal PTDF matrices (Eq. (18)).

$$zptdf_{l,z} = \sum_{i \in N_z} nptdf_{l,i} * gsk_{i,z}, \forall l \in L, z \in Z \tag{18}$$

GSKs are a set of factors describing a linear estimation of the most probable change in the net injection at a node in relation to the change of the net position of this zone (Epexspot 2011). In practice, a precise procedure to define the GSKs is missing. Gebrekiros et al. (2015) show that the GSKs defined based on nodal injections (production minus demand) perform best among three tested schemes. In this paper, we assume the GSKs as the nodal weight of the net position within the zone given by the nodal pricing solution, $gsk_{i,z} = \frac{Q_i^{s^*} + qwind_i - Q_i^{d^*}}{\sum_{i \in N_z}(Q_i^{s^*} - Q_i^{d^*})}, \forall i, z, i \in N_z$, where $Q_i^{s^*}$ and $Q_i^{d^*}$ represent the solution given by the nodal pricing model.

Figure 5-1 illustrates different market clearing models. Among the three models, the nodal pricing model needs most detailed information regarding the grid topology. In the FBMC model, the nodes in the grid are divided into several bidding zones. The approximated laws of physics are only applied to CBs (bold lines); the other lines (i.e., non-CBs) have no physical restrictions. The CBs could be lines connecting two bidding zones (i.e., interties) or lines within a zone. In the ATC model, the network is also divided into several bidding zones. Instead of using the capacity of individual lines, the ATC model limits power transfer between two bidding zones to be less than an aggregate capacity (i.e., ATC value). No physical restrictions are applied to lines within a bidding zone.

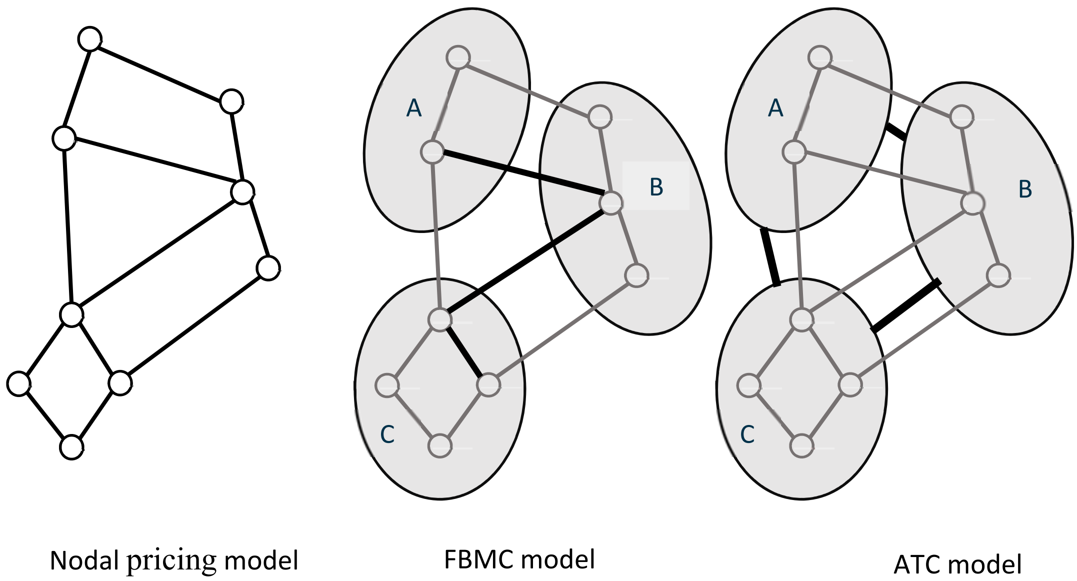

Figure 5-1: Day ahead market models

2.3 Re-dispatching model

In real time, re-dispatching is needed due to the supply and load uncertainties and the incompleteness of the market coupling models (e.g., physical characteristics of the power system are not fully taken into account). A congestion-free network must be guaranteed. The assumptions that we use for the re-dispatching model in this paper, are the following:

a) We assume that the supply uncertainty is caused only by the forecast errors of wind generation.

b) We assume that the load quantities given by the day-ahead market stay unchanged in the real time. However, in order to guarantee the feasibility of the re-dispatching model, the option to curtail load ($LOADSHED_n$) is possible but at a very high cost as displayed in Figure 5-2.

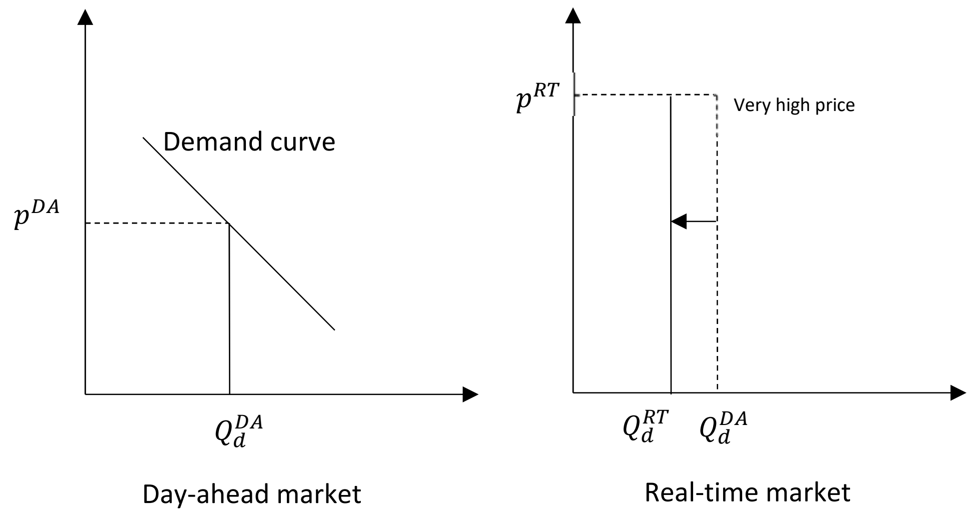

Figure 5-2: Load shedding

c) Conventional generation has high flexibility and can be adjusted accordingly. We assume that the generators still bid at their marginal cost in the re-dispatching model. Generators that fail to dispatch the contracted power would pay their saved marginal cost to the market and generators that increase their generation in order to satisfy the demand would be compensated by their short-run marginal cost of production. In real life, the re-dispatching cost will increase because the generators might bid at a higher price (i.e., marginal price plus the flexibility cost) and because other costs (e.g., start-up cost) would be taken into account.

d) We test two levels of cooperation among the TSOs (i.e., no cooperation and full cooperation). No cooperation refers to the case when the TSOs can only adjust the generation within their own jurisdiction in the real-time market, and the full cooperation case is when the TSOs can adjust the generation within the whole network.

$$\min \sum_i \int_{Q_i^{s'}}^{Q_i^{s'}+GUP_i+GDN_i} P_i^s(Q)dQ + \sum_i lscost * LOADSHED_i \tag{19}$$

Subject to:

$$NI_i = \left(Q_i^{s'} + GUP_i - GDN_i\right) + (rqwind_i - WINDSHED_i) - (Q_i^{d'} - LOADSHED_i), \forall i \in N \tag{20}$$

$$\sum_i NI_i = 0 \tag{21}$$

$$FL_l{}^N = \sum_i nptdf_{l,i} * NI_i, \forall l \in L \tag{22}$$

$$\left|FL_l{}^N\right| \leq CAP_l, \forall l \in L \tag{23}$$

$$GUP_i, GDN_i, LOADSHED_i, WINDSHED_i \geq 0, \forall i \in N \tag{24}$$

The objective of the re-dispatching model is to minimize total re-dispatching costs (Eq. (19)). The generation $Q_i^{s'}$ and the demand $Q_i^{d'}$ from the day-ahead market model are used as input for the re-dispatching model. The generation can be increased by GUP_i or decreased by GDN_i. The option to curtail consumer's load ($LOADSHED_n$) is possible only when the feasibility of the re-dispatching model cannot be guaranteed. We assume the marginal cost of such an option to be significantly higher ($lscost \gg 0$) than any other marginal generation cost. The re-dispatching model guarantees that the solution gives feasible flows by applying the nodal PTDF matrix and thermal capacity limits (Eq.(22) and (23)). We simulate two different levels of cooperation among system operators (i.e., full cooperation and no cooperation). The above formulations assume that the system operators are fully aware of operations by other system operators in the re-dispatching model and the re-dispatching is not restricted within the same bidding zone.

$$\sum_{i \in N_z} \left((GUP_i - GDN_i) + (rqwind_i - qwind_i - WINDSHED_i) - LOADSHED_i\right) = 0, \forall z \in Z \tag{25}$$

Adding Eq.(25) to the above formulations limits re-dispatching within the same bidding zone. That is, the system operators can only increase or decrease generation within their own jurisdiction. Decreased generation should be equal to increased generation within the same bidding zone.

3. Network and Input data

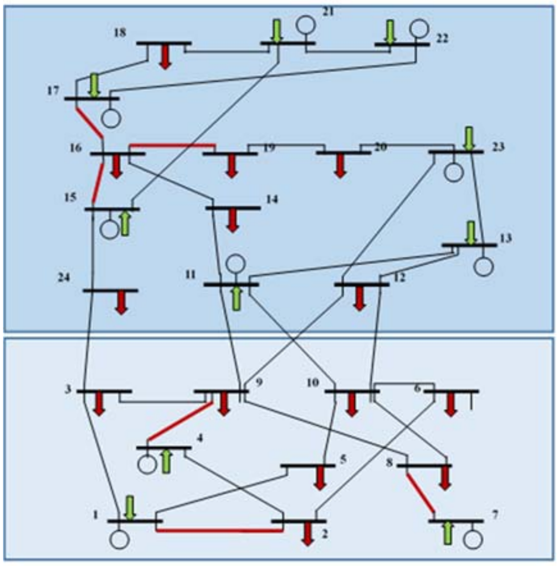

Figure 5-3: IEEE RTS 24-bus system

The models are tested in the IEEE RTS 24-bus test system (Subcommittee 1979, Ordoudis el al. 2014), which is composed of 24 buses and 34 transmission lines, as displayed in Figure 5-3. The supply and demand bid functions are derived from Deng et al. (2010) and shown in Table 5-1. Generators are located at buses 1, 4, 7, 11, 13, 15, 17, 21, 22 and 23. Loads are at the rest of the buses. The parameters for the transmission lines are given in Table 5-2.

Bus-ID	*Supply Bids*	*Bus-ID*	*Demand Bids*
1	15.483+0.0150q	2	65.000−0.0820q
4	20.000+0.0161q	3	75.517−0.1129q
7	12.555+0.0352q	5	63.000−0.0925q
11	29.000+0.0362q	6	42.289−0.0847q
13	39.859+0.1012q	8	62.517−0.1016q
15	29.678+0.0220q	9	50.517−0.0876q
17	23.180+0.0295q	10	59.517−0.0502q

21	30.031+0.0270q	13	45.289−0.0733q
22	20.966+0.0268q	14	64.517−0.0851q
23	35.330+0.0552q	16	58.289−0.1146q
		18	76.547−0.0792q
		19	72.517−0.0682q
		20	63.289−0.1033q
		24	72.289−0.0733q

Table 5-1: Bid functions of generation and load for IEEE24 system

From	To	Capacity MVA	Reactance p.u.	From	To	Capacity MVA	Reactance p.u.
1	2	175	0.0146	11	13	400	0.0488
1	3	175	0.2253	11	14	400	0.0426
1	5	350	0.0907	12	13	400	0.0488
2	4	175	0.1356	12	23	400	0.0985
2	6	175	0.205	13	23	400	0.0884
3	9	175	0.1271	14	16	250	0.0594
3	24	400	0.084	15	16	400	0.0172
4	9	175	0.111	15	21	400	0.0249
5	10	350	0.094	15	24	400	0.0529
6	10	175	0.0642	16	17	300	0.0263
7	8	350	0.0652	16	19	400	0.0234
8	9	175	0.1762	17	18	400	0.0143
8	10	175	0.1762	17	22	400	0.1069
9	11	400	0.084	18	21	400	0.0132
9	12	400	0.084	19	20	400	0.0203
10	11	400	0.084	20	23	400	0.0112
10	12	400	0.084	21	22	400	0.0692

Table 5-2: Reactance and Capacity of Transmission Lines

Wind farms are located at buses 15 and 22 with installed capacity of 1000 MW and 400MW respectively. The expected wind generation in the day-ahead is 500MW at Node 15 and 200MW at Node 22. We generate 1000 scenarios of wind power in real time, as displayed in Figure 5-4.[3] We assume the cost of wind generated power to be zero.

[3] We used the Weibull distribution to simulate wind speed, and then we used the function from the software package WindPRO (https://www.emd.dk/windpro/) to convert wind speed to power production. The wind turbine would stop working if the rated wind speed is exceeded its cut-out speed.

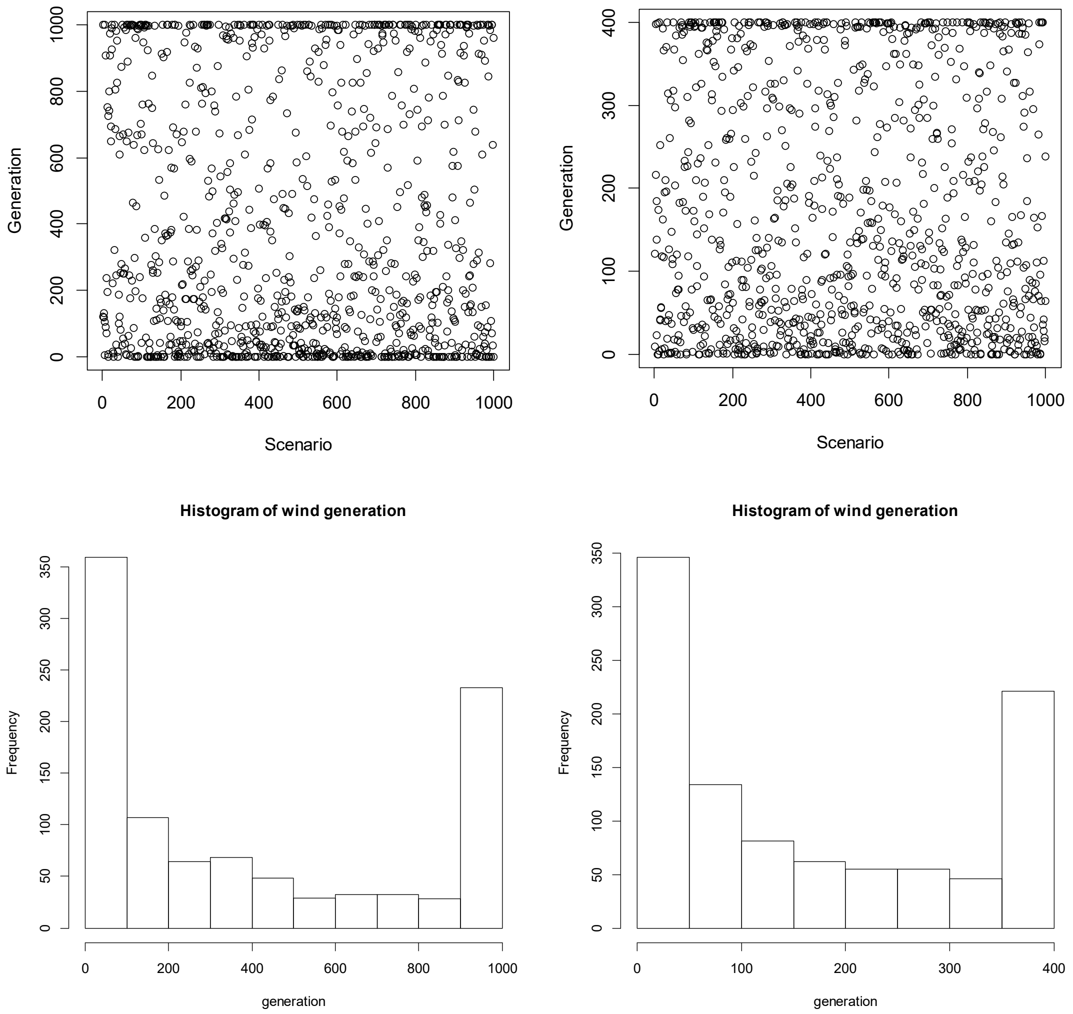

Bus 15 Bus 22

Figure 5-4: Wind generation

The buses are initially divided into two countries according to their geographic location. The southern country contains buses 1 to 10 and the northern country contains buses 11 to 24. We keep the configuration of one of the countries unchanged (i.e., the Southern one) while splitting the other one into more bidding zones, and test how the outcome regarding different congestion models changes. The bidding zones in the northern country are under the control of the same system operator. We need to point out that it is not exactly clear how the number of zones and zone-boundaries are to be determined in both the ATC and FBMC models. Stoft (1996, 1997) shows that the partition of the network into zones generally is not obvious, but states that it should be based on price differences given by the nodal pricing solution. However, Bjørndal and Jörnsten (2001) also point out that even if it depends on price differences in the nodal pricing model, it is not straightforward. In our paper, we first run the nodal pricing model using supply and demand information in the day-ahead market, and then roughly group the nodes in the northern part into 3 and 4 bidding zones based on the price differences and node location, as showed in Figure 5-5.

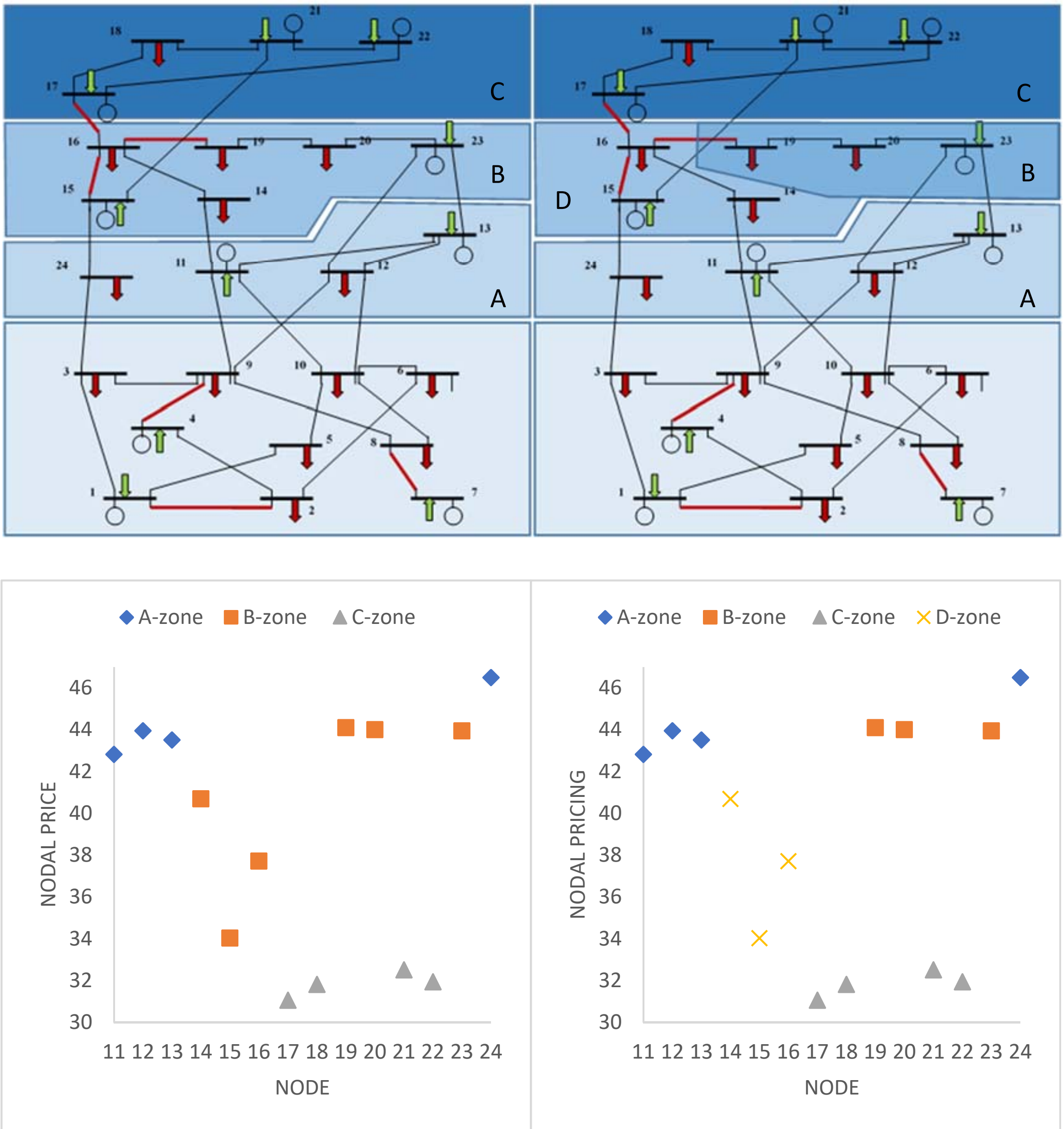

Figure 5-5: zonal configurations

The FBMC model uses the solution of the nodal pricing model, to decide the GSKs (Eq.(18)) and the CBs (lines that are congested given by the FB solution are set to be the CBs in the FBMC model). To make the ATC model comparable to the FBMC model, we use the flows given by the nodal pricing solution as a basis to set the aggregate capacity limits. The limits are equal to the absolute value of accumulated flows between two bidding zones given by the nodal pricing solution. We also assume that the aggregate capacity limits between two bidding zones are the same in both directions. For instance, the aggregate capacity limits from the northern country to the southern country are equal to those from the southern country to the northern country.

In the-real time market (i.e., the re-dispatching model), we assume that the TSOs for these two countries can only adjust the generation within their own jurisdiction (i.e., the southern one and the northern one) in the no cooperation case and can adjust the generation freely within the whole network in the full cooperation case. The cost to reduce the load is 1000 (i.e., $lscost = 1000$).

4. Results

We present the simulation results in this section. We study how the bidding zone configuration affects the performance of different cross-border congestion models with two different cooperation levels.

4.1 Impact on the social surplus

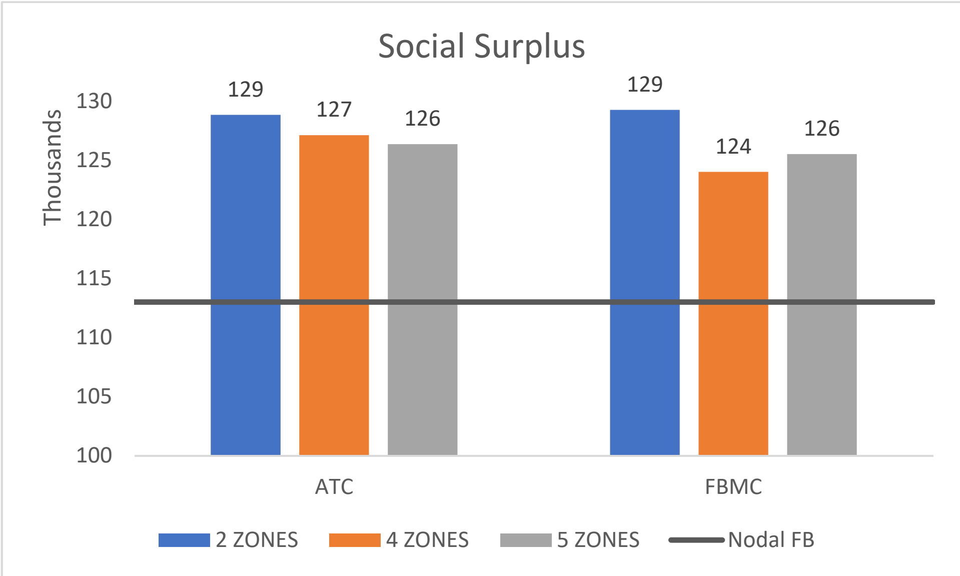

Figure 5-6: Social Surplus in the Day-ahead market

We first look at the impact on social surplus. In all the cases, the social surpluses given by both the ATC and FBMC models are higher than the corresponding value in the nodal pricing model. With the same zone bidding configuration, the ATC model gives higher social surplus than the FBMC model does in both the 4-zone and 5-zone cases. In the ATC model, the social surplus decreases slightly as the number of bidding zones increases. In the FBMC model, the social surpluses in both the 4-zone and 5-zone cases are lower than the one in the 2-zone case. However, the social surplus is a bit higher in the 5-zone case than in the 4-zone case.

The higher social welfare given by both the ATC and FBMC models imply that more power is sold/exchanged in these day-ahead markets (Table 5-3) than in the nodal pricing model. However, it is possible that some contracted power in the day-ahead market could not be dispatched due to network limitations. The following re-dispatching may lead to extra cost for the end consumers. To better understand the performance of different day-ahead market models, we need to take the re-dispatching cost into account. The re-dispatching cost is likely affected by the level of cooperation among the system operators. A higher level of cooperation indicates that it is more likely to re-dispatch cheaper power in the system and the re-dispatching cost would be lower.

	2 ZONES	4 ZONES	5 ZONES
ATC	4733	4568	4529
FBMC	4704	4549	4541
Nodal pricing	3431	3431	3431

Table 5-3: Contracted load in the day−ahead market

4.2 Impact on the re-dispatching cost

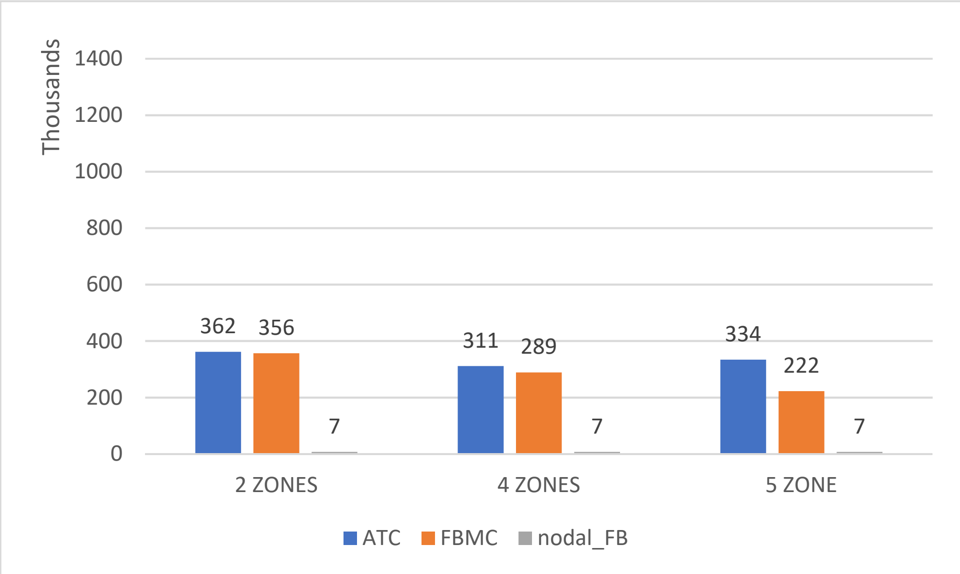

Figure 5-7: Re-dispatching Cost (Full Cooperation)

We first consider cases with a high level of cooperation (i.e., full cooperation). Figure 5-7 shows the average re-dispatching cost for the 1000 scenarios. The average re-dispatching cost is about 7000 given by the nodal pricing model, which is the lowest among the three models. The re-dispatching cost is much higher in both the ATC and FBMC models.

The cost in the ATC model falls from 362,000 in the 2-zone case to 311,00 in the 4-zone case (about 14%). The cost in the FBMC model falls from 356,000 to 289,000 in the 4-zone case (about 19%). However, the cost in the ATC increases from the 2-zone case to 334,000 in the 5-zone case (about 7%) while the cost in the FBMC further decreases to 222,000, a decline by nearly 23%.

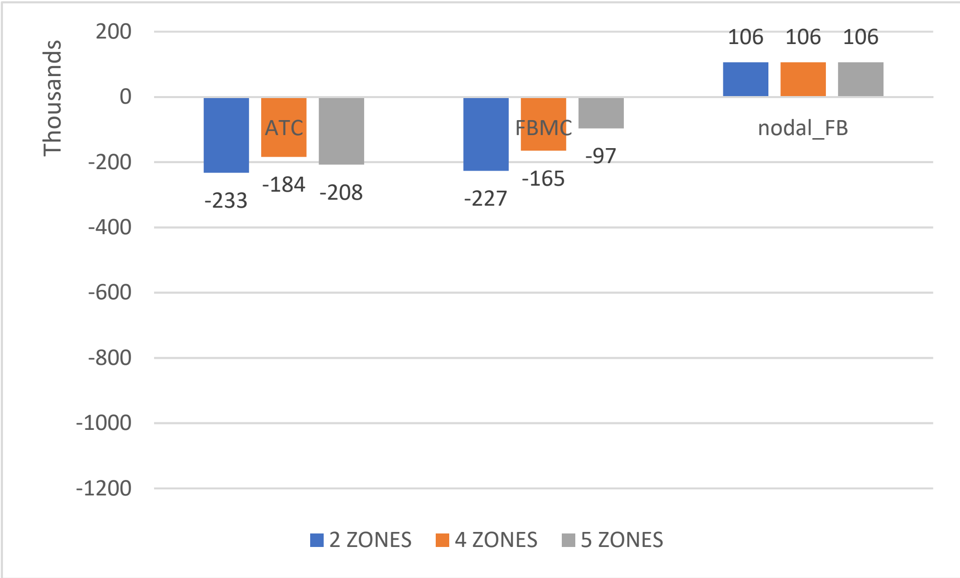

Figure 5-8: Total social surplus[4] in the full cooperation case

In the cases with a higher level of cooperation, the performance of the FBMC model is better if a more detailed network is given (i.e., more bidding zones). In our example, the FBMC model could be greatly improved if a better zone configuration is given in the full cooperation case. The social surplus from the day ahead increases from 124,000 in the 4-zone case to 126,000 in the 5-zone case, while the re-dispatching cost deceases by nearly 23%. As given by Figure 5-8, the total social surplus (i.e., the social surplus given by the day-ahead market minus the re-dispatching cost in the real time) is highest in the 5-zone case when applying the FBMC model.

.[4] As the load shedding cost are assumed to be very high, the total social surplus thus could be negative.

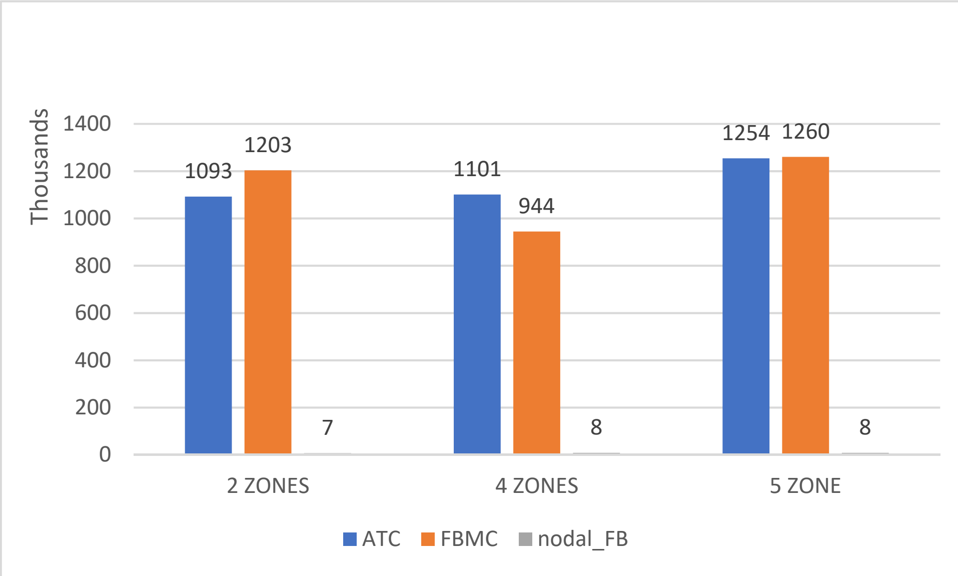

Figure 5-9: Re-dispatching Cost (No Cooperation)

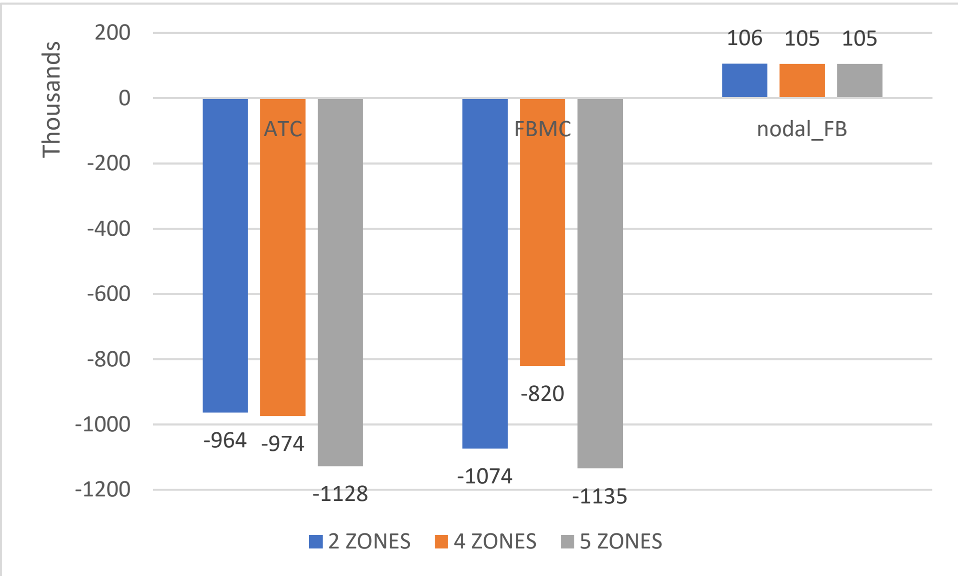

Figure 5-10: Total Social surplus in the no cooperation case

Figure 5-9 shows the average re-dispatching cost in the no cooperation case. Again, the nodal pricing gives much lower re-dispatching cost than both the ATC and FBMC models.

In the no cooperation case, the re-dispatching cost in the ATC model does not decrease even when there are more bidding zones. In fact, the re-dispatching cost increases. In the FBMC model, the re-dispatching cost does not always decline as there are more bidding zones. Compared to the 4-zone case, the re-dispatching cost given by the 5-

zone case increase by 33%.The cost for the 5-zone cases is even higher than that the 2-zone cases. In both the ATC and FBMC models, the total social surplus is lowest in the 5-zone case.

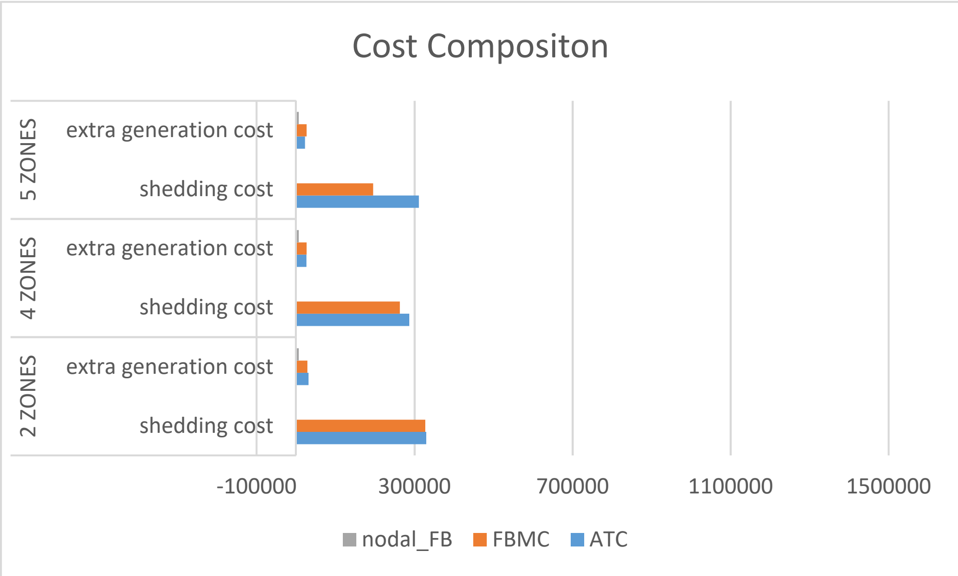

Figure 5-11: Cost Composition (Full Cooperation)

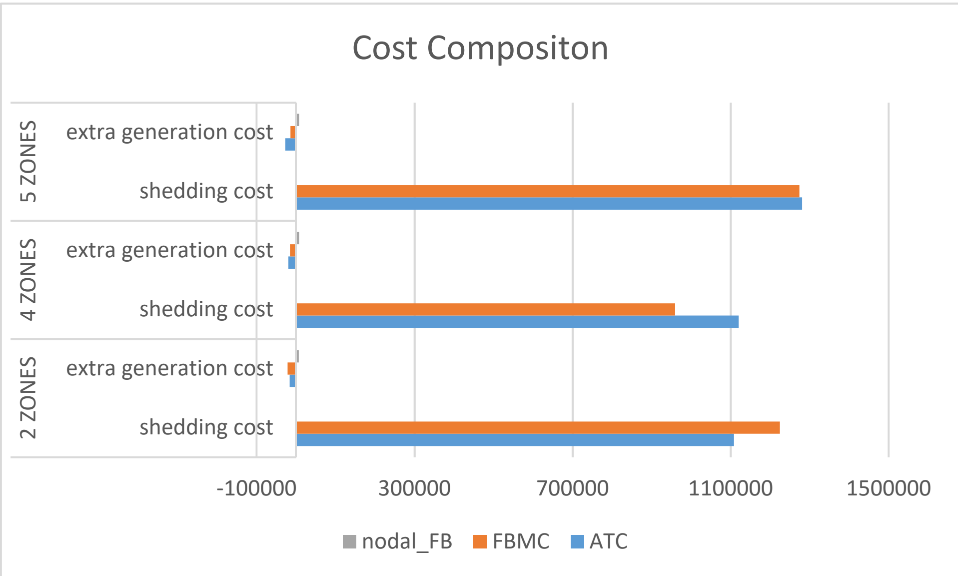

Figure 5-12: Cost Composition (No Cooperation)

We notice that the the cost of up- and down- generation (extra generation cost) given by both the ATC and FBMC models is negative in the no cooperation case, which indicates that a large amount of contracted power in the day ahead market could not be dispatched in the real time as showed in Table 5-4. Correspondingly, the load shedding cost in the no cooperation case is much higher than that in the full cooperation case. By strengthening cooperation among the system operators, the shedding cost could be greatly reduced. This may show the importance for the European countries to intergrate the real-time re-dispatching market.

	Full Cooperation				No Cooperation		
	2 ZONES	4 ZONES	5 ZONES		2 ZONES	4 ZONES	5 ZONES
ATC	7%	6%	7%	ATC	23%	25%	28%
FBMC	7%	6%	4%	FBMC	26%	21%	28%
Nodal pricing	0%	0%	0%	Nodal pricing	0%	0%	0%

Table 5-4: Ratio of load shedding to contracted load

5. Conclusion

Currently the bidding zones of the European power market are defined mostly according to national boundaries. In this paper, we attempt to test how the bidding zone configuration might affect the performance of different network flow models in the day ahead market, given the fact that more and more renewable energy has been connected to the European grid. The paper runs a simulation in the IEEE RTS 24-bus test system by defining different bidding zone configurations and setting two levels of cooperation among the transmission system operators.

In our example, we show that in general, compared to the ATC model, the FBMC model helps to reduce more re-dispatching cost if the zone configuration is improved. We also find that, the FBMC model might perform better in a higher cooperation level. In our example, compared to the 4-zone case, the 5-zone case has a higher social surplus. The re-dispatching cost deceases by almost 23% in the full cooperation case but increases by about 33% in the no cooperation case.

We further notice the main reason for a high re-dispatching cost is that a large amount of contracted power in the day ahead market could not be dispatched in the real time.

By strengthening cooperation among the system operators, the re-dispatching cost could be greately reduced.

Finally, we aslo show that the nodal pricing model will result in a much lower re-dispatching cost than both the ATC and FBMC in both cooperation level, which might indicate the nodal pricing model is a better option for the European power market.

Reference

[1] Bjorndal, E., Bjorndal, M. H., Cai, H., & Panos, E. Hybrid Pricing in a Coupled European Power Market with More Wind Power. NHH Dept. of Business and Management Science Discussion Paper, 2015

[2] Bjorndal, E., Bjorndal, M. H., Cai, H., " Efficiency of the flow-based market coupling model in the European market" Discussion Paper, 2016

[3] Bjørndal, Endre, Mette Helene Bjørndal, Kjetil Trovik Midthun, and Asgeir Tomasgard. "Stochastic Electricity Dispatch: A challenge for market design." (2016).

[4] Bjørndal, Mette, and Kurt Jörnsten. "Zonal pricing in a deregulated electricity market." The Energy Journal (2001): 51-73.

[5] Christie, Richard D., Bruce F. Wollenberg, and Ivar Wangensteen. "Transmission management in the deregulated environment." Proceedings of the IEEE 88.2 (2000): 170-195.

[6] Deng S J, Oren S, Meliopoulos A P. The inherent inefficiency of simultaneously feasible financial transmission rights auctions[J]. Energy Economics, 2010, 32(4): 779-785.

[7] Deutscher Bundestag, "Rahmenbedingungen für den Aufbau eines Overlay Stromnetzes, Drucksache 17/4336. 2010. "

http://dipbt.bundestag.de/dip21/btd/17/043/1704336.pdf.

[8] Epexspot (2011), "CWE_Flow_Based_Questions_and_Answers"

https://www.epexspot.com/document/14065/CWE_Flow_Based_Questions_and_Answers.pdf

[9] Epexspot et al., "EUPHEMIA public description - PCR market coupling algorithm," Price Coupling of Regions (PCR), Public, Feb. 2013.

[10] Gebrekiros, Y., Doorman, G., Preda, T., & Helseth, A. (2015, October). Assessment of PTDF based power system aggregation schemes. InElectrical Power and Energy Conference (EPEC), 2015 IEEE (pp. 358-363). IEEE.

[11] Hogan, William W. "Contract networks for electric power transmission." Journal of Regulatory Economics 4, no. 3 (1992): 211-242.

[12] Leuthold, Florian U., Hannes Weigt, and Christian von Hirschhausen. "Efficient pricing for European electricity networks–The theory of nodal pricing applied to feeding-in wind in Germany." Utilities Policy, 2008: 16(4), 284-291.

[13] Nordpool (2014), "4M Market Coupling launches successfully by using PCR solution." http://www.nordpoolspot.com/globalassets/download-center/pcr/pcr-pr_4m-mc-launch.pdf

[14] Ordoudis, C., P. Pinson, J.M. Morales, M. Zugno (2014). An updated version of of the IEEE RTS 24-bus system for electricity market and power system operation studies. Course material, Technical University of Denmark, 31761 - Renewables in Electricity Markets.

[15] Schavemaker, P.H., et al., "Flow-based allocation in the Central Western European region", paper C5-307, CIGRE, 2008.
http://citeseerx.ist.psu.edu/viewdoc/download?doi=10.1.1.459.7550&rep=rep1&type=pdf

[16] Stoft, Steven (1996), "Analysis of the California WEPEX Applications to FERC", PWP-042A, University of California Energy Institute.

[17] Stoft, Steven (1997), “Zones: Simple or Complex?”, The Electricity Journal, Jan/Feb, pp. 24-31

[18] Van den Bergh, Kenneth, Jonas Boury and Erik Delarue, The Flow-Based Market Coupling in Central Western Europe: Concepts and definitions, In The Electricity Journal, Volume 29, Issue 1, 2016, Pages 24-29, ISSN 1040-6190

[19] Venkatesh, P., et al. "Electrical Power Systems: Analysis." Security And Deregulation, Phi Learning Pvt Ltd. 2012